University of Alberta

Tripartite-motif family members in the White Pekin duck (*Anas platyrhynchos*) modulate antiviral gene expression

by

Alysson Heather Blaine

A thesis submitted to the Faculty of Graduate Studies and Research
in partial fulfillment of the requirements for the degree of

Master of Science
in
Physiology, Cell and Developmental Biology

Biological Sciences

Fall 2013
Edmonton, Alberta

Abstract

Wild waterfowl, including mallard ducks, are the natural reservoir of avian influenza A virus and are resistant to highly pathogenic strains. This is primarily due to the robust innate immune response of ducks. Shortly after exposure to both highly pathogenic (A/Viet Nam/1203/04 (H5N1)) and low pathogenic (A/mallard/BC/500/05 (H5N2)) avian influenza, many immune genes are upregulated including members of the diverse tripartite-motif (TRIM) family. TRIM proteins have species-specific antiviral roles in a variety of viral infections. I have identified a contig of TRIM genes located adjacent to the MHC locus in the White Pekin duck (*Anas platyrhynchos*) genome. A duplication of the *TRIM27.1* gene (*TRIM27.1a* and *TRIM27.1b*) has occurred. Using quantitative real-time PCR (qPCR) I determined that both *TRIM27.1a* and *TRIM27.1b* are upregulated 34- and 5-fold, respectively, at 1 day post-infection with VN1203. In a co-transfection experiment I determined that *TRIM27.1a* and *TRIM27.1b* have opposite effects on expression, decreasing and increasing transcription of antiviral genes, respectively.

Acknowledgements

Firstly, I would like to thank my supervisor, Dr. Kathy Magor for inviting me to join her lab and giving me the tools and opportunities rarely offered to a M.Sc. I am grateful for the support, direction and encouragement I have received throughout my degree from you and know that you have made me a better scientist, student and presenter. I could not have chosen a better lab or environment to work in and know that I have had amazing experiences in my three years in your lab, so thank you.

Thank you also to my committee members, Dr. James Stafford and Dr. Jim Smiley for your guidance. To Dr. Miodrag Belosevic for both your time and your constructive feedback. Thank you to Dr. Brad Magor for your expertise in cell culture and for the use of your equipment.

Domingo, thank you for your guidance in planning experiments and the motivation you provided me with. Megan, although I only overlapped for a short period of time, I cherish that time and connection and your help and confidence in me that I sometimes lacked. Thank you for being you, and being me, all at the same time. Ximena, for being so generous with your technical skills and for your friendship, I thank you. Hillary and Kristina, you were both supportive in times of need and willing to help whenever I needed it. Thank you for all the good times, you both made grad school fun. Thank you to Laura, Graham, Bianca, and Michelle for your friendship and support. Finally, I would like to thank and acknowledge all the members of the K. Magor lab, past and present and from the ether of BioSci - Brittany, Herman, Emmanuel and Barb I have learned so much from each and every one of you. And thank you to everyone at CanBiocin. Without the training and exposure I received, and continue to receive, from the company and everyone involved, I would not have pursued graduate studies.

Thank you to my funding sources, NSERC for funding this work, Alberta Innovates Technology Futures, the department, the GSA and FGSR for the financial support in completion of this degree.

Finally, and perhaps most profoundly, I would like to thank my family; both blood and chosen. Thank you Mum for being a pillar of strength and constancy and for trying to keep me sane and grounded throughout this endeavour. And thank you Mum for the ongoing encouragement, pride and for embracing my need for furry companions. Thanks to my sister, Amanda for the laughs and for listening. To Aunt Mary for her belief and support and the reminders of how proud Uncle Eric would have been. To my adopted families; Christina, Amy (and all the Pura and Higgins family) and Erin. Under no circumstance could I have made it through this without you three.

Table of Contents

List of Tables

List of Figures

Abbreviations

abqPCR	Absolute quantification real-time PCR
AP-1	Activator protein 1 (a.k.a. C-Jun)
B30.2	Alternate name for PRY/SPRY domain (see below)
BC500	A/mallard/British Columbia/500/05 (H5N2)
BLAST	Basic local alignment search tool
BTN(-L)	Butyrophilin
BR	B30.2-related gene
BSA	Bovine serum albumin
C-I to C-XI	Categories 1 through 11
cDNA	Complementary DNA
ChIFN-2	chicken IFN-β
CDS	Coding sequence
d2CARD	Duck two tandem caspase-recruitment domains
DF1	Chicken embryonic fibroblast cell line
DNA	Deoxyribonucleic acid
dpi	Days post infection
EST	Expressed sequence tag
FML	Familial murine leukemia
GAPDH	Glyceraldehyde 3-phosphate dehydrogenase
GST-I	Glutathione S-transferase 1
HIV	Human immunodeficiency virus
IAV	Influenza A virus
IκB	Inhibitor of NFκB
IKKα/β/ε	IκB kinase family alpha/beta/epsilon

IFN-β	Interferon-beta (ch – chicken)
MEFV	Mediterranean fever protein
MHC	Major histocompatibility complex/loci
MX1	Myxovirus resistance gene 1(ch – chicken)
NCBI	National Centre for Biotechnology
NFκB	Nuclear factor kappa-light-chain-enhancer of activated B cells
ORF	Open reading frame
PAMP	Pathogen associated molecular pattern
PCR	Polymerase chain reaction
PML	Promyelocytic leukemia protein (a.k.a. TRIM19)
PRR	Pattern recognition receptor
PRY/SPRY	Preryanodine spore lysis A/ryanodine receptor domain
PT	Post-transfection
qPCR	Quantitative real-time polymerase chain reaction
RBCC	RING, B-box and coiled-coil
RFP	Ret-finger protein (a.k.a. human TRIM27)
RNA	Ribonucleic acid
RIG-I	Retinoic acid-inducible gene 1
RING	Really interesting new gene
RT-PCR	Reverse transcription-polymerase chain reaction
SNPs	Single nucleotide polymorphisms
SSH	Suppressive subtractive hybridization
SUMO	Small ubiquitin-like modifier
TRAF	Tumor necrosis factor receptor associated factor family
TRIM	Tripartite-motif family
TRIM5α(rh)	Tripartite-motif protein 5 alpha (rhesus monkey)

UBE2	Ubiquitin-conjugating enzymes E2 family
VN1203	A/Viet Nam/1203/04 (H5N1)
WCL	Whole cell lysate

Chapter 1. INTRODUCTION

1.1 Overview

The tripartite-motif (TRIM) family is a recently discovered protein family. Some members of the TRIM family have direct roles in antiviral restriction of important human pathogens like human immunodeficiency virus (HIV) (Keckesova *et al.* 2004; Stremlau *et al.* 2004; Barr *et al.* 2008). Although this direct restriction is of great interest, TRIM proteins also have diverse roles in modulating the intracellular immune responses (Kawai & Akira 2011; Uchil *et al.* 2013; Versteeg *et al.* 2013). Interestingly, the TRIM family appears to be rapidly evolving (Sawyer *et al.* 2007; Sardiello *et al.* 2008) and both the repertoire of TRIMs (Boudinot *et al.* 2011; Marin 2012) and the functional roles TRIMs play are often species-specific (Stremlau *et al.* 2004; Stremlau 2005; Taylor *et al.* 2011). Species-specific antiviral TRIMs are often found in organisms that are the natural host of a virus due to coevolution of virus and host; examples of species-specific restriction include HIV by TRIM5α in old world monkeys (Stremlau *et al.* 2004; Stremlau 2005) and tick borne encephalitis virus by TRIM79α in mice (Taylor *et al.* 2011). Co-evolution of viruses and their preferred, or reservoir, host species is a balancing act between viral replication strategies and host immune responses.

Ducks (*Anas platyrhynchos*) are the reservoir hosts of influenza A virus (IAV) (Kim *et al.* 2009). The balancing act between the virus pathogenesis and reservoir host immune response is clear in the context of the duck and IAV relationship. Highly pathogenic IAV strains, that will cause great pathology and rapid death in other birds – like members of the Galliformes order, chickens (*Gallus gallus*) and turkeys (*Meleagris gallopavo*) – have limited to no observable pathology in ducks (Mundt *et al.* 2009).

Ducks, and other wild waterfowl, harbor all serotypes of IAV (Webster *et al.* 1992) and the virus often replicates asymptomatically in the intestines which will readily shed into the environment (Kim *et al.* 2009). The differential susceptibility of ducks and chickens demonstrates co-evolution in host organisms, and thus will drive changes not only in the virus replication strategies, but in the intracellular immune responses and immune arsenal of the host organism.

Previous studies have demonstrated that chickens lack an essential component of the IAV intracellular cytoplasmic viral detection system, retinoic acid-inducible gene I (RIG-I) (Barber *et al.* 2010), which may contribute to the observed pathology differences between ducks and chickens during an IAV infection. The RIG-I bioset, or antiviral intracellular immune gene repertoire, that is turned on in IAV infected ducks will help to control the infection and the pathology associated with immune reactions to IAV (Kobasa *et al.* 2007); this response will be lacking in chickens due to the absence of RIG-I. As such, what is likely contributing to the successful responses of ducks to IAV are the rapid and robust innate immune responses initiated shortly after infection.

Elucidating the IAV relevant innate antiviral genes is the first step in narrowing the field of candidate duck and IAV specific TRIMs. Previously, suppressive subtractive hybridization (Vanderven *et al.* 2012), a microarray approach (Barber *et al.* 2013) and 454 deep sequencing has unearthed a large number of potential, differentially expressed candidate genes, among which are differentially expressed *TRIM* genes. As lung is the predominant site of highly pathogenic IAV replication, a suppressive subtractive hybridization (SSH) approach demonstrated key differentially expressed genes in infected duck lung (Vanderven *et al.* 2012); a minor component of these identified genes were members of the TRIM family. A chicken cell microarray approach that was used to determine the duck RIG-I bioset also identified a number of candidate immune relevant

TRIMs, results not shown (Barber *et al.* 2013). These approaches however would not clearly expose species-specific duck TRIM(s) nor did they clearly convey the repertoire of the duck TRIM family. As repertoires and functionality of TRIMs are often species-specific, our goal was to use the newly available draft duck genome sequence to determine what TRIMs ducks have and compare it to the available genomes of chickens and turkeys. I determined that ducks have a unique TRIM (which is absent in chickens) in their immune arsenal. Here, I show that ducks possess a duplicated immunomodulatory *TRIM* gene, *TRIM27.1b*, that is upregulated during highly pathogenic IAV infection, increases antiviral gene expression in a RIG-I activated cell and is absent in the chicken and the turkey genomes.

1.2 Characteristics of TRIMs and their roles in innate immunity

1.2.1 The tripartite-motif and classifications of TRIMs

The TRIMs derive their name from the conserved three part domain architecture that characterizes the family. Presence of an N-terminal tripartite-motif composed of RING-, B-box and coiled-coil domains (most stringently the B-box domain) are characteristic of the family (Nisole *et al.* 2005; Ozato 2008). An organizational paradigm has been proposed based on the N-terminal motif components and variable C-terminal domain (Ozato 2008). However, there is still debate about the accuracy and relevance of the paradigm to the family and a contrary more evolutionary based organizational paradigm has also been proposed (Marin 2012). Organization scheme based on evolutionary characteristics of the TRIMs categorizes the family into two groups (group 1 have C-terminal domains that are found in vertebrates and invertebrates, and group 2 represent TRIMs with a C-terminal PRY/SPRY (PRY/SPLa/RyR (PreRYanodine/spore

lysis A/Ryanodine) receptor domain (Ponting *et al.* 1997; Sardiello *et al.* 2008) which is only found in vertebrates). Conventionally, an organizational scheme of 11 categories (C-I to C-XI) of TRIMs classifies the family in terms of the N- and C-terminal composition (Ozato *et al.* 2008). The most immune relevant C-terminal domain is the PRY/SPRY domain (or B30.2 domain) – which often dictates protein targets and interactions – due to the largest number of immune relevant TRIMs sharing the common PRY/SPRY C-terminal architecture.

1.2.2 Functional implications of the RING domain as an E3-ligase

Beginning at the N-terminus, the RING (or, really interesting new gene) domain predominates in the TRIM family. RING domains, which confer the general ability of TRIM proteins to possess E3-ligase abilities, are ubiquitous in the human genome; RING domains are found in the TRIM family (Meroni & Diez-Roux 2005), the tumor necrosis factor receptor associated factor (TRAF) family (Song & Donner 1995) and many other proteins. The presence of RING domains is conserved across vertebrates and invertebrates including cnidarians, nematodes and arthropods (Marin 2012). Interestingly, the RING domains of TRIM and TRAF families have been shown recently to have an early evolutionary link (Marin 2012). TRAF family members are adaptor components of immune signaling cascades (Ware 2011), apoptosis (Micheau & Tschopp 2003) and cytokine signaling (Inoue *et al.* 2000; Lamothe *et al.* 2008). As such, it is very interesting that the RING domain of TRIMs share a common origin with the TRAFs as immune signaling roles have been associated with a number of TRIM proteins (Kawai & Akira 2011; McNab *et al.* 2011; Versteeg *et al.* 2013).

For some TRIMs, RING domains are dispensable; in the case of C-IV members TRIM14, -16, -20, -51, -70 and -1L and C-VI member TRIM66 (Versteeg *et al.* 2013). The best characterized function of the RING domain in TRIM dependent E3-ligase

activity is TRIM25 (Gack *et al.* 2007) which will be discussed in greater detail below (section 1.3). Ubiquitination is a cellular process that modifies target proteins through conjugating one or more ubiquitin moieties to proteins which can result in altered function of the target or degradation by the proteasome. Ubiquitination is a step-wise process that requires three different proteins including the E1-, E2- and E3-ligase (Deshaies & Joazeiro 2009). E1-ligases are the ubiquitin-activating enzymes, which provide ubiquitin-conjugating E2-ligases with ubiquitin which is transferred to the ubiquitin-ligating E3-ligases. E3-ligases are responsible for transferring the ubiquitin moiety to the target and dictate direct interactions with the target protein. Indeed a large array of interactions of TRIM family members with cognate E2-ligases has been elucidated (Napolitano *et al.* 2011) including notable TRIMs such as TRIM27 association with UBE2 E2-ligase enzymes although no functional relationship for TRIM27 ubiquitinylation has been elucidated which will be discussed in detail below.

Ubiquitinylation is not the only modification ability attributed to the TRIMs. SUMOylation is similar to the ubiquitination process but instead of ubiquitin, another protein is conjugated to the target protein, small ubiquitin-like modifier or SUMO. Human TRIM19 (or Promyelocytic leukemia factor, PML) and TRIM27 (Chu & Yang 2011) have been shown to associate with SUMOylating E2-ligases. Additionally, TRIM27 has been observed to induce apoptosis through the N-terminal RBCC motif (Dho & Kwon 2003).

1.2.3 Protein-protein interactions can be mediated by the B-box and coiled-coil domains

The least well characterized motif within the TRIM family is also the most defining feature of the group. The B-box domain is found in all TRIM proteins (Ozato *et al.* 2008) and is unique to the TRIM family. There may be a single B-box domain (B-box

2) within a TRIM protein or there may be tandem B-box domains (B-box 1 and B-box 2), but B-box 2 is always present (Reymond *et al.* 2001). Outside of self-association very little is known about the function of the B-box domain (Ganser-Pornillos *et al.* 2011) and protein-protein interactions (Li *et al.* 2007). Aside from the self-associations, the B-box domain has been implicated in binding specificity to HIV viral capsid by TRIM5α (Li & Sodroski 2008). Coiled-coil domains are also responsible for protein-protein interactions and function in homo- and hetero multimerization (Bell *et al.* 2012).

1.2.4 Immune relevance of the C-terminal PRY/SPRY (B30.2) domain

There are a wide variety of C-terminal domains described for members of the TRIM family, but perhaps the best characterized domain, and immune relevant, in the TRIM family is the PRY/SPRY domain. Often, the difference between a SPRY and B30.2 (or PRY/SPRY domains) is unclear and the terms are often used interchangeably, but the two domains denote key structural differences. SPRY are C-terminal domains that are found in a wide variety of species and have an ancient evolutionary origin as they are found in vertebrates and invertebrates (Rhodes *et al.* 2005). PRY/SPRY (or B30.2) domains are only found in vertebrates and are a more recent evolutionary domain found in organisms with an adaptive immune system (D'Cruz *et al.* 2013). SPRY and B30.2 domains are found in a wide variety of protein families (11 have been characterized) (Rhodes *et al.* 2005). The most notable members of the SPRY or B30.2 families are the TRIMs and the butyrophilin (BTNs). Recently, the BTNs and BTN-like gene family have been shown to be rapidly expanding in ducks and have been determined to be relevant in innate immune responses to highly pathogenic IAV infections in ducks (Huang *et al.* 2013).

PRY domains, a component of the PRY/SPRY domain, is a short (approximately 50 to 60 amino acid long) domain that is found in all PRY/SPRY containing (B30.2)

proteins and is far less well characterized than the SPRY domain. There are conflicting reports and speculations on the origins of the PRY domain. It has been reported that the PRY domain evolved later (Rhodes *et al.* 2005; Perfetto *et al.* 2013) and separately in vertebrates than the ancestral SPRY domain and a contrary hypothesis is that the PRY/SPRY domain are likely ancestral and SPRY domains are divergent (Woo *et al.* 2006). However, polymorphisms in both PRY and SPRY domains contribute to some altered functions of TRIM proteins.

PRY/SPRY domains of TRIMs have been shown to be critical determinants of species-specific viral restriction (TRIM5α), contribute to autoimmunity (TRIM21) and to cause disorders in humans (TRIM18). Interactions of the PRY/SPRY domain of human TRIM27 have also been associated with changes in cell cycle regulation and cancers (Krutzfeldt *et al.* 2005), which will be discussed below. The best studied example of PRY/SPRY dependent TRIM functions are in human and rhesus monkey TRIM5α (TRIM5α(rh) for rhesus, the natural host of simian immunodeficiency virus). As mentioned previously, TRIM5α is the canonical antiviral TRIM and TRIM5α(rh) is effective at restricting HIV-1 replication (Stremlau *et al.* 2004; Sawyer 2005; Stremlau 2005; Stremlau *et al.* 2006). A physical interaction of TRIM5α with the HIV-1 retroviral capsid is mediated through the C-terminal PRY/SPRY domain (Stremlau *et al.* 2006) and single amino acid changes within the PRY/ SPRY (Yap 2005) confer enhanced suppression of HIV replication in old world monkeys versus human homologs (Sawyer 2005; Stremlau 2005). Although a large amount of work has determined PRY/SPRY contributions of TRIM5α(rh) to be of high importance recent work has also shown that a contributory role of the RING domain of TRIM5α to HIV restriction (Lienlaf *et al.* 2011). This not only suggests unique species-specific functions for TRIMs, but also suggests multiple roles for individual TRIMs in the context of a single viral infection.

Other TRIM proteins have an association between the PRY/SPRY domain and immune roles. Mutations in the PRY/SPRY domain of TRIM21 (also known as Ro52) contribute to development of autoimmunity and systemic lupus erythematous (James *et al.* 2010). TRIM21 is an Fc binding protein that has been hypothesized to be involved in clearing high molecular weight immune complexes during viral infection (Mallery *et al.* 2010). James *et al.* (2010) showed that the mutations in TRIM21 that are linked to development of autoimmunity. Polymorphisms in the PRY/SPRY domain of TRIM21 map to the same regions of TRIM5α that confer species-specific antiviral function. Similarly, changes in the PRY/SPRY domain of TRIM18 (also known as pyrin, MEFV (Mediterranean fever protein) and marenostrin) are associated with disease generation in familial Mediterranean fever, a spontaneous and hereditary fever disorder (Grutter *et al.* 2006; Weinert *et al.* 2009).

1.3 Intracellular detection of influenza and the intracellular immune signaling pathways

Viruses are obligate intracellular parasites that co-opt the host cell machinery to produce viral progeny. Critical to a successful antiviral response is recognition of pathogen associated molecular patterns (PAMPs) by extracellular, intracellular and endosomal pattern recognition receptors (PRRs). PRRs will initiate signaling cascades which culminate in induction of an antiviral state in the infected cells and surrounding tissues. The type of PAMP, and therefore the PRRs that respond to available ligands, will depend on the virus and pathogen type that is infecting the cells.

Influenza is a single stranded (ss) segmented negative sense RNA virus of the family *Orthomyxoviridae*. Detection of IAV in an infected cell is mediated through two major PRR systems; the toll-like receptors (in ducks, primarily TLR 3 and 7 as ducks

lack TRL8 (MacDonald *et al.* 2008)) and the retinoic acid inducible gene 1-like receptors (RIG-I (Yoneyama *et al.* 2004) and MDA5 (Kato *et al.* 2006)). Replication of IAV will result in rapid and robust innate immune responses in ducks. Detection will culminate in the production of type I interferons (primarily IFN-β and IFN-α), interferon stimulated antiviral genes (ISGs) under control of the interferon regulatory factor (IRF) family (these pathways are nicely and concisely reviewed in (Randall & Goodbourn 2008)). Extensive work has gone into elucidating the effectors, or ISGs, that are turned on when ducks are infected with IAV. This will be discussed in greater detail below.

1.3.1 Signaling components downstream of RIG-I and TLR7 PAMP recognition

Signaling through PRRs follows a well characterized cascade of adapters, phosphorylation and ubiquitination steps. As signaling components in the RIG-I and TLR cascade have been shown to interact with members of the TRIM family (Zha *et al.* 2006), and TRIMs have been shown to alter responses of promoters downstream of these pathways (Versteeg *et al.* 2013), it important to review the pathway and to highlight some of the key players that will be discussed further below. The most important pathway for this work and for susceptibility to influenza infection (Kato *et al.* 2006) is RIG-I that detects virally derived 5'-triphosphate single stranded RNA (Hornung *et al.* 2006). Once bound to the ligand, the two tandem caspase recruitment domains (CARD) (Glusman *et al.* 2000) domains of RIG-I are ubiquitinated by TRIM25 through the E3-ligase activity of the RING domain (Gack *et al.* 2007). Ubiquitinated (Ub) CARD domains then interact with an adapter protein IPS-1 (also known as MAVS, VISA and Cardif) (Kawai *et al.* 2005; Seth *et al.* 2005; Kumar *et al.* 2006) which translocate to the mitochondria via actin trafficking (Ohman *et al.* 2009). RIG-I and another member of the RIG-I-like receptor family, Melanoma Differentiation-Associated protein 5 (MDA5) signal through the same downstream pathway converging at mitochondrial IPS-1; the IPS-1 downstream

pathway is intact in both ducks and chickens (Barber *et al.* 2010) as chickens can respond through MDA5, although MDA5 contribution to IAV responses appears to be minor in comparison to RIG-I (Kato *et al.* 2006). It is also important to point out that the function of the two tandem CARD domains of human (Glusman *et al.* 2000) and duck (Miranzo-Navarro *et al.* unpublished) RIG-I can function in this signaling cascade independent of the regulatory and RNA binding N-terminal domain. I use a constitutively active duck 2 tandem CARD (d2CARD) domain construct in this study (Miranzo-Navarro *et al.* unpublished).

At the point of mitochondrially located RIG-I/ssRNA/Ub/IPS-1, there are two arms of signaling that diverge; both are mediated by members of the TRAF family (TRAF3 for the IRF pathway and TRAF6 for the NFκB pathway). The RIG-I signal is potentiated through a number of different components including NF-kappa-B essential modulator (NEMO, also known as IKK-γ) and two canonical members of the IκB kinase family (IKK-α and IKK-β). IKKs will phosphorylate the inhibitor of NFκB (IκB) which is subsequently ubiquitinated and degraded. With removal of IκB, the nuclear localization signal of nuclear factor of kappa light polypeptide gene enhancer in B-cells 1 (NFκB) is exposed and translocation of NFκB to the nucleus ensues. NFκB is a transcriptional regulator that will, in combination with phosphorylated IRF family members (see below), drive the production of type I interferons (IFN-β and IFN-α) which will activate an antiviral state in an autocrine and paracrine fashion and turn on IRF-1, -7 and -9 (Kamijo *et al.* 1993; Kawakami *et al.* 1995; Sato *et al.* 1998; Sato *et al.* 1998; Sato *et al.* 2000).

The second arm of signaling that is activated by RIG-I/ssRNA/Ub/IPS-1 mitochondrion localization is through the TRAF6 dependent IRF7 activation. In ducks, and chickens no IRF3 homolog has been identified (Cormican *et al.* 2009; Huang *et al.* 2010), it is suspected that IRF7 provides redundancy and takes over the role of IRF3 that

is observed in humans (Magor *et al.* 2013). Another member of the IKK family (IKK-ε) is involved in recruiting interleukin-1 receptor-associated kinase 1 (IRAK-1) and subsequent phosphorylation of avian IRF7 (in humans, this would be IRF3) which can feedback on the type I interferon production and stimulate production of ISGs through interferon stimulation response elements (ISREs).

Subsets of toll-like receptors (TLRs) are responsible for detecting viral PAMPs. TLR3 detects ssRNA and dsRNA and is located in the endosome (Alexopoulou *et al.* 2001); as such, TRL3 will recognize IAV viral genomic ssRNA when the virion uncoats in the acidifying endosome. TRL7 will recognize ssRNA (Lund *et al.* 2004) and TLR9 recognizes CpG DNA of bacterial origin (Hemmi *et al.* 2001) (which is not directly relevant to IAV infection). TLR3 and TLR7 signal through two different primary adapters. TLR3 uses TIR domain-containing adapter protein inducing IFN-β (TRIF) where TLR7 uses the myeloid differentiation primary response 88 (MyD88) adaptor. The pathways converge on signaling components shared in the RIG-I pathway, but culminate in activation of IRF-3 (for TLR3, in avian species it would be IRF7) and IRF-7 (for TLR7), predominantly. TLR7 signaling through TRAF6 will follow the same general cascade of interactions previously outlined above which include NEMO/IKKα/IKKβ phosphorylation of IκB and nuclear translocation of NFκB. It is important to note that there is intricate cross talk in all signaling cascades and stimulation of multiple transcription factors during an infection will occur more as a network than a linear cascade.

TLR3 signaling through TRIF will predominantly stimulate IRF3 activation in humans, and is predicted to culminate in avian IRF7 activation. When TRL3 recognizes viral RNA (be it ssRNA or dsRNA) TRIF associates with the cytoplasmic Toll IL-1 receptor (TIR) domain to initiate the signaling cascade. TRAF3 association with TRIF

will perpetuate the signal down the IRF3 (human) or IRF7 arm (avian) of the pathway. TRAF3 will associate with TRAF family member-associated NFκB activator (TANK) and will subsequently recruit a kinase, TANK-binding kinase 1 (TBK-1). This association recruits another non-canonical member of the IKK family, IKKε, which will directly phosphorylate IRF3 (in humans) and is assumed to be IRF7 (avian).

Cross talk is also observed between IKK family members in the TRIF, MyD88 and NFκB pathways (Clark *et al.* 2011). And members of IKKs from TLR3 and RIG-I/TLR7 signaling cascades interact directly with human TRIM27 (Zha *et al.* 2006), which will be discussed in greater detail below. Although it is easiest to pictographically represent and talk about signaling cascades as linear and predictable, they are a complex network of interactions dictated from multiple PRR based recognition of different ligands within a single infection. Interplay between different cascades converge and cross-talk with each other in order to fine-tune intracellular responses. Since I focus on the RIG-I dependent signaling cascade the contributions of the TLR component is represented (Figure 1-2) by an ambiguous endosomal TLR.

1.3.2 The importance of RIG-I in differential susceptibility

Genetic susceptibility in humans to IAV infection has been hypothesized based on familial relationships in highly pathogenic IAV (H5N1) deaths (Zhang *et al.* 2009; Horby *et al.* 2012) but the breadth of knowledge of IAV susceptibility comes from animal models (Trowsdale & Parham 2004; Kato *et al.* 2006; Kobasa *et al.* 2007). Early, robust and effective innate immune responses to IAV are of paramount importance to controlling IAV replication and pathology (Baskin *et al.* 2009) which can also be detrimental to the host in highly pathogenic infections (Kobasa *et al.* 2007). Although the determinants of susceptibility to death by IAV, and conversely control of IAV pathology observed in ducks, likely is the result of interplay in the network of multi-gene and virally

determined responses, RIG-I detection plays an integral role during IAV infection and other RNA viral infections (Trowsdale & Parham 2004). Loo *et al.* (2008) demonstrate that mouse cells deficient in the cytoplasmic receptor RIG-I will experience increased pathology during IAV infection and ISGs downstream of RIG-I will be all but absent. RIG-I recognition and subsequent activation of intracellular signaling cascades is also integral in survival of mice infected with other RNA viruses (Kato *et al.* 2006). Differential susceptibility of ducks and chicken to IAV infection is also likely a concerted network of host and virus dependent mechanisms.

Chickens are highly susceptible to highly pathogenic IAV infection (predominantly H5 and H7 subtypes of IAV) and will die rapidly when little pathology is observable in ducks (Kim *et al.* 2009; Pantin-Jackwood & Swayne 2009). Differential susceptibility of chickens to IAV is not predicated on the replication of the virus in developing pathology (Morales *et al.* 2009) and therefore likely is contributed by either the host dependent detrimental immune responses, as was demonstrated in macaques (Kobasa *et al.* 2007), or because of a lack of IAV detection and response in chickens as indicated by the absence of RIG-I (Barber *et al.* 2010) which has been shown to be detrimental to RNA viral responses in mice (Kato *et al.* 2006). Previously, duck RIG-I has been shown to activate robust innate immune responses in chicken cells (Barber *et al.* 2013), which lack endogenous RIG-I (Barber *et al.* 2010), and stimulate production of the RIG-I bioset in chicken cells which will be discussed below. However, one locus will not likely confer general susceptibility nor resistance.

1.3.3 The RIG-I bioset in ducks and the antiviral program during IAV infection

As chickens lack endogenous RIG-I, this provided a clear and extremely valuable way to elucidate genes under control of the RIG-I receptor termed the RIG-I bioset. This diverse set of genes has been the focus of ongoing research in our lab and overlap

between RIG-I bioset is observed through microarray analysis of transfected chicken cells (Barber *et al.* 2013) and tissue RNA expression profiles of ducks infected with IAV (Vanderven *et al.* 2012). Infection of ducks with highly pathogenic IAV results in massive increases in expression levels of key antiviral ISGs after only 24 hours of infection (Vanderven *et al.* 2012). Robust innate immune responses are short lived but profound, generally tapering off by 3 days post infection (dpi). Expression of immune relevant genes like *MHC class I*, *OASL* and *ISG12* were observed during the SSH screen (Vanderven *et al.* 2012). Previously, *RIG-I* was observed to be dramatically upregulated in duck lung tissue at 1 dpi with a highly pathogenic IAV isolate which suggests a strong association with early innate immune response of ducks to IAV (Barber *et al.* 2010). Three previously known IAV responsive RIG-I genes (Trowsdale & Parham 2004) were shown to be upregulated in RIG-I transfected chicken cells infected with IAV (Barber *et al.* 2010); *protein kinase R* (*PKR*), *myxovirus resistance gene 1* (*MX1*) and *IFN-β*. The recent microarray analysis of infected chicken cells has confirmed the relevance of these genes and others in the avian innate immune responses to IAV (Barber *et al.* 2013) including members of the IFIT family, chemokines, TLR3, and members of the IRF family. It is important to note here that although *MX1* in mice has been shown to play an integral role in highly pathogenic IAV infection by decreasing pathology and increasing survival of mice expressing murine MX1 (Salomon *et al.* 2007). Interestingly, chicken *MX1* does not appear to have the same protective effects as murine MX1 (Bernasconi *et al.* 1995) even though *MX1* expression is upregulated in RIG-I transfected chicken cells (Barber *et al.* 2010). Additionally, although ducks upregulate expression of their *MX1* gene upon infection with both low and highly pathogenic IAV(Barber *et al.* 2013), like chicken, duck *MX1* has also been shown to lack the protective effect (Bazzigher *et al.* 1993) that mouse *MX1* confers during influenza infection (Bernasconi *et al.* 1995). When

avian cell lines were transfected with the duck derived *MX1* gene, no enhanced resistance to IAV was observed (Bazzigher *et al.* 1993). In the diverse range of important ISGs in the RIG-I bioset that have been elucidated, members of *TRIM* family are among some of the less profound contributors.

1.4 TRIMs and innate immune pathways

It is becoming more and more apparent that a large number of TRIMs are contributing to not only to direct viral restriction but innate immune signaling. A comprehensive review of all immunomodulatory TRIMs is outside of the scope of this work, but has been reviewed recently and thoroughly (Kawai & Akira 2011). Mentioned previously, are TRIM21, and TRIM18. TRIM23 has also been shown to be essential for antiviral defense and to be a SUMOylating E3-ligase (Arimoto *et al.* 2010). In recent months, two very thorough examinations of the innate immune signaling contributions have been published that outline signaling capabilities of much of the human TRIM repertoire using luciferase reporter assays and canonical promoters of NFκB, AP-1 and IFN-β, ISREs and NFκB (Uchil *et al.* 2013; Versteeg *et al.* 2013). Some TRIMs examined in these works are even capable of directly affecting promoter activity in the absence of a previously activated pathway. Direct signaling modulation through NFκB has been observed for TRIM1, -5, -8, -13, -25, -32, and -62 (Uchil *et al.* 2013). Direct signaling has also been observed for the Akt dependent transcription factor AP-1. TRIMs that influence AP-1 signaling directly include TRIM1, -5, -14, -15, -21, -22, -25, -31, -32, and -62 (Uchil *et al.* 2013). However, TRIMs may also play immunomodulatory roles in cells were the antiviral signaling cascade is active. I will focus on the known immunomodulatory roles for TRIMs relevant to this work below.

1.4.1 TRIM25 is integral to RIG-I signaling

As mentioned previously, the cytoplasmic RNA sensor RIG-I requires ubiquitination of the two tandem CARD domains in order to become active (Glusman *et al.* 2000). In addition to the TRIM25 ubiquitination, RIG-I activation can also be attributed to modification by RING finger protein 135 (RNF135/Riplet), independent of TRIM25 (Oshiumi *et al.* 2009; Oshiumi *et al.* 2010; Oshiumi *et al.* 2012). RIG-I activation through unlinked polyubiquitin chains (Jiang *et al.* 2012) has also been observed. Currently, the E3-ligase activity of TRIM25 is the best understood mechanism of activation of RIG-I (Gack *et al.* 2007). The RING domain of TRIM25 is responsible for the activation and has been shown to be indispensable to activation (Glusman *et al.* 2000). Interestingly, IAV NS1 protein, the primary virulence factor of influenza, specifically targets TRIM25 and interferes with its ability to ubiquitinate RIG-I (Gack *et al.* 2009; Rajsbaum *et al.* 2012). Targeting of TRIM25 by NS1 likely confers an advantage to IAV replication, and therefore indicates relevance of the RIG-I pathway in IAV infection. As such, the role TRIM25 plays in innate immune signaling pathways is integral to detection of IAV infection. Interestingly, the contribution of TRIM25 to RIG-I activation is not its only role. Mouse TRIM25 over expression is also directly restrictive to release of HIV from infected cells (Uchil *et al.* 2008). In the same study, human TRIM25 had the opposite effect on HIV release, where silencing of the endogenous TRIM25 in human cells actually depressed HIV release. TRIMs, therefore, can have many faces and roles in intracellular responses to viral pathogens.

1.4.2 TRIM19/PML is a transcriptional modifier that localizes to nuclear bodies

A number of TRIM family members were originally identified because of a link to development of cancer or human disease. TRIM19 or promyelocytic leukemia factor (PML) is one of those TRIMs. TRIM19 is a TRIM protein family member of the C-V

group, and has the characteristic N-terminal RBCC motif, but does not possess a C-terminal PRY/SPRY domain (Ozato 2008). Blastp analysis of human TRIM19 shows homology in the C-terminus to a DUF3583 domain, which has unknown function, and an exonuclease domain. TRIM19 localizes to peri-nuclear punctate foci in healthy cells termed nuclear bodies (NBs, also known as PML bodies) (Dyck *et al.* 1994) and was originally characterized due to the associated NB disruption observed in acute promyelocytic leukemia (De Thé *et al.* 1990). TRIM19 is not oncogenic by itself, but fusion with retinoic acid receptor alpha (RARα) results in oncogenic activity characterized by aberrant cytoplasmic localization of TRIM19 outside of the NBs (De Thé *et al.* 1990). TRIM19 is also interferon inducible and confers enhanced resistance to infection to negative sense ssRNA viruses (IAV and vesicular stomatitis virus) through the coiled-coil domain, but conferred no resistance to a positive sense ssRNA virus (encephalomyocarditis virus (EMCV)) (Chelbi-Alix *et al.* 1998). Direct viral restriction of murine leukemia virus (MLV) by release inhibition has also been observed for both human and mouse TRIM19, although no observed change in replication in viral transcript was observed (Uchil *et al.* 2008). TRIM19 is a tumor repressor in healthy cells that is dependent on functions of the RING domain (Le *et al.* 1996) and will induce apoptosis through the same RING domain (Borden *et al.* 1997; Wang *et al.* 1998). The pro-apoptotic effects of TRIM19 can be attributed in part to the interactions with the NFκB survival pathway. TRIM19 has been shown to interact with NFκB subunits downstream of the IκB inhibitors to decrease anti-apoptotic signals and shift the balance in the cell towards caspase-dependent apoptosis (Wu 2003). Interestingly, the authors showed co-localization of TRIM19 and the p65 NFκB subunit into NBs. This suggests that NBs are important organizational centers and have roles in cell cycle, and signaling regulation. Contrary to previous data suggesting a role of the RING domain in apoptosis, Wu *et al.*

(2003) show that the interaction between TRIM19 and p65 subunit of NFκB is through the C-terminal domain. Interestingly, TRIM27, or Ret-finger protein (RFP) co-localizes with TRIM19 in NBs in normal cells and follows the same aberrant distribution in cancer cells (Cao *et al.* 1998). Early studies on TRIM locations within the cells identified a physical hetero-multimerization ability of TRIM19 and TRIM27 (Reymond *et al.* 2001) and co-localization of TRIM19 and TRIM27 in NBs is dependent on a physical interaction between N-terminal B-Box and coiled-coil domains (Cao *et al.* 1998). Interactions between TRIM27 and immune signaling pathways will be discussed in greater detail below.

1.4.3 TRIM14 is a newly identified signaling component of AP-1

There is very little known about the biological roles of TRIM14. Previous data from 454 deep sequencing suggested that TRIM14 may be relevant to IAV responses as a statistically significant increase in expression of the predicted duck TRIM14 transcript was observed in highly pathogenic IAV lung tissue (Table A-1). Human TRIM14 localizes to discrete cytoplasmic bodies (Reymond *et al.* 2001), and has been reported to increase expression levels in autoimmune disease (Sjöstrand *et al.* 2012). There is also a putative association with a developmental disorder, and it has been predicted to be one of a number of loci of interest in cleft palate development (Vieira *et al.* 2008). TRIM14 has also been recently identified as having a role in restriction of hepatitis C virus (HCV), where over expression of human TRIM14 decreases HCV replication (Metz *et al.* 2012).

1.5 The TRIMs, the MHC and evolution

The major histocompatibility complex (MHC) is the foremost immune centre of the genome. It is rapidly evolving and large numbers of gene families are located in this

region. In humans, the MHC is located on chromosome 6, mouse on chromosome 17, and in chickens on microchromosome 16 (National Centre of Biotechnology Information, National Library of Medicine). In the MHC locus, large expanded gene families are located including the HLA family in humans (in mice it is the H-2 and chickens the BF/BL) of MHC class I and class II genes, members of the olfactory receptor family, members of the tumor necrosis factor family, butyrophilin family and TRIM family (Horton *et al.* 2004).

The MHC is a rapidly evolving region of the genome for a number of reasons. Primarily, the MHC locus is the region that encodes the class I antigen presentation gene, or MHC class I genes, which are integral to the adaptive immune system of vertebrates and which are highly polymorphic (Trowsdale & Parham 2004) due, in part, to selective pressure of pathogens. In addition, members of the rapidly changing olfactory receptor family are located in this region in mammals (Gruen & Weissman 1997; Niimura & Nei 2007). MHC and olfaction has been associated with detection of related kin and unrelated mate selection in mammals and is therefore subject of intense selective pressures (Milinski *et al.* 2005; Chaix *et al.* 2008). As the MHC has the highest concentration of immune genes of any other location in the genome, genes residing within this locus will likely be subject to selective pressures resulting from changes in the other genes of the locus and indicate a potential role in immunity.

Segmental duplication events which elaborate species-specific repertoire is not uncommon to this locus. In humans, the TRIM rich region lies telomeric to the MHC class I genes, and there is a concentration of 8 TRIM genes in the human MHC (Meyer *et al.* 2003). In keeping with the theme of rapid evolution of genes in the MHC locus, expansion of the TRIM family, both located within the MHC and outside of the MHC locus, is unique to each species and species-specific gene duplications are often observed

(Ando *et al.* 2005; Sawyer *et al.* 2007; Tareen *et al.* 2009; Boudinot *et al.* 2011). The mouse TRIM repertoire has many murine specific TRIMs; TRIM12 is murine specific (Tareen *et al.* 2009) and implicated in IAV resistance (Boon *et al.* 2009) and TRIM79α which is restrictive to tick borne encephalitis virus (TBEV) (Taylor *et al.* 2011) and absent from the human repertoire. The mouse has a particularly robust region of species-specific TRIM5α expansion, and although not located in the MHC, this is a clear example of recent mammalian TRIM family duplication (Tareen *et al.* 2009). Compared to the human TRIM5α locus (which encodes four TRIM genes and one TRIM-like pseudo gene), the murine locus has dramatically expanded to 12 paralogous TRIMs (or partial TRIMs) originating from the homolog of human TRIM5α, one of which is IAV resistance marker TRIM12, as mentioned above. Indeed this same TRIM5 locus has expanded dramatically in cows where in dogs, the TRIM5 locus has contracted (Sawyer *et al.* 2007).

Aside from species-specific duplications, the TRIM family members that are rapidly evolving are evolutionarily younger TRIMs that contain the PRY/SPRY domains (or B30.2) and, as discussed previously, are only found in vertebrates with an adaptive immune system. A very thorough evolutionary study of the human TRIM repertoire has grouped the TRIM family into two groups or evolutionary clades (Sardiello *et al.* 2008); group 1 are the conserved TRIMs with highly variable C-terminal domains (including TRIM19) which are highly conserved between vertebrates and have representatives in invertebrates (Sardiello *et al.* 2008), and group 2 which are more variable, younger, characterized by the PRY/SPRY domain and are likely a reservoir for new TRIMs and for species-specific duplication events (Sardiello *et al.* 2008; van der Aa *et al.* 2009). Sardiello *et al.* (2008) examine TRIM repertoires from mammals, invertebrates, birds, and teleosts and even plants. They show that group 1 TRIMs were found to be present in

1:1 ratios in humans and mice and represent a more ancient clade, as some group 1 TRIMs are found in both vertebrates and invertebrates. Group 2 are decidedly more evolutionarily recent as only vertebrate genomes have group 2 C-terminal PRY/SPRY TRIM family members and they are species-variable. Of the group 2 TRIMs examined, only 17 of the genes are shared between the different vertebrate species (Sardiello *et al.* 2008). This clearly reinforces the need for individual species examination of the TRIM family, as no assumptions of number or function of TRIMs between species are definite.

1.5.1 The chicken and turkey MHC has TRIM rich regions

The BF/BL locus of the chicken is the homologous region to the human HLA locus (MHC). The locus itself is extremely compact, spanning only 92 kb of genomic DNA and contains the classical (MHC class I and MHC Class II) and non-classical MHC genes (Kaufman *et al.* 1999). The TRIM-rich region of the chicken MHC lies telomeric to the chicken BF/BL, MHC class I, locus (as is observed in humans) (Ruby *et al.* 2005). Originally, in the extended map of the MHC, 5 full length *TRIM* genes (TRIM 7, -39, -X (now known to be -27.2), -27 and -41) were predicted and 1 incomplete *TRIM* gene (BR, for B30.2 Related) that contains part of the coiled-coil and PRY/SPRY domains (Ruby *et al.* 2005). The map of the extended chicken MHC has since been elaborated and refined to include a variety of TRIM and non-TRIM genes, tRNAs, the MHC class I , class II and class III genes and the peptide loading machinery (Shiina 2007). Shiina *et al.* (2007) predict within the TRIM rich region of the chicken MHC a total of 7 independent *TRIM* genes, *TRIM7.2, -7.1, -39.2, -27.2, -39.1*. However, *TRIM39.1* is actually the incomplete *TRIM* corresponding to the BR locus described above (Ruby *et al.* 2005)), *-27.1* and *-41* (for a schematic, see Figure 1-1A).

The more recently elucidated turkey MHC B locus bears striking resemblance and synteny with the chicken MHC B locus (Figure 1-1B). Spanning a slightly larger

region of the turkey genome, with the same TRIM genes and conservation in the ORF directional pattern between the two galliforms (Chaves *et al.* 2009).

Currently, there is very little known about the avian TRIM genes, with only expression based work conducted thus far on a single TRIM in this locus, chicken *TRIM39.2* (ch*TRIM39.2*) (Pan *et al.* 2011). The authors refer to this gene as *TRIM39* and show that the organ where ch*TRIM39.2* is most highly expressed is in spleen, closely followed by liver. No functional work has been published on what role this chicken MHC locus encoded ch*TRIM39.2* is playing in the spleen nor if there is an immunological relevance or immunomodulatory role played by ch*TRIM39.2*. However, as the spleen is the quintessential immune organ, and the expression level of chicken *TRIM39.2* is significantly higher in the spleen than in any other organ (Pan *et al.* 2011), there may be an as yet undetermined immunological role for *TRIM39.2* in the chicken.

1.6 TRIM27/Ret finger protein (RFP)

1.6.1 TRIM27/RFP, cancer development and intracellular signaling

TRIM27 was originally identified as the C-terminal half of an oncogenic fusion protein; the RBCC motif of the human TRIM27 (huTRIM27 a.k.a. Ret-finger protein, or RFP) is fused to Ret-tyrosine kinase that causes dysregulation in cell growth (Takahashi *et al.* 1988), but our understanding of the association of human TRIM27 with different cancers and oncogenesis is unclear. Increased expression of full length, unaltered, huTRIM27 in different isolated tumor cells from colon, breast and ovarian cancers (Zoumpoulidou *et al.* 2012) coupled with the correlation of increased huTRIM27 expression in tumors that do not respond well to treatment (Horio *et al.* 2012) and invasiveness of breast cancers (Tezel *et al.* 2009) suggest an involvement of endogenous

huTRIM27 in cancer. Association of TRIM proteins in general with cancer is not surprising considering the hallmark of oncogenesis is cell cycle dysregulation; TRIMs that contribute at least in part to signaling, cell cycle regulation (Patel & Ghiselli 2005) and/or cell survival could be potential oncogenes or cancer cell markers. Although cellular locations of huTRIM27 vary greatly with the experimental cell type and origin (Morris-Desbois *et al.* 1999; Tezel *et al.* 1999; Shimono *et al.* 2000; Harbers *et al.* 2001; Matsuura *et al.* 2005; Tezel *et al.* 2009), an interesting co-localization (Cao *et al.* 1997) and interaction between huTRIM27 and huTRIM19 in PML NBs has been observed (Cao *et al.* 1998) (section 1.4.2). Perinuclear and nuclear localization of huTRIM27 has been a well-studied characteristic of huTRIM27. In fact, association of huTRIM27 and the nucleus seems intimate as huTRIM27 has been shown to interact directly with promoters and transcription factors in the nucleus (Shimono *et al.* 2003) and to have direct interactions with epigenetic transcriptional control mechanisms including DNA methylation processes (Shimono *et al.* 2000; Matsuura *et al.* 2005). Conflicting reports suggest multiple opposing roles for TRIM27 expression and cancer; whether TRIM27 speeds tumorigenesis (Zoumpoulidou *et al.* 2012) or promotes cellular apoptosis through the N-terminal domains (Dho & Kwon 2003). Although the role of TRIM27 in oncogenesis is elusive and may not be defined, there is much evidence indicating involvement.

What seems to be abundantly clear about TRIM27 is that different domains of huTRIM27 will interact with a myriad of proteins and each domain of this TRIM has been shown to have many diverse functions. TRIM27 belongs to the C-IV category of TRIMs and possesses the typical RBCC-PRY/SPRY domain architecture (Ozato *et al.* 2008). Given the association of TRIMs with E3-ligase activity (Meroni & Diez-Roux 2005), it is not surprising that TRIM27 is implicated in ubiquitination processes (Niimura

& Nei 2007; Napolitano *et al.* 2011; Hao *et al.* 2013). One study showed TRIM27 to be a promiscuous E3-ligase associating with 12 different E2-ligases, although the strengths of associations varied (Napolitano *et al.* 2011). Ubiquitinylation of TRIM27 is also increased when it associates with a group of proteins known as the MAGE family (melanoma antigen family) (Doyle *et al.* 2010) that have roles in intracellular trafficking and cancer development (Hao *et al.* 2013). TRIM27 has also been shown to function as a fairly robust SUMOylating E3-ligase (Chu & Yang 2011). HuTRIM27 also shares a pro-apoptotic role (Lee *et al.* 2013) with TRIM19 (Wu 2003). The N-terminal RBCC motif of huTRIM27 induces apoptosis when over expressed in cells (Dho & Kwon 2003) through a caspase-dependent and mitochondrial cytochrome-C release independent mechanism.

TRIM27 also has direct effects on intracellular immune signaling pathways by direct binding and ubiquitination of the intracellular PRR NOD2 (Niimura & Nei 2007). NOD2 is a members of the NOD-like receptor (NLRs) and NOD2 is specifically responsible for intracellular cytosolic detection of bacterial peptidoglycan moieties (Bonen *et al.* 2003). TRIM27 binds to NOD2 through the C-terminal PRY/SPRY domain and subsequent ubiquitination targets NOD2 for degradation (Niimura & Nei 2007). Negative regulation of signaling pathways seems to be a recurring theme with TRIM27 as recent evidence suggests a role for TRIM27 in ubiquitin-dependent negative regulation of T-cells (Cai *et al.* 2011; Srivastava *et al.* 2012).

1.6.2 Human TRIM27/RFP interacts with the IKKs to supress IFN

HuTRIM27 has been shown to interact with the inhibitor of NFκB kinase family (IKKs) (Zha *et al.* 2006). The physical interaction of huTRIM27 and members of the intracellular immune signaling pathways that are relevant to IAV responses has been shown to be immunosuppressive to a number of transcriptional response elements including NFκB, ISREs and IFN-β (see above in section 1.3). The authors show that

huTRIM27 physically interacts with IKKα, IKKβ downstream of the RIG-I pathway and IKKε and TBK-1 (TANK-binding kinase 1) which are directly involved in phosphorylating and activating IRF3 (or presumably IRF7 in avian cells). The authors focus of the IKKε association by using a yeast two-hybrid system. The C-terminal domain of huTRIM27 is responsible for the direct interaction with IKKε (and phosphorylation) indicating the PRY/SPRY domain is the integral domain in regulating this signaling pathway (Zha *et al.* 2006). The cytoplasmic retention of IKKε was also demonstrated which has an immunosuppressive response by preventing IRF3 activation and translocation to the nucleus (Figure 1-2). Although no direct evidence for cytoplasmic retention interactions with either IKKβ or IKKα were presented in this paper, the authors do demonstrate that huTRIM27 physically interacts with both IKKα and (to a greater extent) IKKβ through yeast two-hybrid screens and co-immunoprecipitations. Transcriptional repression of key immunomodulatory transcriptional response elements are inhibited by the over-expression of huTRIM27 in a dose dependent manner; including the response of IFN-β promoter activity. By interacting with IKKβ, huTRIM27 would decrease the phosphorylation of IκB and subsequent degradation which would in turn prevent NFκB translocation to the nucleus. The observation of physical interaction between huTRIM27 and members of the IKK family is central to our hypothesis (Zha *et al.* 2006). In this work, I hypothesized that one, or both, of two duck TRIM27.1 proteins may function in a similar manner to the huTRIM27 homolog to depress the intracellular antiviral pathway (Figure 1-2). In our study I employ the use of ISG production via RIG-I mediated intracellular antiviral immune responses in order to measure the interplay of our two candidate *TRIM27.1*s with the intracellular innate immune signaling pathways (Figure 1-3).

1.7 Research aims

Aim 1. To determine the duck TRIM repertoire

Using the newly available draft duck genome, I will generate a list of predicted or recognizable (containing the canonical RBCC tripartite-motif) TRIM genes. From this list I will annotate the genes located within a single locus and compare the repertoire to other available avian genomes. I will use an *in silico* approach for this and available genome analysis tools and software to generate a clear annotated genomic map of the draft duck genome. As ducks are the natural host of influenza, I will determine if ducks have any unique TRIMs that could be playing a species specific role in influenza virus infection. I will narrow the list of candidate TRIM genes through comparison of the literature and by previous data to suggest differential expression during influenza infection.

Aim 2. To examine the transcriptional profile for our TRIM genes

To determine if any of the identified candidate duck TRIMs are differentially expressed during IAV infections, I will design a number of probes and primers to look at gene expression during infection using quantitative real-time PCR (qPCR) focusing on *TRIM*s within scaffold618. I will use RNA isolated from the ducks infected with either a low pathogenic IAV (A/mallard/BC/500/05 (H5N2)) or highly pathogenic (A/Viet Nam/1203/04 (H5N1) IAV.

Aim 3. To test the candidate antiviral TRIMs for antiviral function.

I will clone the identified upregulated TRIM gene(s) into an expression vector to test by transfection. I will use a chicken cell line (embryonic fibroblasts) (because there is

no available duck cell line) to transiently transfect in the TRIM genes and measure the immunomodulatory effects of the candidate genes.

Table 1-1. Evolutionary group assignments of TRIM family members in the human repertoire.
Group 1 and group 2 assignments of *TRIM* genes according to their evolutionary properties assigned as per Sardiello *et al.* (2008).

Group Number	TRIM number	Group Number	TRIM number
1	1	2	4
	2		5
	3		6
	8		**7**
	9		10
	12		11
	13		15
	14		17
	16		20
	18		21
	19		22
	23		26
	24		**27**
	25		31
	28		34
	29		35
	32		38
	33		**39**
	36		40
	37		**41**
	42		43
	44		48
	45		49
	46		50
	47		52
	54		58
	55		60
	56		61
	59		64
	62		68
	63		72
	65		73
	66		74
	71		75

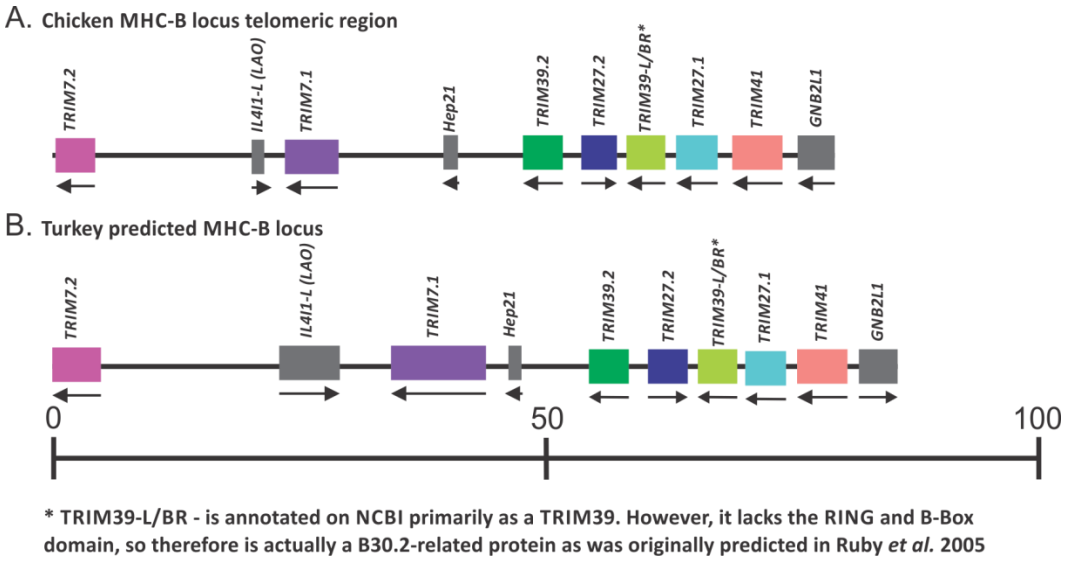

Figure 1-1. Genomic organization of the published chicken and turkey MHC locus. Scale image of the genomic organization of the (A) chicken and (B) turkey. Depicted are boxes annotating the coding region for each gene with *TRIM*s represented in colour and non-TRIM genes in the locus represented in grey. The region of representation has been scaled back from the original published loci and represents the region which is syntenic with the duck predicted MHC presented in this work. TRIMs of the same lineage are depicted in shades of the same colours. Arrows indicate direction of coding regions. The scale drawings are based on and modified from published chicken and turkey papers as NCBI does not have a complete annotation for the turkey locus (Ruby *et al.* 2005; Shiina 2007; Chaves *et al.* 2009).

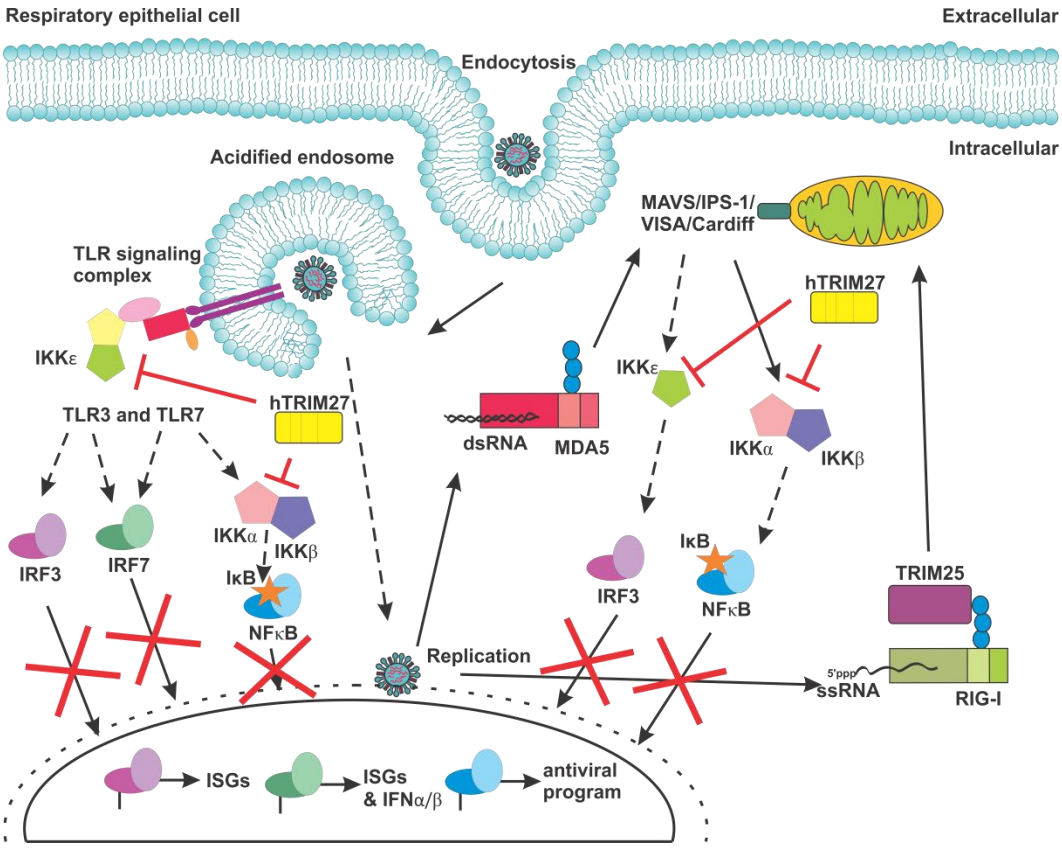

Figure 1-2. Interaction of human TRIM27 with members of the IKK family will depress the intracellular antiviral program.
Human TRIM27 has been shown to interact with canonical (IKK-α and IKK-β) and non-canonical (IKK-ε) members of the IκB Kinase (IKK) family. Interaction of TRIM27 with IKKs has been demonstrated through yeast two-hybrid system and co-immnoprecipitation studies (Zha *et al.* 2006). The interaction will decrease signaling and intracellular innate immune responses by decreasing activation and nuclear translocation of members of the interferon regulatory factor (IRFs) family of transcription factors and NFκB. Figure adapted from (Zha *et al.* 2006; Carty & Bowie 2010; Ryu *et al.* 2010; McNab *et al.* 2011; Yan & Chen 2012)

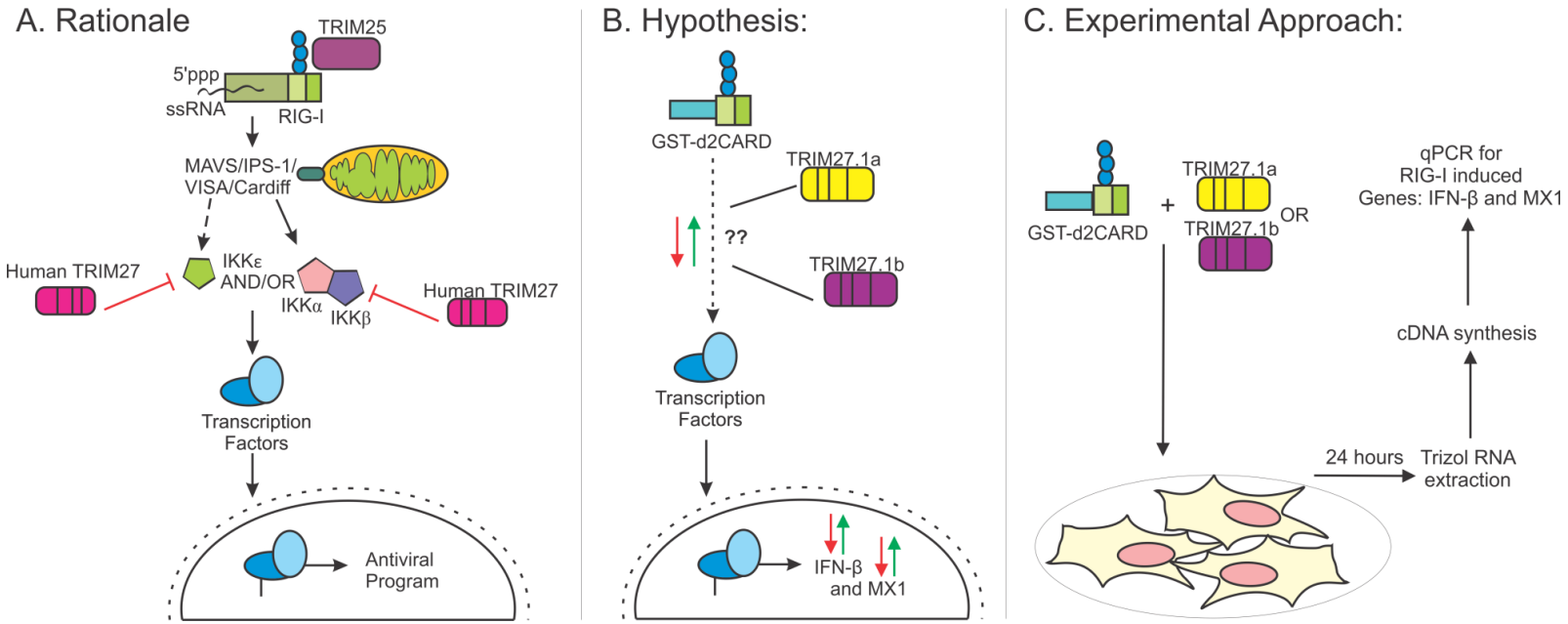

Figure 1-3. Interaction of huTRIM27 with the IKKs is the foundation for further experiments with duck *TRIM27.1a* and *TRIM27.1b* in cell culture.

Zha *et al.* (2006) showed that (A) Human TRIM27 interacts with IKKα/β/ε downstream signaling components of the RIG-I pathway which would inhibit the antiviral program in the cell. (B) To determine if duck *TRIM27.1a* and *TRIM27.1b* play a similar role in immune modulation I used a (C) cell culture based experiment with a constitutively active GST-fused duck RIG-I CARD domains construct (GST-d2CARD) in a chicken embryonic fibroblast (DF1) line. I co-transfected with *TRIM27.1a* and *TRIM27.1b* for 24 hours and measured relative expression of two genes downstream in the signaling pathway, *interferon beta* (*IFN-β*) and *myxovirus resistance gene 1* (*MX1*) with qPCR.

Chapter 2. MATERIALS AND METHODS

2.1 *In silico* analysis and annotation of the TRIM genes in the draft duck genome

Using the draft genome of the White Pekin duck (Pre Ensembl release 66, July 2012), the assembled scaffolds, predicted CDS and peptides were analyzed and annotated. Differential map to gene analysis was previously conducted and identifiable, annotated TRIMs formed the framework for further analysis. Vector NTI Advanced 10 (Invitrogen) and Lasergene v7.0 and 9.0 (DNASTAR Inc.) programs were used to analyze genomic and CDS sequences to confirm predicted sequences. SeqBuilder and SeqMan (Lasergene) are used to analyze sequence information. Alignments were conducted using ClustalW alignments in MegAlign (Lasergene) and MultAlin online interface (Corpet 1988). Coding sequence predictions are also made using the web based server GenScan (MIT server, Stanford University; (Burge & Karlin 1998)). Alignments and syntenic analysis is conducted using BLAST® (Basic local alignment search tool) and NCBI (National Centre for Biotechnology) databases and alignment tools. Phylogenetic trees and bootstrapping analysis was conducted using MegAlign programs (Lasergene) and bootstrapping procedure with 1000 trials and 111 seeds.

2.2 RNA extraction of infected tissues and cDNA synthesis

Previously, infections of 6 week old White Pekin ducks were carried out using a highly pathogenic isolate, A/Viet Nam/1203/04 (H5N1) (VN1203) from a fatal human infection, and a low pathogenic environmental isolate, A/mallard/British Columbia/500/05 (H5N2) (BC500), using an eye, nares and trachea drip. Infections with VN1203 and BC500 were previously done in biosafety level 3 facilities in St. Jude's Research hospital; the mock birds were treated just as BC500 and VN1203 infected birds,

but eye, nares and tracheal drips were done using sterile PBS. At 1, 2 and 3 dpi, total RNA was isolated from the tissues. Total RNA was quantified using a nano-drop and used for cDNA synthesis using samples of 1000 ng (for RT-PCR) or 500 ng (qPCR). RNA was DNAse treated (DNAse I Amp grade, Invitrogen) prior to synthesis; SuperScript III (Invitrogen) and an oligo (dT) primer (IDT Technologies) was used for extension. Quality of cDNA was verified using RT-PCR for a house keeping gene, glyceraldehyde 3-phosphate dehydrogenase (GAPDH) using gene specific primers GAPDHF1 (5′-CCGTGTGCCAACCCCCAATGTCT-3′) and GAPDHR1 (5′-GCCCATCAGCAGCCTTCACTAC-3′) using in-house Taq enzyme (a recombinant Taq enzyme produced in the Department of Biological Sciences, University of Alberta). Amplification procedure is a 1 minute initial denaturation (95°C), and 28 cycles of 15 seconds melt (95°C), 15 seconds annealing (60°C) and 30 seconds extension (72°C) to amplify a 107 bp product.

2.3 Expression analysis by reverse-transcription (RT-PCR) and qPCR

Primers used for RT-PCR were designed *in silico* from the coding sequence predictions from the draft genome using Vector NTI Advance 10 and primers were synthesized by IDT (primer pairs for each gene is available in (Table 2-1). Primer pairs were tested using sample 401 (male sex matched VN1203 infected ducks) in lung or spleen samples of cDNA. Products were amplified with Platinum® Taq DNA polymerase (Invitrogen). The resulting product was sequenced before RT-PCR was done. qPCR probes were designed using standard conditions on Primer Express v3.0 (Applied Biosystems) or using the online RealTime PCR design tool (IDT). PrimeTime Probes (6-FAM/ZEN/IBFQ) and primers were ordered as mixes (qPCR assays, IDT) and are resuspended in nuclease free Tris-EDTA (TE) buffer pH 8.0 (IDT); Primer and probe sequences are available in Table

2-2. FastStart TaqMan® master mix (Roche) was used for the qPCR assay in the Prism 7500 Real Time PCR machine (Applied Biosystems). Analysis was either using a relative expression assay (ΔΔCT) based on expression of an endogenous control (Glyceraldehyde 3-phosphate dehydrogenase, GAPDH) and the gene of interest, or by using an absolute quantification approach with standard curve analysis of a known copy number of the gene of interest. The absolute quantification based analysis used a pCR2.1-TOPO clone of each target gene, *myxovirus resistance gene 1* (*MX1*) and *interferon beta* (*IFN-β*). Specifically, a fragment of chicken *MX1* (*ChMX1*) and the full length transcript of chicken interferon (*ChIFN-β*) were used in order to generate a standard curve for copy number analysis. A total of 4 separate experiments were completed to demonstrate the consistent immunomodulation of *IFN-β* and *MX1* expression by *TRIM27.1aV5* and *TRIM27.1bV5* using abqPCR. Standard curves of each gene (*IFN-β* and *MX1 fragment*) were run on every analysis plate with dilutions of vector back calculated from $1x10^8$ down to $1x10^1$ copies/well using Avogadro's number and nano-drop values of the minipreps of *IFN-β* and *MX1fragment.* This generated a reliable standard curve with predictable values for slope and intercept. I calculated the copy number from the Ct values of triplicate samples of each cDNA sample using the plate endogenous standard curve and by using the following equation.

Equation 1. Calculation for copy number by using Ct values of abqPCR and slope/intercept of each standard curve.

$$y = mx + b$$

y is the Ct
m is the slope
b is the intercept
x is the copy number

$$\text{Copy number} = 10 \wedge ((Ct - b)/m)$$

2.4 Cloning and sequencing

TOPO-TA cloning system (Invitrogen) was used to clone A-overhang PCR products into the TOPO pCR2.1 vector system. Sequencing of inserts is done with TOPO backbone specific primers M13r (5' - CAGCAAACAGCTATGAC-3') and M13F-20 (5' - GTAAAACGACGGCCAG-3'). Products produced with non-taq enzymes (such as Phusion, see below) were A-tailed using a dATP (1mM) (Invitrogen) solution and running a second A-tailing PCR on purified product with house taq enzyme in a single 20 minute extension (72°C) in order to clone into pCR2.1. Sequencing was through the use of BigDye Terminator v3.1 (Applied Biosystems) and the 3730 DNA sequencer (MBSU, University of Alberta, Applied Biosystems). All sequencing reactions were in a total volume of 10 μl using 0.5 μl of template and 0.5-1 μl of BigDye. DNA was precipitated using 1/10 final volume of 3M sodium acetate pH 5.2. A 2:1 volume of 95% (v/v) ethanol incubated for 1/2 hr at 4°C and centrifuged at 16,100 x g for 10 minutes to precipitate. The pellet was washed in 70% ethanol and resuspended in 10μl of water. Chromatograms were analyzed using ContigExpress (Invitrogen).

2.5 Amplification of *TRIM27.1a* and *TRIM27.1b* and allele screening

Amplification of *TRIM27.1a and TRIM27.1b* from cDNA was performed using lung sample from duck 401, infected with high pathogenic IAV (VN1203). AmpliTaq Gold® PCR Master Mix (Invitrogen) was used for the first amplification of both *TRIM27.1a* and *TRIM27.1b* (primer sequences and conditions are specified in Table 2-3). Allelic clones were amplified from lung cDNA samples from VN1203 infected ducks 310, 312 and 401 with both AmpliTaq Gold® PCR Master Mix and Phusion high fidelity PCR master mix with GC buffer (conditions are listed in Table 2-4). PCR products were extracted, A-tailed (when necessary) and cloned into pCR2.1-TOPO. Polymorphism

screening was necessary as clones were observed to be polymorphic. Analysis of all allele screening and alignments were done using ContigExpress (Vector NTI suite v11, Invitrogen). Identified clones were sequenced completely in the forward and reverse direction using backbone and *TRIM27.1a* and *TRIM27.1b* specific primers (Table 2-5 and Figure 2-1) with sequence overlap along the entire length for allele screening. Full clone consensus was exported and aligned with other clones from the same bird to determine allele of the clones. Clone contigs were aligned with other clones from the same allele and then allele contigs were aligned in order to determine single nucleotide polymorphisms (SNPs) in the sequence. A heat map was generated from alignment of the allele contigs from ducks 310, 312 and 401.

2.6 Expression constructs and design

Expression constructs were made by engineering primers for directional cloning with restriction sites (3'-NheI, Not-I-5') from confirmed TOPO clones of *TRIM27.1a* and *TRIM27.1b*; a single 3'-primer and two different 5'-primers were used to generate an untagged, and a V5 epitope-tagged (GKPIPNPLLGLDST-C-terminal) insert (Table 2-6). Template clones (clone 2-2 for *TRIM27.1a* and clone 4-4 for *TRIM27.1b*) were selected because their sequences were the closest to predicted CDS (from the draft duck genome) and to the consensus sequence of the allele screening alignments. Phusion high fidelity master mix with GC content enhancer was used to produce inserts for *TRIM27.1a-NT (No Tag)*, *TRIM27.1a-V5*, and *TRIM27.1b-NT*. Due to repeated failure of PCRs with Phusion and the reverse primer for *TRIM27.1b-V5*, AmpliTaq® Gold was used for amplification of the *TRIM27.1b-V5* insert. The sequence was confirmed for all clones. Double digestion of the pcDNA3.1/Hygro+ expression vector (Invitrogen) and insert with NheI and NotI (New England Biolabs) was employed. Ligation of the insert into the digested vector was

done with T4-ligase (Invitrogen). Clones were confirmed with PstI digestion and identified clones were sequenced. Positive clones containing the confirmed insert fragments of pcDNA3.1/Hygro+/TRIM27.1aNT, pcDNA3.1/Hygro+/TRIM27.1aV5, pcDNA3.1/Hygro+/TRIM27.1bNT and pcDNA3.1/Hygro+/TRIM27.1bV5 were sequenced completely using the primers listed in Table 2-5 (Figure 2-2). The constructs were transformed into *Escherichia coli* DH5α, grown in 50 ml of LB + 100 μg/ml ampicillin. DNA was isolated by midi-prep (Qiagen MidiPrep Kit), and concentration was determined by nano-drop for use in transient transfections. Two constructs used for the expression experiments and the GST-pulldowns were designed, cloned and provided by Dr. Domingo Miranzo-Navarro. Two constructs were provided, one containing the GST-I protein for control (DOG109) and one construct which contains Glutathione-S-transferase (GST) gene fused to the two tandem CARD domains from duck RIG-I (GST-I/RIG-I-duck2CARD, DOG110 or *d2CARD,* Figure 2-3).

2.7 Transfection and expression

DF1 chicken embryonic fibroblasts (passage 18) were recovered from frozen stocks at a concentration of 1.5 x 10^6 cells/ml in 5% DMSO. DF1 cells were cultured in Dulbecco's modified eagle medium (DMEM) + 10% v/v non-heat-inactivated fetal bovine serum (FBS) (Invitrogen) and incubated at 39°C, humid environment and 5% CO_2. Passages 20 to 31 were used for transient transfection experiments. 24 well plates were used for RNA extraction experiments (ThermoScientific) and for protein expression 6-well plates were used (ThermoScientific). Adherent cells were harvested using a 1x PBS wash, a 1 minute 0.25% (w/v) trypsin EDTA incubation, and resuspended in DMEM + 10% v/v FBS. Cells were counted using trypan blue and a haemocytometer, with two counts per culture and the average was used to calculate concentration. Cells were seeded

onto 24 well or 6 well plates with 500μl or 2 ml, respectively, at a concentration of 4 x 10^5 cells/ml. 24 hrs after seeding, the cells were transiently transfected using Lipofectamine 2000 reagent (Invitrogen) according to manufacturer's instructions. A ratio of 1 μg:2.5 μl DNA:lipofectamine was used for transfection in OptiMEM media (Invitrogen), and 100 μl and 500 μl volumes of DNA/Lipofectamine/OptiMEM complexes were aliquoted onto 24 well and 6 well plates, respectively. Four hours after transfection, the OptiMEM media was aspirated and replaced with DMEM + 10% FBS. The luciferase assays were cultured immediately with 500 μl of DMEM + 10% (v/v) FBS and incubated overnight with no observable changes in general cell health. Transfection efficacy was verified visually with transfection of the pDsRed-N1 vector and fluorescence microscopy.

2.8 RNA extractions from tissue culture

RNA experiments were performed in 24 well seeded plates and RNA extractions were performed at either 24 or 48 hrs post-transfection (PT) depending on the experiment. Media was aspirated, cells were washed with ice cold 1x PBS and 200 μl of TRIzol® reagent (Invitrogen) was used per well to lyse and extract RNA from the adherent cells. RNA was isolated from 3 wells per replicate (a total of 600 μl of TRIzol® per replicate), and 2 or 3 repetitions within a single experiment were done in order to ensure accuracy of results and three or four experimental replicates were done as specified. RNA extraction was conducted by chloroform extraction. RNA was precipitated a 0.5:1 volume of isopropanol to original volume of TRIzol® regent (e.g. 600 μl of isopropanol to the original 1200 μl of TRIzol®) incubated at room temperature for 10 minutes. RNA was pelleted by centrifugation at no more than 7,500 x g for 5 minutes

at 4°C. The RNA pellet was washed in a 1:1 volume of 75% (v/v) ethanol original volume of TRIzol® reagent with 3 to 5 washes with 75% v/v ethanol. RNA was resuspended in 30 - 50µl of nuclease-free H_2O (Ambion® Life Technologies). Concentration and purity of RNA was determined by nano-drop.

2.9 Protein extraction from tissue culture and GST-pulldown

Protein experiments were performed in 6 well seeded plates and protein extractions were performed at 24 hours PT. Cells were washed once in ice cold 1x PBS, aspirated and transferred immediately to ice. Lysis buffer (50 mM Tris-HCl (pH 7.2), 150 mM NaCl, 1% (v/v) Triton X-100) with cOmplete Mini, EDTA-free proteinase inhibitor cocktail pellets (Roche Diagnostics) was used to lyse the cells, 250 µl per well, and extract cytoplasmic proteins. Cells were incubated and then scraped in the Lysis buffer and lysate (1500 µl) was collected in 1.5 ml microcentrifuge tubes (Axygen®). Large complexes were pelleted and discarded and 50 µl of whole cell lysates (WCL) were boiled for 10 minutes in 12.5 µl of Laemmli buffer (0.25 M Tris-HCL (pH 6.8), 8% (w/v) SDS, 20% (v/v) β-mercaptoethanol, 40% (v/v) glycerin, 0.2% (w/v) bromophenol blue). The whole cell lysate was incubated with glutathione-coated sepharose beads (GE Healthcare) for three hours with constant agitation in order to allow the GST-tags to bind to glutathione. GST-pulldowns were processed by boiling for 10 minutes in 25 µl of Laemmli buffer. Non-specific binding was observed when using raw beads, so TIF (150 mM NaCl, 20 mM Tris-HCl (pH 8.0), 1mM MgCl2, 0.1% (v/v) Triton X-100, 10% (v/v) Glycerol) wash with 5% (w/v) BSA blocking overnight was employed.

2.10 Western blotting and imaging

SDS-page gels of 8% acrylamide were run for the western blot at 100 mA. PageRuler™ Plus prestained ladder (Pierce) was used for size measurements. Transfer to Trans-Blot® Nitrocellulose transfer membrane (BioRad) was conducted for 2 hours at 75 mA. Membranes were blocked overnight at 4°C in PBS + 5% (w/v) skim milk. Primary mouse antibodies were bound for 2 hours at 24°C in a hybridization oven, and were either mouse α-GST (1:1000) or mouse α-V5 (1:5000, Invitrogen). Secondary antibody binding was a goat anti-mouse:HRP (horse radish peroxidase) conjugate antibody (1:5000, BioRad) and was conducted at 24°C for 1 hour. Imaging of membranes was through chemiluminescent substrate cleavage, either Amersham® Enhanced Chemiluminescence (ECL) solution (GE Healthcare) or ECL prime (GE Healthcare).

2.11 Chicken interferon-2 promoter activation

To assess level of transcriptional activation I employed a luciferase reporter experiment which utilizes the pGL3-ChIFN-2 construct which is the pGL3-Basic firefly luciferase reporter (Promega) with 173 base pairs of the chicken IFN-2 (the avian homolog of IFN-β) promoter region as previously reported (Sick *et al.* 1998; Barber *et al.* 2010). The ChIFN-2 promoter, which has an NFκB binding site and two putative IRF binding sites (presumably IRF7 in chickens), was used to drive the expression of firefly luciferase. A dual luciferase reporter assay was employed (Promega) which uses expression of the renilla (*Renilla reniformis*) luciferase construct, phRG-TK, to measure transfection efficiency. GloMax® 20/20 luminometer measured the *Renilla* luciferase activity in the presence of Luciferase Assay Reagent II (Promega) reagent over 12 seconds – with a 2 second delay and a 10 second read. Stop & Glo® reagent (Promega) was added and the level of firefly (*Photinus pyralis*) luciferase activity was measured. Luciferase activity

was represented as a normalized (to GST-I Only transfection control = 1.0) ratio of firefly:renilla luciferase activity. Transient transfections of each group were performed in triplicate wells of a 24 well plate seeded and transfected as described. In order to reflect what had been demonstrated previously with RIG-I promoter responses (Versteeg *et al.* 2013), 5 ng of the d2CARD contrsuct was used to stimulate the RIG-I pathway in the transfected cells. Increasing amounts of each gene of interest was added to constitutively actvated (d2CARD trasnfected) cells, from 25 ng to 500 ng. To maintain and control for exogenous DNA additive effects, the total amount of DNA was normalized with addition of empty vector (pcDNA3.1/Hyrgo+). Each transfection was run in a single experiment three times. Four experimental transfection replicates were performed.

Table 2-1. Primers used for RT-PCR of the candidate duck TRIM genes.

Gene of Interest	Product Size (bp)	Primer Name	Sequence (5' XXX…X 3')	Primer Bank #	Tm (°C)
GAPDH	107	GAPDH-F1	CCGTGTGCCAACCCCCAATGTCT	452	64.2
		GAPDH-R1	GCCCATCAGCAGCCTTCACTAC	453	60.3
TRIM7.2	238	D-TRIM7EX3F	TGAGAGGCAGAGGCAGAGCG	736	61
		TRIM7aEx8-R	CCGCCAGCACGCAGAAGGAATAAT	744	61.8
TRIM7.1	512	TRIM7bEx8-F2	CTGCTGGTGGAGTTCGAGGG	835	60.2
		TRIM7bEx10-R2	CCCACCTCCACCTCCCAGTAAT	836	60.6
TRIM14-Exon1	268	TRIM14a/Ex1-F1	GGGTCCATCCATCCCCCAGGAGCAA	831	66.8
		TRIM14a/Ex1-R1	AGTCAGGGAGCAACACTGGGTGGGC	832	66.5
TRIM14-Exon6	277	TRIM14a/Ex6-F2	CAACCTGGGAATACGACAGCC	833	58
		TRIM14aEx6-R2	GATGCTCGATTCCAGCCCAG	834	58.3
TRIM27.2 (Set 1)	278	TRIM27aEx3/4-F	CTGGAGGACATCAGAGGCACC	747	60.3
		TRIM27aEx7-R	TCATCGGATGAGTCCTGCTGG	748	61.9
TRIM27.2 (Set 2)	516	TRIM27aEx6-F1	CATCTTGATGTTTGAGCTGCCTG	911	60.2
		TRIM27aEx7-R1	CGCTCCACACCAAGAACCAGG	912	58.2
TRIM27.1a	286	TRIM27bEx4/5-F	AGACTCTTGAAAAGCTGTGAGG	749	54.8
		TRIM27bEx7-R	GCTCGAAGTCGAATCTCTCTGG	750	57
TRIM27.1b	324	TRIM27cEx3/4-F	GAATAAATCCCTGCAGGATGCC	751	56.1
		TRIM27cEx7-R	AAATCTCTGCGGGTTGTCAGG	752	57.5
ψ*TRIM27d*	374	pTRIM27d-F	GATGGGAATACATGCTGCAGG	753	56.1
		pTRIM27d-R	GGCTGGAGGAAAAGTGAAGATGG	754	57.9
TRIM39.2	317	TRIM39b-F1	TCTTCTCAGGTCGCCACTACTGG	829	60.2
		TRIM39b-R1	GTCGGTCACGTTGTAGAAGGAGAT	830	58.2
TRIM41	382	TRIM41aEx4-F2	TCAGCCGCCTCATCGCCGAA	837	63.7
		TRIM41aEx8-R2	CGTCTGCTCGGTGGCCGTC	815	63.7

Table 2-2. Primer and probe sequences for target genes used for quantitative real-time PCR (qPCR).
Both duck and chicken probes used for analysis are included.

Gene of Interest		Sequence (5' - /56-FAM/X../ZEN/X../31ABkFQ/-3')	Amplicon (bp)	Region of Amplification
	Probe	TCTCCGCGG/ACCTCAAGAT		
	Primer F	TGCTTCCTACAGCCCATCCT		In the first region of the 'PRY' domain
TRIM7.2	Primer R	GGCGAACCACCTCCTCAT	63	
	Probe	AGAAAACGG/CCCCGGGAACCA		Within the coiled-coil region in the last 400 bp of the gene
	Primer F	TGCAAAACATCCAGCTCTCAA		
TRIM7.1	Primer R	GCCCAGCTCGATAAGTTGTTG	112	
	Probe	TGGCCCCCA/GCGGTTCGA		Between coiled-coil domain and before beginning of the PRY/SPRY
	Primer F	GCAACTGGAGGAGGATATTTTACC		
TRIM14	Primer R	AAATTGTGGCAGGTGCTAAGC	68	
	Probe	CCTCAGCGT/GCATCTCACGAGGAC		In the coiled-coil domain right before the start of 'PRY' domain
	Primer F	CCCATCTGGAAAGAAGACTTGAG		
TRIM27.1a	Primer R	GGTTGGCTCTTGCAATTTAAACA	107	
	Probe	CAGACACAG/CAAACCCCCACCTTGTC		The very beginning of the 'PRY' domain
	Primer F	GGGTGTTTCGTCCCATCTCA		
TRIM27.1b	Primer R	GGGCAAACGTGACTCTGGAT	89	
	Probe	TTTCCTCA/TGCCCAGACAGCG		Spans the linker region of the coiled-coil and the PRY/SPRY
	Primer F	AAGTTCCAGACCCCTAAAG		
TRIM39.2	Primer R	CATGCACCTCCCAGTAG	124	
	Probe	CTCCCTCAG/CTGATGCCCCCATG		
Chicken GAPDH	Primer F	GGTGCTAAGCGTGTTATCATCTCA		Position 394 to 463 of ChGAPDH
	Primer R	CATGGTTGACACCCATCACAA	70	
	Probe	AGCAGCCCACAC/ACTCCAAAACACTG		
Chicken IFNβ	Primer F	TCCAACACCTCTTCAACATGCT		Position 258 to 326 of ChIFNβ
	Primer R	TGGCGTGTGCGGTCAAT	69	
	Probe	CTTCACCTCCG/CAATCCAGCAAGA		
Chicken MX1	Primer F	GGACTTCTGCAACGAATTG		Position 948 to 1131 of ChMX1
	Primer R	TCCCACAAGTTCATCTGTAAG	148	

Table 2-3. *TRIM27.1a* and *TRIM27.1b* amplification primers.

Gene of Interest	Size (bp)	Primer Name	Sequence (5' XXX…X 3')	Primer Bank #
TRIM27.1a	1506	TRIM27.1bAmplificationF	ATGGCTTCGCAGAGCCCCTCGGA	960
		TRIM27.1bAmplificationR	AGGACAAATCCGGAGGGGAGACCTG	961
TRIM27.1b	1425	TRIM27.1cAmplificationF	ATGGCCGAGTGCGACCCGCTG	962
		TRIM27.1cAmplificationR	TCAGGGAGCCAGCTGGATCTTGGACTCC	963

Table 2-4. Parameters for AmpliTaq® Gold and Phusion PCR amplification of *TRIM27.1a* and *TRIM27.1b*.

Gene of Interest	Enzyme	Primer Name	Number of cycles	Tm (°C)/ Duration (sec)	Ta (°C)/ Duration (sec)	Text (°C)/ Duration (sec)
TRIM27.1a	AmpliTaq® Gold	TRIM27.1bAmplificationF TRIM27.1bAmplificationR	35	95.0/30	57.0/30	72.0/180
	Phusion	TRIM27.1bAmplificationF TRIM27.1bAmplificationR	35	98.0/10	60.0/30	72.0/60
TRIM27.1b	AmpliTaq® Gold	TRIM27.1cAmplificationF TRIM27.1cAmplificationR	35	95.0/30	60.0/30	72.0/180
	Phusion	TRIM27.1cAmplificationF TRIM27.1cAmplificationR	35	98.0/10	63.0/30	72.0/60

Table 2-5. Sequencing primers.

Target	Gene of Interest	Sequence (5' XXX…X 3')	Primer Bank Number	Tm (°C)
TOPO Backbone	M13F-20	GTAAAACGACGGCCAG	450	50.7
	M13r	CAGGAAACAGCTATGAC	451	47.0
pcDNA3.1 Backbone	BGHR	TAGAAGGCACAGTCGAGG	731	53.6
	T7-pgem	TAATACGACTCACTATAGGG	461	47.5
TRIM27.1a	TRIM27.1bEx1-F2	TTGCAAGCAGGCAGAGGAGCA	1002	62.0
	TRIM27bEx4/5-F	AGACTCTTGAAAAGCTGTGAGG	749	54.8
	TRIM27.1bEx7-F	ATTCGACTTCGAGCCTTGTGTGCT	1004	60.8
	TRIM27.1bEx2-R	AGCTCGAGGCGAGCCTGGATTTCTT	1005	64.0
	TRIM27.1bEx5/4-R	GGTTGAACTTCATCACCTCACAGC	1006	58.1
	TRIM27bEx7-R	GCTCGAAGTCGAATCTCTCTGG	750	57.0
TRIM27.1b	TRIM27.1cEx7-F	ATTTGACACCTACTGCTCGGTGCT	1008	60.5
	TRIM27.1cEx2/1-5	ATATGTTCTTTGCACTCCTGGGCG	1009	59.5
	TRIM27.1cEx5/4-R	CACACCTGGTCAAGGCACTCCT	1010	61.5
	TRIM27.1cEx1/2-F	GCCCAGGAGTGCAAAGAACATATC	1007	58.1

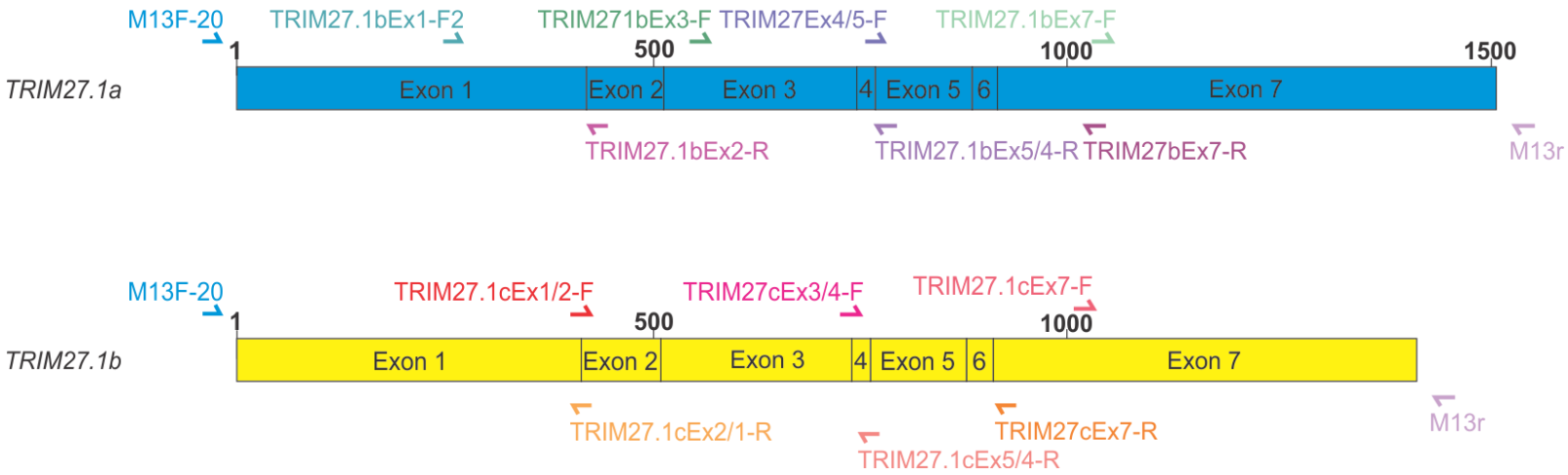

Figure 2-1. Sequencing primers used for allele screening of cDNA amplified *TRIM27.1a* and *TRIM27.1b* genes.
This is a schematic of the primer binding sites in the length of the coding sequence of TRIM27.1a and TRIM27.1b used for sequencing and allele/polymorphism analysis. Different combinations of primers depending on the read per clone were used in order to achieve full and complete forward and reverse strand coverage for a single clone template.

Table 2-6. Primers for directional cloning of expression construct with and without C-terminal modifications (V5-epitope tags).

To facilitate directional cloning within the multiple cloning site (MCS), restriction sites were engineered into the amplification primers. NheI and NotI are compatible enzymes which appear only once in the MCS of pcDNA3.1/Hygro(+) and which will facilitate directional cloning. NheI is the enzyme at the 5' end of the multiple cloning site, and NotI is the enzyme on the 3' end of the MCS. SS indicates engineering of a 5'- TGA TGA – 3' double stop codon to ensure termination of the transcript. The V5 epitope was engineered into the ultramer and corresponds to the amino acid code for the canonical V5 epitope-tag (GKPIPNPLLGLDST-C-terminal-SS-NotI). The manufacturer's melting temperature (Tm) specified on the primers overestimates the template binding region of the primer. So the PCR annealing temperature was estimated based on the region of the primer which will overlap the existing template in order to ensure binding of the primer to the template. Specified in the Tm (°C) column here is the calculated Tm (°C) primers that overlaps the template. Clones 2-2 (*TRIM27.1a*) and clone 4-4 (*TRIM27.1b*) were used as template for the amplification.

Gene of Interest	Product Size (bp)	Primer Name	Sequence (5' XXX…X 3')	Primer Bank Number	Tm (°C)
TRIM27.1a	1532	TRIM27.1bAmpF-NheI	GGCGCTAGCATGGCTTCGCAGAGCCCCTCGGA	1016	67.2
		TRIM27.1bAmpR-SS-NotI	GCCGCGGCCGCTCATCAAGGACAAATCCGGAGGGGAGACCT	1017	63.5
	1574	TRIM27.1bAmpR-V5-SS-NotI	GCCGCGGCCGCTCATCAGGTGGAGTCCAAGCCAAGCAAGGGG TTGGGGATGGGCTTGCCAGGACAAATCCGGAGGGGAGACCT	1018	63.5
TRIM27.1b	1451	TRIM27.1cAmpF-NheI	GGCGCTAGCATGGCCGAGTGCGACCCGCTG	1019	67.2
		TRIM27.1cAmpR-SS-NotI	GCCGCGGCCGCTCATCAGGGAGCCAGCTGGATCTTGGACTCC	1020	64.8
	1493	TRIM27.1cAmpR-V5-SS-NotI	GCCGCGGCCGCTCATCAGGTGGAGTCCAAGCCAAGCAAGGGG TTGGGGATGGGCTTGCCGGGAGCCAGCTGGATCTTGGACTCC	1021	64.8

Table 2-7. Parameters for AmpliTaq® Gold and Phusion PCR amplification of construct inserts of *TRIM27.1a* and *TRIM27.1b*.

Phusion high fidelity enzyme was used to amplify *TRIM27.1aNT*, *TRIM27.1aV5* and *TRIM27.1bNT*. AmpliTaq Gold was used to amplify *TRIM27.1bV5*. Sequence of all constructs were confirmed prior to use in transefections.

Gene of Interest	Construct	Enzyme	Primer Name	Number of cycles	Tm (°C)/ Duration (sec)	Ta (°C)/ Duration (sec)	Text (°C)/ Duration (sec)
TRIM27.1a	*TRIM27.1a-NT*	Phusion	TRIM27.1bAmpF-NheI TRIM27.1bAmpR-SS-NotI	35	98.0/10	70.0/30	72.0/45
	TRIM27.1a-V5	Phusion	TRIM27.1bAmpF-NheI TRIM27.1bAmpR-V5-SS-NotI	35	98.0/10	70.0/30	72.0/45
TRIM27.1b	*TRIM27.1b-NT*	Phusion	TRIM27.1cAmpF-NheI TRIM27.1cAmpR-SS-NotI	35	98.0/10	66.0/30	72.0/45
	TRIM27.1b-V5	AmpliTaq® Gold	TRIM27.1cAmpF-NheI TRIM27.1cAmpR-V5-SS-NotI	35	95.0/10	62.0/30	72.0/120

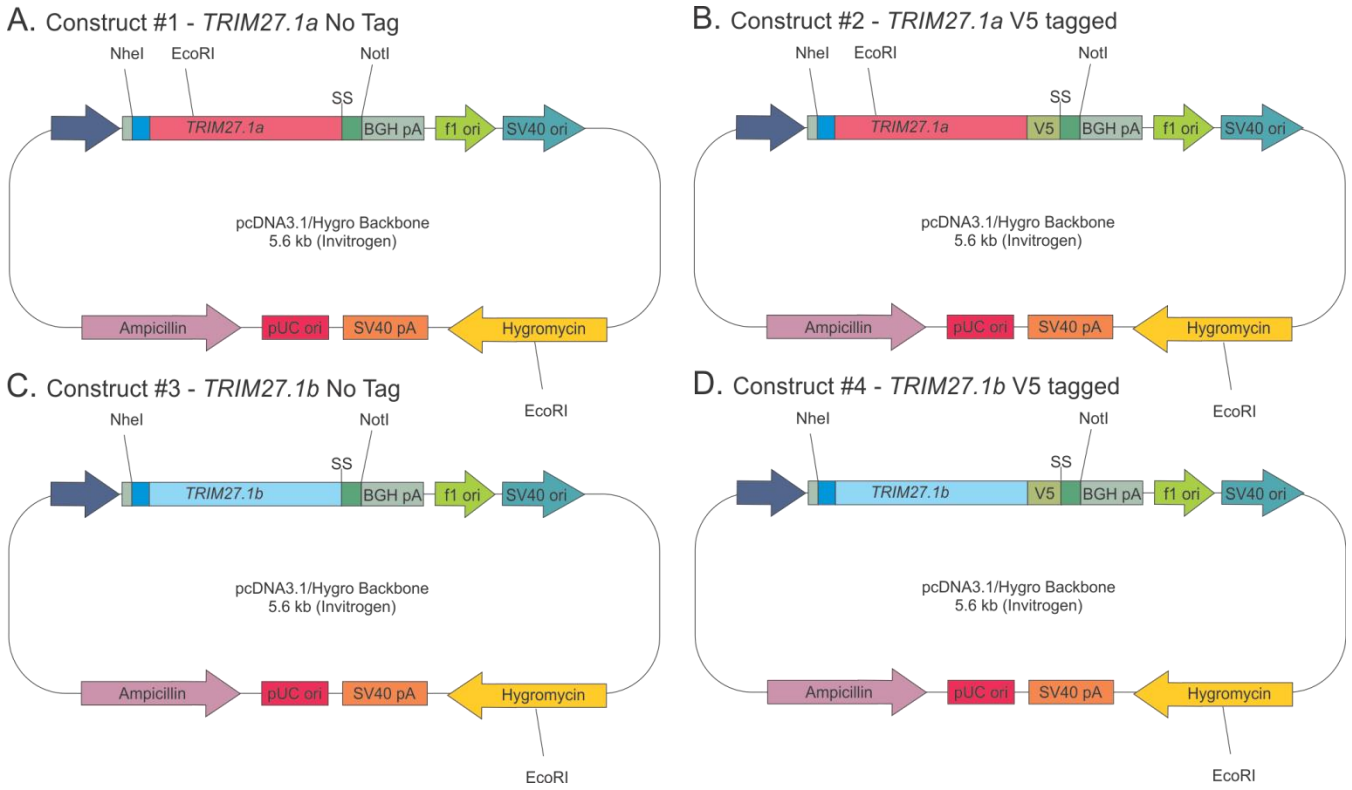

Figure 2-2. pcDNA3.1 expression vector maps generated from directional cloning of the four engineered TRIM27.1a and TRIM27.1b inserts.

All clones were identified with EcoRI digestion (empty vector has another EcoRI site in the MCS) and confirmed with sequencing. Diagrams of the 4 constructs used for transient transfection, or co-transfection, and gene expression are A) pcDNA3.1/Hygro+/TRIM27.1aNT; B) pcDNA3.1/Hygro+/TRIM27.1aV5; C) pcDNA3.1/Hygro+/TRIM27.1bNT; and D) pcDNA3.1/Hygro+/TRIM27.1bV5 construct.

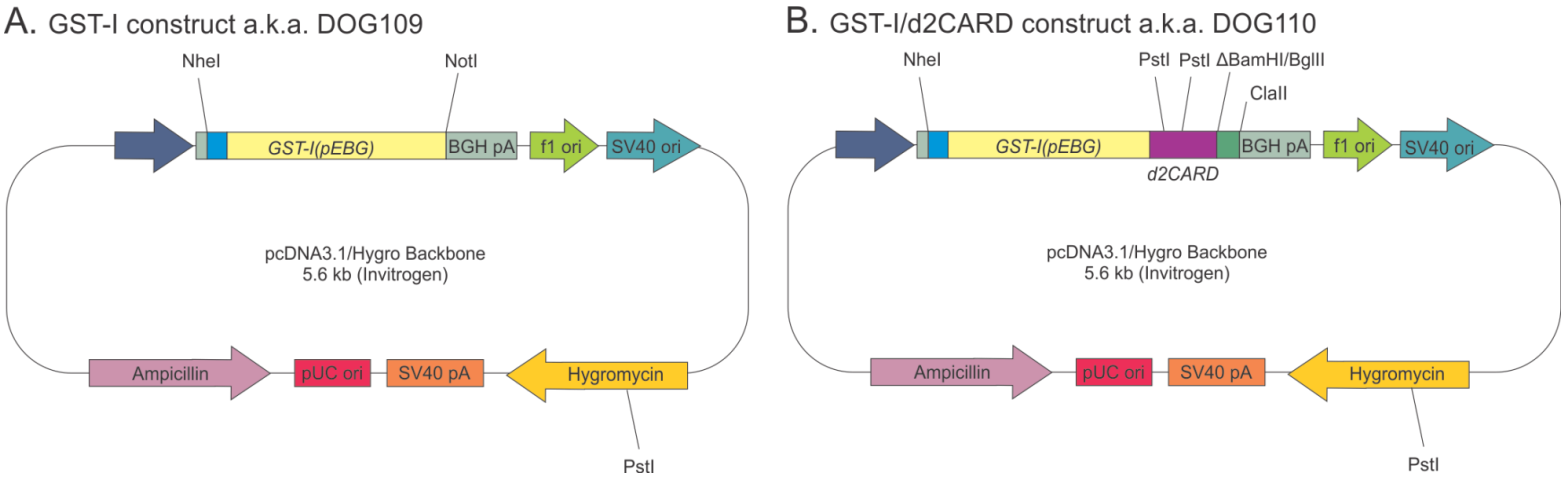

Figure 2-3. pcDNA3.1 expression vector maps of the glutathione-S-transferase (GST) fusion proteins.
These two constructs were made by Dr. Domingo Miranzo-Navarro and were employed to mimic an activated antiviral state in the transiently transfected DF1 cells. A fully sequenced clone of DOG109 was confirmed with BstNI digestion (BstNI sites not shown on diagram, but at positions 340, 534, 509 (in insert), 1088, 1769, 1824, 1811, 3522, 3813, 3934, and 3947 in the vector backbone). A fully sequenced clone of DOG110 was confirmed with PstI digestion and a 156 bp digestion product in the d2CARD insert differentiates the positive clones. Diagrams of the 2 constructs used for transient transfection, or co-transfection, and gene expression are a) DOG109, or GST-I, the plasmid containing GST into which the duck-2-CARD domains were fused; and b) DOG110, or GST-d2CARD, the construct containing the fusion gene of the duck RIG-I tandem CARD domains fused to the C-terminal end of GST.

Chapter 3. RESULTS AIM 1 AND AIM 2

3.1 Repertoire of TRIM genes in White Pekin ducks

In order to focus our search for an antiviral or immune relevant *TRIM*, I first had to determine which recognizable *TRIM*s were in the draft White Pekin duck genome. Previously, two ducks, one infected (duck number 408) with highly pathogenic IAV A/Viet Nam/1203/04 (H5N1) (VN1203) and one mock (duck number 70) animal (PBS) were sacrificed at 3 dpi and the RNA from lung tissue was used for cDNA synthesis and 454 deep sequencing (454 Life Sciences). Previously, comparison of the expressed duck sequences with the sequenced Beijing duck genome (Huang *et al.* 2013) generated a differential map to gene analysis between lung tissue of duck number 408 and compared to duck lung tissue infected with a low pathogenic IAV isolate sacrificed at 3 dpi (duck number 70). I first searched this list for any annotated or recognizable *TRIM*s. A total of forty-seven *TRIM*s (or partial *TRIM*s) were originally predicted in the White Pekin duck repertoire (Table 3-1). A large number of *TRIM*s (seven predicted genes) were located within a single *TRIM*-rich scaffold, scaffold618 (highlighted yellow in Table 3-1). This list was reduced down to a manageable number of candidate genes for further investigation by examining location within the genome, searching the literature for a homolog that has an immune relevant function. The list of candidate antiviral or immune relevant genes which include *TRIM*s located within the MHC of chickens (*TRIM7, TRIM27, TRIM39* and *TRIM41*), *TRIM14,* which were noted as being differentially expressed from the differential map to gene analysis and *TRIM19* which is well known to be involved in immune responses in mammals.

3.1.1 Annotation of the predicted duck MHC TRIM-rich region

It was immediately apparent that a single scaffold, scaffold618, within the draft White Pekin duck genome was predicted to contain a concentration of *TRIM* or *TRIM*-like genes. It is important to note before continuing that I had to completely revise the prediction scaffold618 after closer examination. Although the map of scaffold618 has since been revised, and will be discussed in greater detail below, in order to develop a clear idea of the annotation of scaffold618 from the prediction annotated by the automated prediction programs (Huang *et al.* 2013) I need to elaborate on the process of annotation and provide a schematic of our starting point (Figure 3-1) and end point (Figure 3-2) of scaffold618 annotation.

Originally predicted by the automated annotation of scaffold618 (NCBI accession # KB742989.1) were 7 *TRIM* genes and 4 non-*TRIM* genes (Table A-1). I mapped the exons and ORFs to the genomic scaffold and developed a schematic of genomic organization (Figure 3-1). Although since revised, the genomic organization of the genes predicted within scaffold618 is conserved with the annotated genes from the major histocompatibility locus of two comparison species of the Galliform order, chicken (*Gallus gallus*, GenBank) (Figure 3-1). As such, we hypothesized that duck scaffold618 is a contig that will likely map to the same chromosome as the duck MHC. Of an original 11 internal accession numbers for predicted ORFs in scaffold618 were 6 predicted full length (beginning and ending with a predicted start (ATG) and stop (TGA) codon) *TRIM*-genes. The accession numbers are represented here by both the internal reference number/NCBI protein ID: Apl_13515/EOB02161.1 (*TRIM7.2*), Apl_13518/EOB02162.1 (*TRIM7.1*), Apl_13519/EOB02159.1 (*TRIM27.2*), Apl_13520/EOB02163.1 (*TRIM27.1a*), Apl_13521/EOB02164.1 (*TRIM27.1b*) and Apl_13522/EOB02160.1 (*TRIM41*). Also predicted by the automated genome assembly program was a *TRIM*-like

gene, Apl_13524/EOB02166.1 (*ΨTRIM27d*), which is a gene fragment of the C-terminal PRY/SPRY domain which lacks the N-terminal RBCC motif (Table A-1). Also originally predicted from scaffold618 are 4 non-*TRIM* genes: Apl_13514/EOB02156.1, Apl_13516/EOB02157.1, Apl_13517/EOB02158.1 and Apl_13523/EOB02165.1 (Table A-1). These are the CDS predictions I first mapped to scaffold618 genomic sequence in order to generate a rough schematic for the genomic organization (Figure 3-1A). However, some clear differences existed in this original schematic (Figure 3-1A) as compared to chicken (Figure 3-1B). Duck *TRIM7.1* spans a larger region of the genome in comparison to chicken *TRIM7.1*. The duck prediction lacks *TRIM39* which is found in the chicken. The duck scaffold does not have a predicted Hep21 gene which is located in the chicken MHC B locus (NM_204521.2) and predicted in the turkey (XM_003211139.1). Unrelated to the *TRIMs*, Hep21 is a member of the uPAR/CD59/Ly-6/snake toxin family and is found at high concentrations in egg whites of developing chicken embryos, but the role Hep21 plays is unknown (Bazzigher *et al.* 1993). Duck scaffold618 also contains two predicted *TRIM27.1* genes (*TRIM27.1a* and *TRIM27.1b*) (Figure 3-1A) not predicted in the syntenic region of the chicken MHC (Figure 3-1B) which has only a single *TRIM27.1* (NM_001099359.1, NCBI). The last gene predicted within scaffol618 (Apl_13524, *pTRIM27d*) is a fragment which contains only the C-terminal domain of a TRIM and does not contain the N-terminal TRIM components, the RING, B-Box or coiled-coil domain. So, in order to accurately represent and clarify the scaffold, I re-annotated the entire scaffold using *in silico* prediction and manual approaches. I predicted CDS and peptide sequences from the scaffold618 genomic DNA by running the entire scaffold through an online open-reading frame (ORF) prediction program, GenScan (MIT server, Stanford University; (Burge & Karlin 1998). I elaborated the original annotation of 7 TRIM and 4 non-TRIM genes within the scaffold and refined

the prediction of a total of 13 complete genes within the revised duck scaffold618 (Figure 3-2A) including duck *Hep21* and *TRIM39* which were not in the original computer based annotations. I also predicted 20 tRNAs which is not shown on the schematic (Table A-2). I performed synteny analysis with a scale schematic of the chicken (Figure 3-2B) and turkey (Figure 3-2C) MHC loci derived from NCBI and publications (Ruby *et al.* 2005; Shiina 2007; Chaves *et al.* 2009). In comparison with the annotated chicken and turkey MHC locus, our revised prediction of duck scaffold618 (Figure 3-2A) is syntenic with both avian MHC loci.

3.1.2 Duck scaffold618 contains four predicted *TRIM27* genes

Within the TRIM-rich scaffold618, the draft duck genome had predicted 4 separate coding sequences which were annotated as *TRIM27*s; Apl_13519/EOB02159.1, Apl_13520/EOB02163.1, Apl_13521/EOB02164.1 and Apl_13524/EOB02166.1 (Table A-1). Due to the large number of *TRIM27* homologs within scaffold618, I deemed this group of *TRIM*s to be of special interest as candidate antiviral or immune relevant *TRIM*s. The chicken genome predicts only two *TRIM27* genes within the MHC B locus TRIM-rich region; *TRIM27.1* (NM_001030671.2) and *TRIM27.2* (NM_001099359.1). The turkey MHC locus has two annotated TRIM27 proteins; TRIM27.1 (ACA64760.1) and TRIM27.2 (ACA64758.1). At first glance it would appear that the duck possess an additional two *TRIM27* homologs not observed in the chicken or the turkey.

We first annotated the predicted coding sequences by homology searches to the known avian TRIM27 genes. I assigned names to the genes by looking at synteny within the locus, and conservation in the amino acid and nucleotide sequences; Apl_13519 is *TRIM27.2*, Apl_13520 is *TRIM27.1*, Apl_13521 is a novel avian gene not characterized in either chicken or turkey, but has high homology (51% identity) to *TRIM27.1* and

finally Apl_13524 is a fragment of a gene with a PRY/SPRY domain and homology in the C-terminal domain to TRIM27 (Figure 3-2). Although the C-terminal SPRY domain has high sequence homology to other TRIM27 proteins, it is likely just a member of the SPRY domain containing butryrophilin-like family and not a TRIM. As such, I have annotated this as a *TRIM27-like butyrophilin* gene (*TRIM27-L BTN*).

3.1.3 RT-PCR amplification of *TRIM7.1* and annotation of *TRIM7.1* and *TRIM39.2*

In order to determine if *TRIM7.1* was a candidate immune relevant TRIM, RT-PCR was performed in order to amplify and clone a region of the *TRIM7.1* transcript from infected tissues, confirm the sequence and look at expression in infected duck tissues. The sequenced cloned fragments when aligned to the predicted sequence resulted in two additional (not predicted) exons in 5 separate positive clones (Figure 3-3). When I re-annotated scaffold618 CDS predictions, I determined that the genome predicted CDS for Apl_13518/EOB02162.1 was inaccurate and the amino acid sequence translation for TRIM7.1 coded for two separate RING-domains. The CDS for Apl_13518/EOB02162.1 spans a region of the genomic material which includes two separate *TRIM* genes, coding for *TRIM7.1* and *TRIM39.2*, and duck *Hep21* (Figure 3-2A).

3.1.4 *TRIM39.1-like/BR* gene is not a member of the TRIM family

The chicken genome annotation predicts two *TRIM39*-like genes (AB268588.1and AY694127.1) the first of which is located within the chicken MHC locus between *TRIM27.2* and *TRIM27.1*. The genes are annotated as *TRIM39.1* (AB268588.1) and *BR* (AY694127.1), and translate to a 256 amino acid protein with a single amino acid difference at position 240 (H240R from TRIM39.1(BAF62987.1) to

BR (AAW82326.1)). Although there is homology between BR and the C-terminal end of chicken TRIM39.2 (NP_001006196.2) the 256 amino acid protein prediction for TRIM39.1 lacks both a RING domain and a B-box domain.

In all of the ORF predictions of scaffold 618, an ORF was never predicted for the duck *TRIM39.1-like/BR* gene, which is predicted in both the chicken (AB268588.1) and the turkey (ACA64759.1) *TRIM39.1* sequences. I manually scanned and aligned the genomic region of scaffold618, which is flanked by *TRIM27.1a* (upstream) and *TRIM27.2* (downstream) in order to locate a homologous region to the *BR* gene within the duck (Figure 3-2) and ran the isolated *TRIM27.1a* and *TRIM27.2* intragenic region with an ORF prediction server (GenScan). I located a putative start and stop that corresponds to a PRY/SPRY domain containing gene, which translates to 309 amino acid protein that contains a coiled coil and a C-terminal PRY/SPRY domain with 78% identity (221/282 amino acids) to the chicken BR (Figure A-1).

3.1.5 Analysis of *TRIM14* as a candidate antiviral TRIM

Previous data had suggested that *TRIM14* is highly upregulated at 3 dpi with a highly pathogenic IAV virus (VN1203). Differential map to gene analysis during the 454 deep sequencing showed a statistically significant increase in *TRIM14* transcript in duck 408 compared to duck 70 of 15 hits to 0, respectively (Table A-1). As such, I pursued this as a candidate immune relevant *TRIM* gene. The predicted transcript for *TRIM14* (Apl_15985, NCBI accession EOA95592.1) is only a partial sequence located within scaffold1806 (KB744240.1) (Figure 3-4). Our first step was to conduct RT-PCR of cDNA samples at different time points of influenza infection in immune and influenza relevant organs, namely the lung and spleen. Two cycle numbers yielded the most reliable and obvious comparison of band intensity in the samples (25 and 28 cycles)

(Figure 3-5). Relative expression of *TRIM14* using RT-PCR at 1 dpi does not indicate an immune relevant role during IAV infection, regardless of pathogenicity. At 3 dpi in spleen, there is also no discernible pattern of differential expression between the mock, low pathogenic IAV or highly pathogenic IAV. However, in lung tissue isolated at 3 dpi I do observe higher intensity of bands at both 25 cycles and 28 cycles of amplification in highly pathogenic IAV (VN1203) infected samples (Figure 3-5).

I then designed *TRIM14* specific probe and primer sets to quantify the gene expression in infected tissues. Based on the previous data from the differential map to gene analysis from the draft genome I was expecting massive upregulation in tissues infected with highly pathogenic IAV (VN1203). In lung tissue I observed relatively consistent expression of *TRIM14* in both 1 dpi and 3 dpi (Figure 3-6A). In spleen at 1 dpi, I observed an increase from an average expression level of 3.95-fold in the mock samples to 12.16-fold in highly pathogenic IAV (VN1203) infected spleen. At 3 dpi in spleen, elevated expression is no longer observed, where mock expression averages at 2.31-fold and highly pathogenic IAV infected average expression is 3.32-fold (Figure 3-6B).

3.1.6 Ducks have two *TRIM19* or *TRIM19-like* genes

TRIM19, also known as promyelocytic leukemia factor (PML) is a well characterized antiviral TRIM (Chelbi-Alix *et al.* 1998) and transcription factor (Wu 2003). The chicken genome annotation predicts three separate coding regions for PML (XM_413690.3 and XM_413692.3) or PML-like (XM_003641812.1) genes (NCBI, 2012). The draft duck genome originally predicted three separate partial transcripts for TRIM19 (Apl_10900 (EOB00009.1), Apl_10902 (EOB00003.1) and Apl_10903 (EOB00004.1) located within duck scaffold878 (KB743248.1) (Table A-1) (a schematic of this scaffold is available in Figure 3-7). Conversely, annotated in the available duck

genome assembly on Ensembl indicates a single partial PML transcript (ENSAPLG00000001534) in scaffold878 (KB743248.1).

Human TRIM19, or PML, has a number of different annotated isoforms, the longest being isoform 1 (or TRIM19α) which is an 882 amino acid long transcription factor. To determine which of the coding sequences in the draft genome corresponds to a legitimate prediction, I aligned the protein sequences to the human homolog TRIM19 isoform 1 (NP_150241.2). The first coding sequence prediction in the draft genome (Apl_10900) corresponds to a 204 amino acid protein which aligns most closely to the B-Box region of human TRIM19. The second coding sequence prediction in the draft genome (Apl_10902) corresponds to the B-Box and coiled-coil region of human TRIM19. The third coding sequence prediction in the draft genome (Apl_10903) corresponds a region of human TRIM19 located between the B-Box and the extreme C-terminus of TRIM19 known as the DUF3583 domain which has an unknown function. As such, the duck genome annotation did not predict a full length TRIM19, only parts of the predicted transcription factor.

We used the gene prediction software to verify the predictions (GenScan, MIT server) using scaffold878 and predicted a total of 13 ORFs within the scaffold. I predicted only two ORFs in scaffold 878 which have homology to TRIM19. I were able to predict two PML-like coding regions within scaffold878, and eleven other putative non-TRIM genes within the scaffold which display syntenic organization with the available chicken genome (NCBI). The first GenScan predicted protein (PML-1 or TRIM19-1) is a 342 amino acid protein which corresponds to the B-Box region of TRIM19 and has high percent identity to the 204 amino acid genome predicted Apl_10900 (Figure A-2). The second protein predicted by GenScan (PML-L2 and PML-L3 or TRIM19-2) is a 643 amino acid long protein which aligns to both Apl_10902 and

Apl_10903 on its N- and C-terminal domain, respectively (Figure A-3). What I have predicted for the duck scaffold878 is two coding regions which correspond to two TRIM19-like homologs. As the chicken genome predicts 3 separate TRIM19 or TRIM19-like genes, and our duck genome prediction only two there is a possibility that ducks lack a TRIM19 homolog that is present in the chicken. However, due to low sequence quality in this region of the duck genome, I am unable to accurately predict this without further investigation. I prepared a schematic of the draft duck genome prediction of scaffold878 which shows the orientation and location of the predicted coding sequences within the scaffold (Figure 3-7) as no RT-PCR or sequencing analysis was pursued for duck PML I cannot be sure if the GenScan predictions are accurate or if the draft duck genome prediction is accurate of three separate PML and PML-like genes (as depicted).

3.2 Expression of immune relevant TRIM genes during influenza A infection.

In order to determine what TRIMs to pursue as candidate duck specific immune *TRIM* genes, I had to first determine if our short list of candidates are upregulated during an IAV infection. Using cDNA samples from ducks infected previously with low pathogenic IAV (BC500), highly pathogenic IAV (VN1203) or with mock infection, I looked at the expression level of *TRIMs* located within scaffold618. In order to verify the coding sequence predictions, narrow our pursuit and assess the immune relevance of each scaffold618 *TRIM*, I used RT-PCR to amplify the transcripts from cDNA at different cycle numbers to estimate the relative expression level of each *TRIM* in lung tissue (Figure 3-8). All four TRIMs examined by RT-PCR were shown to be upregulated in cDNA from 1 dpi lung tissue.

We were unable to amplify *TRIM27.2* or *TRIM41* from cDNA samples using a variety of primer combinations, annealing temperatures and enzymes. I designed one set

of qPCR probes and primers for both *TRIM27.2* and *TRIM41* to amplify them with highly sensitive TaqMan gene specific probe system. The probes for *TRIM41* yielded no detectable product after 40 cycles from highly pathogenic IAV infected lung (data not shown) and the probes for *TRIM27.2* detects only at 39.1 cycles or higher which is over the threshold of reliable information and is less than a single cycle away from being undetected (data not shown). Most samples with the *TRIM27.2* probe were undetectable indicating no transcript amplification. Due to time constraints no further exploration of these candidates was pursued

We were able to amplify *TRIM7.1* (Apl_13518 that was determined to be *TRIM7.1* and *TRIM39.2*) and the product was sequenced to confirm the new predicted CDS. I designed two sets of qPCR probes for *TRIM7.1* in order to assess expression with highly sensitive TaqMan gene specific probe system. Both sets of probes for *TRIM7.1* failed validation (data not shown). Due to time constraints no further exploration of this candidate was pursued.

3.2.1 Quantification of expression of *TRIM27.1a* in infected ducks

qPCR shows that *TRIM27.1a* is highly upregulated in 1 dpi highly pathogenic IAV (VN1203) infected lung tissue (Figure 3-9A). The mean expression level of the three ducks is 34.36-fold above the level of mock samples. This upregulation is very short lived however, and by 2 dpi in lung tissue expression is consistent between infected and uninfected samples.

We also looked at relative expression in intestine and spleen samples from the same ducks. These are influenza or immune relevant organs, so expression of candidate TRIMs in either of these organs indicated involvement in viral restriction or immune modulation. As low pathogenic IAV replicates in the duck intestine, I used intestine samples from 1 and 3 dpi to look at relative expression (Figure 3-9B). Expression level of

TRIM27.1a was not affected by low pathogenic IAV (BC500) infection in the intestine. Apart from a single duck which had a slightly upregulated amount of transcript for *TRIM27.1a* in the intestine 1 dpi, the expression remained relatively constant compared to mock birds. The same is true for spleen samples at 1 and 3 dpi (Figure 3-9C). No differential expression was observed in spleen during the course of both low and highly pathogenic IAV infections.

3.2.2 Quantification of expression of *TRIM27.1b* in infected ducks

qPCR shows that *TRIM27.1b* is also upregulated in 1 dpi highly pathogenic IAV (VN1203) infected lung tissue (Figure 3-10A), although to a lesser extent than *TRIM27.1a* (Figure 3-9A). The mean expression level of the three ducks is 5.32-fold above the level of mock samples, with a range between 3.38- and 7.78-fold. However, upregulation of *TRIM27.1b* is more prolonged compared to *TRIM27.1a* and slowly decreases 2 dpi to an average of 3.42-fold above mock and down to 1.29-fold above mock by 3 dpi in lung (Figure 3-10A).

In intestine, expression level of *TRIM27.1b* was not affected by low pathogenic IAV (BC500) as expression was similar to mock samples (Figure 3-10B). In highly pathogenic IAV (VN1203) infected spleen at 1 dpi there was a slight upregulation of TRIM27.1b above mock samples; expression was 2.74-fold higher in VN1203 spleen than mock spleen. Slightly elevated levels of expression persist in spleen at 3 dpi for both IAV infected samples (BC500 and VN1203).

3.2.4 Quantification of *TRIM7.2* expression

Based on the RT-PCR amplification of TRIM7.2 (Apl_13515) and the apparent upregulation at 25 cycles, I designed gene specific TaqMan probes and primers for quantitative real-time PCR (qPCR). cDNA samples were consistently calculated to be 500 ng based on nano-drop concentrations. For all qPCR, 1/10 dilutions were made of each sample to be used as template. Relative quantification (ddCT) of *TRIM7.2* shows that in highly pathogenic IAV (VN1203) infected lung tissues, *TRIM7.2* is upregulated an average of 4.24-fold above mock expression levels (Figure 3-11A) with a range of 1.85- to 5.81-fold in VN1203 infected lung tissue. Comparatively, there is no increase in level of expression of *TRIM7.2* during infection with a low pathogenic IAV (BC500) isolate in lung tissue, nor in intestine samples (where the virus will replicate) at either 1 dpi or 3 dpi (Figure 3-11B).

3.2.5 Quantification of expression of *TRIM39.2* in infected ducks

Relative quantification (ddCT) of *TRIM39.2* shows that at 1 dpi, relative expression of *TRIM39.2* remains constant in both lung and intestine samples (Figure 3-12A and B). However, at 3 dpi in intestine there is an upregulation of TRIM39.2 in low pathogenic IAV (BC500) infected samples; mean expression is 5.30-fold greater than mock samples (Figure 3-12B). In 1 dpi spleen samples, *TRIM39.2* expression is elevated (5.14-fold) in highly pathogenic IAV (VN1203) infected samples over mock and low pathogenic IAV (BC500) infected samples (Figure 3-12C).

3.2.6 RT-PCR expression of pTRIM27d displays no patterns of expression

The draft genome has annotated Apl_13524/ EOB02166.1 as a *TRIM27-like* gene (*pTRIM27d* for partial TRIM27); however the predicted sequence, as stated earlier, is a

fragment of a gene with a PRY/SPRY domain and homology in the C-terminal domain to TRIM27. Through sequence alignments of TRIM27 homologs from multiple species, manual queries for conserved amino acid sequences and gene prediction software – I were able to predict a larger ORF for *pTRIM27d*. Although, I were never able to predict a RING-domain. As a result, I am no longer annotating Apl_13524/ EOB02166.1 as a TRIM because it lacks one of the essential components of the tripartite-motif. Due to the sequence homology with other TRIM27-like PRY/SPRY containing butyrophilin, I am annotating this gene – not as *pTRIM27d* – but as a *TRIM27-like BTN* gene (or BR gene meaning *B30.2*-related gene) as per the original chicken annotation (Ruby *et al.* 2005).

Regardless of nomenclature, I examined the expression of this gene through RT-PCR to look at the potential for it to be involved in immune response. An inconsistent expression pattern was observed for the gene product which does not seem to follow any pattern of expression relative to infection (Figure 3-13). As a result, I did not pursue expression work on this gene.

3.3 Diversity in *TRIM27.1a* and *TRIM27.1b*

The MHC is the most rapidly evolving region of the genome (Kelley *et al.* 2005). As such, the genes located within the MHC, or the telomeric regions around MHC class I genes, would be subject to mutation, selection and evolution. When I amplified and sequenced *TRIM27.1a* and *TRIM27.1b* from infected lung samples, I observed polymorphisms in the sequences such that it warranted further investigation of diversity in the two genes. I attempted to assemble a clear picture of single nucleotide polymorphisms (SNPs) in the two genes from both alleles in three different White Pekin ducks.

3.3.1 *TRIM27.1a* and *TRIM27.1b* are polymorphic genes

A total of 16 individual clones for *TRIM27.1a* were fully sequenced (complete coverage in both the forward and reverse orientations) and aligned from all three ducks. I sequenced 2 clones fully for allele A and allele B for duck 310,4 clones for allele A and 3 clones from allele B from duck 312, and 5 clones of only allele A from duck 401 (Table A-3). Once the alleles were identified, the aligned consensus of each allele was exported and aligned with the consensus sequence of the other alleles from all three birds. Alignment of alleles showed that *TRIM27.1a* is highly polymorphic. In the 1506 base pairs, there are 27 SNP sites in the length of the sequence when the available alleles for all 3 ducks are aligned.

Translated sequences from each allele of *TRIM27.1a* were also aligned (Figure A-4) to look at amino acid changes in the sequence (Figure A-5). The 27 different SNP sites in TRIM27.1a correspond to only 3 different positions of amino acid changes in the length of the 502 amino acid protein. Position 116 in allele A of duck 310 changed from a methionine to a threonine (M to T); hydrophobic to polar. Position 210 in allele B of duck 312 changed from a threonine to a serine (T to S); polar to polar. Finally, position 356 in both alleles of duck 312 changed from threonine to isoleucine (T to I); polar to non-polar. When plotted on the protein domains, the amino acid substitutions are located within the B-box domain (M116T), coiled-coil domain (T312S) and the PRY domain (T356I) (Figure 3-14).

A total of 19 individual clones for *TRIM27.1b* were fully sequenced and aligned from all three ducks (Table A-4). I were able to sequence 4 clones from allele A and 1 clone from allele B from duck 310, 4 clones from both allele A and allele B from duck 312 and 4 clones of allele A and 2 clones from allele B from duck 401. Alignment of

alleles showed that *TRIM27.1b* is less polymorphic than *TRIM27.1a*. In the 1425 base pairs, there are 10 SNP sites in the length of the sequence when the available alleles for all 3 ducks are aligned.

Translated sequences from each allele of *TRIM27.1b* were also aligned to look at amino acid changes in the sequence (Figure A-6). The 10 different SNP sites in *TRIM27.1b* correspond to only 2 different positions of amino acid changes in the length of the 475 amino acid protein. Position 18 in allele B of duck 401 changed from isoleucine to threonine (I to T); polar to non-polar. Position 320 in allele A of duck 310 changed from valine to alanine (V to A); non-polar to non-polar. When plotted on the protein domains, the amino acid substitutions are located within the RING domain (I18T) and the PRY domain (V320A) (Figure 3-15).

Table 3-1. The recognizable TRIM genes within the draft White Pekin duck genome.

This list includes the predicted TRIM family member, internal accession number and scaffold location. Purple colour denotes group 1 *TRIM*s and pink colour denotes group 2 *TRIM*s. *TRIM*s indicated in yellow are located within scaffold618 and are all members of the group 2 *TRIM*s.

TRIM Name	Accession #	Scaffold #	TRIM Name	Accession #	Scaffold #
TRIM2	Apl_07723	800	*TRIM29*	Apl_09494	1071
TRIM2	Apl_07724	800	*TRIM32*	Apl_17261	2638
TRIM2	Apl_13416	2573	*TRIM33*	Apl_02969	191
TRIM7	Apl_13518	618	*TRIM35*	Apl_09916	1179
TRIM7	Apl_19037	11780	*TRIM36*	Apl_15966	408
TRIM7.2	Apl_13515	618	*TRIM37*	Apl_03938	337
TRIM8	Apl_10359	140	*TRIM39.2*	Apl_04891	436
TRIM9	Apl_07920	548	*TRIM39.2*	Apl_04892	436
TRIM13	Apl_09271	402	*TRIM41*	Apl_13522	618
TRIM14	Apl_15985	1806	*TRIM41*	Apl_12894	1764
TRIM19 (PML)	Apl_10900	878	*TRIM41.1*	Apl_18738	7870
*TRIM19 (PML)**	Apl_10902	878	*TRIM42*	Apl_15133	928
	Apl_10903	878	*TRIM45*	Apl_15448	380
TRIM23	Apl_12966	245	*TRIM47*	Apl_10274	95
TRIM24	Apl_02850	821	*TRIM50*	Apl_04886	436
TRIM25	Apl_03154	202	*TRIM54*	Apl_16433	3250
TRIM27	Apl_13519	618	*TRIM55*	Apl_08276	662
TRIM27	Apl_13520	618	*TRIM59*	Apl_09116	1824
TRIM27	Apl_13521	618	*TRIM62*	Apl_10231	324
TRIM27	Apl_13524	618	*TRIM63*	Apl_14136	803
TRIM28	Apl_18731	2775	*TRIM66*	Apl_11973	1265
TRIM28	Apl_18504	unassigned	*TRIM67*	Apl_05239	759
TRIM29	Apl_09489	1071	*TRIM69 or 47*	Apl_10275	95
TRIM29	Apl_09493	1071	*TRIM71*	Apl_06226	581

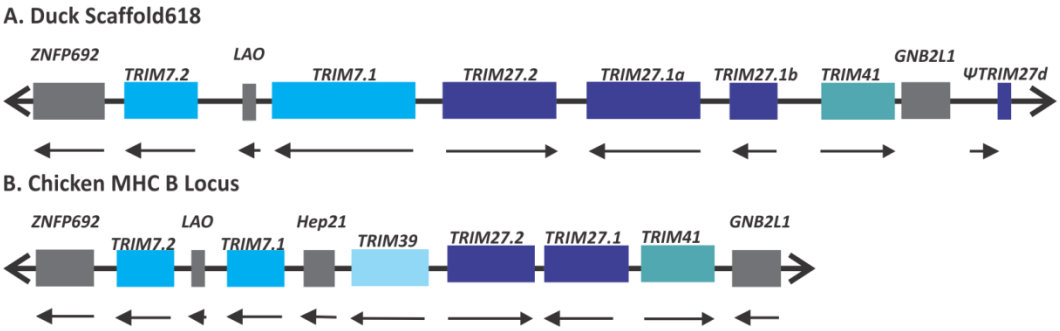

Figure 3-1. Schematic representation of the recognizable genes predicted in scaffold618 as originally annotated in the draft genome and the genomic organization of the chicken MHC B locus.
For syntenic comparison between (A) the draft White Pekin duck (*Anas platyrhynchos*) genome and (B) the available domestic chicken (*Gallus gallus*) genome (NCBI, GenBank: AADN03007209.1). This map has since been edited and revised, but is indicative of the automated draft genome prediction.

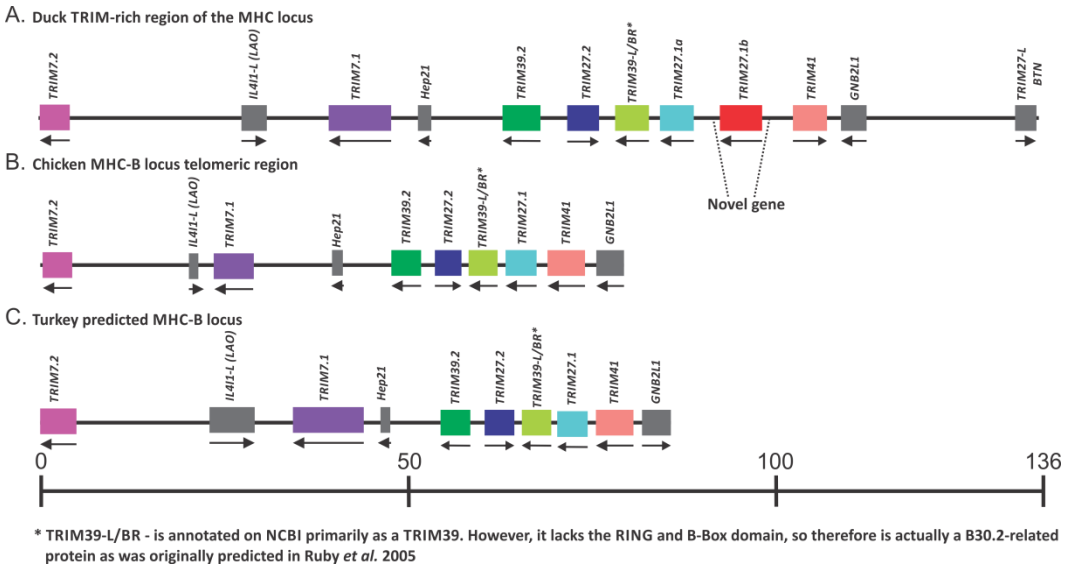

* TRIM39-L/BR - is annotated on NCBI primarily as a TRIM39. However, it lacks the RING and B-Box domain, so therefore is actually a B30.2-related protein as was originally predicted in Ruby *et al.* 2005

Figure 3-2. Scale revised schematic representation of genomic organization of the TRIM-rich region of avian MHC B loci.

This image demonstrates the conserved gene synteny of (A) duck TRIM genes and the (B) chicken and (C) turkey TRIM-rich regions. The gene length and positions are to scale and are based on the annotation of scaffold618 and previously published scale schematics (Ruby *et al.* 2005; Chaves *et al.* 2009). Non-TRIM genes are depicted in grey, homologs are depicted in different shades of the same colour.

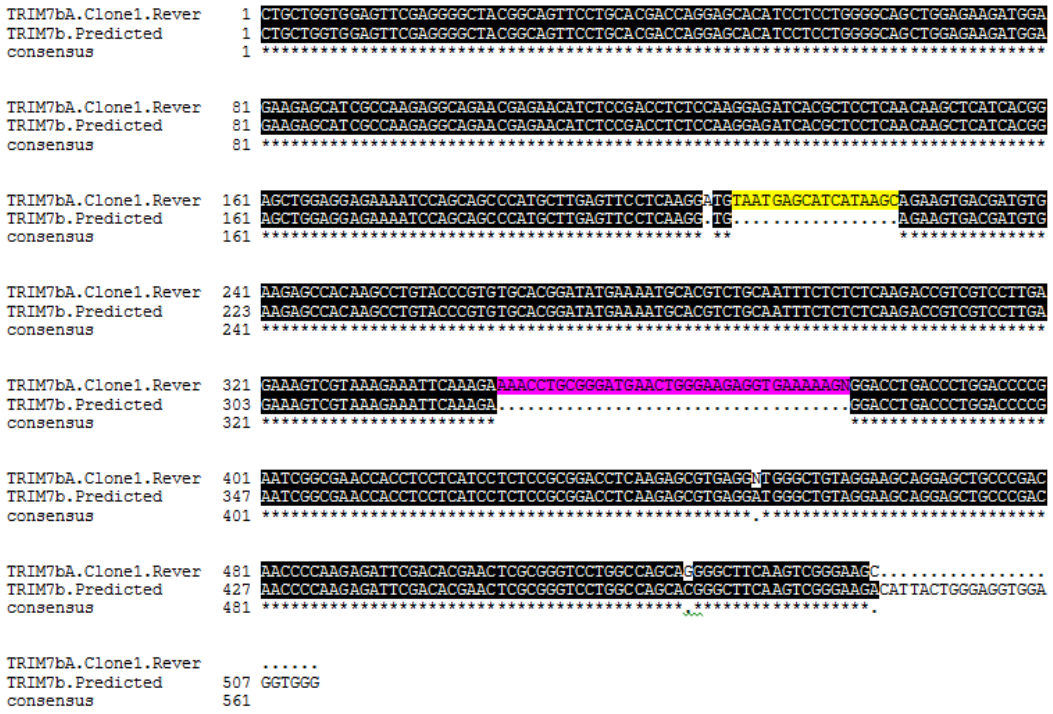

Figure 3-3. Alignment of the original *TRIM7.1* CDS predicted in scaffold618 and the sequence derived from RT-PCR of the C-terminal end of duck *TRIM7.1*.
The regions highlighted indicate a previously unannotated exon 8 (yellow) and exon 10 (pink). Five individual clones for TRIM7.1 were analyzed and confirm the sequence.

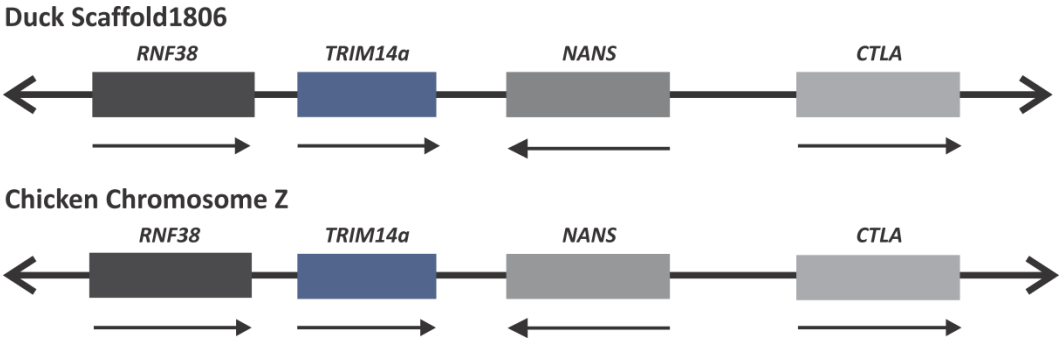

Figure 3-4. Schematic of duck scaffold1806 which contains the putative *TRIM14* coding sequence.
In the draft White Pekin genome is a single predicted TRIM14 ORF that is located within scaffold1806. This CDS falls between two genes, *ring finger protein 38* (*RNF38*) and *N-acetylneuraminic acid synthase* (*NANS*). Downstream is *clathrin light chain A* (*CTLA*). In the chicken, all 4 of these genes are located on chromosome Z.

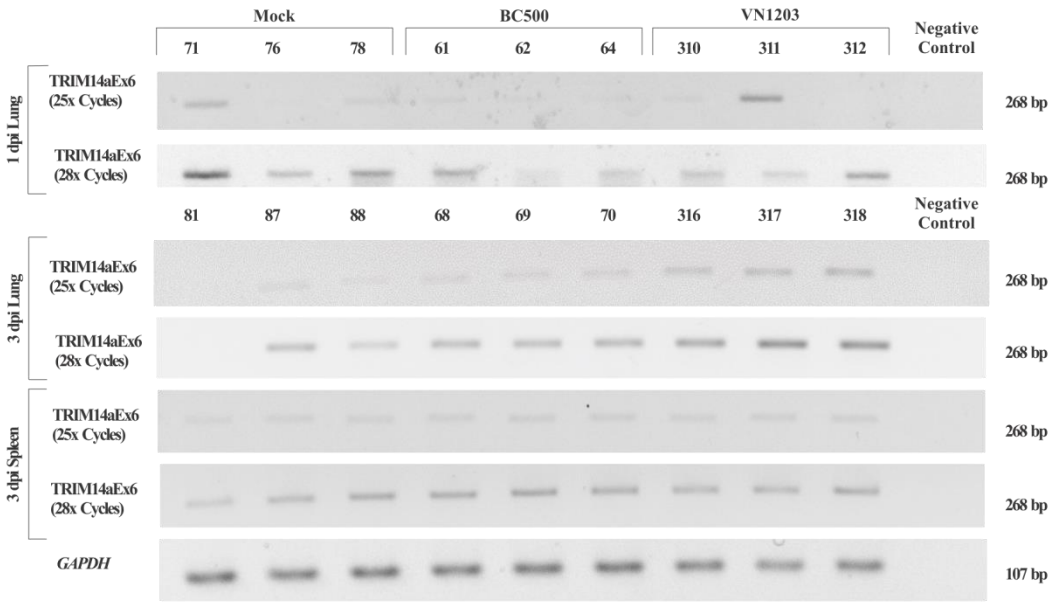

Figure 3-5. RT-PCR amplification of duck *TRIM14* transcript to determine relative expression level in infected tissue samples.
Primers amplified C-terminal coding sequence at different time points. Samples of 1000 ng cDNA were used to amplify the sequence confirmed transcript of duck TRIM14 (Apl_15985). Expression of *TRIM14* at 1 dpi in lung displays no obvious trend. By 3 dpi, expression of *TRIM14* is higher in the highly pathogenic IAV (VN1203) infected lung tissue than the mock samples (by visual inspection of band intensity). At 3 dpi in the spleen, no obvious changes in expression levels are observed, indicating relatively common expression levels regardless of infection. Numbers indicate unique internal duck identifying numbers for the experimental infection.

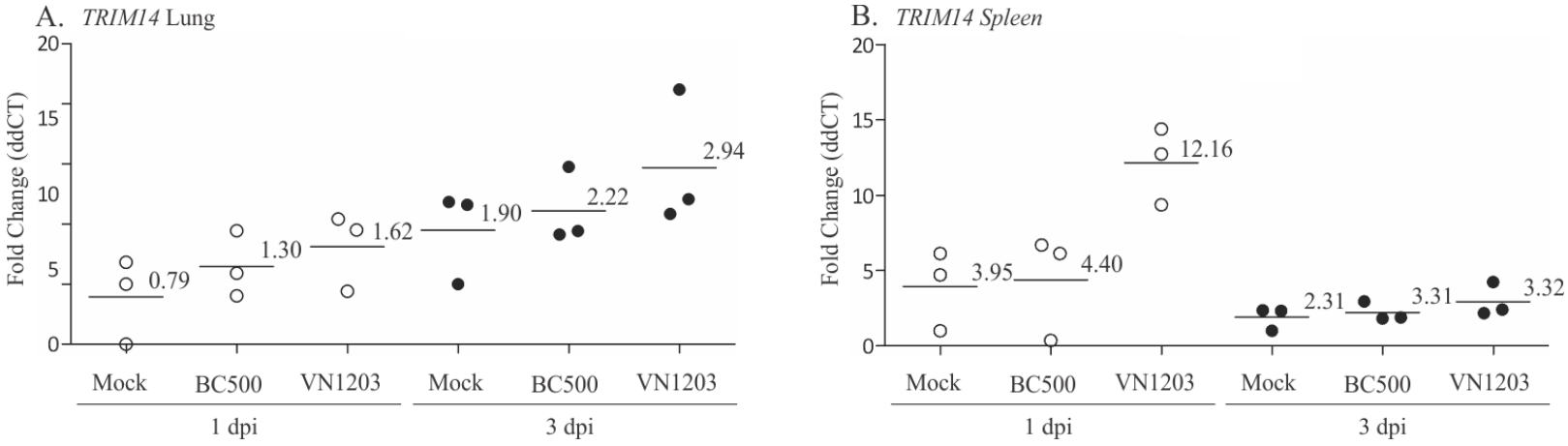

Figure 3-6. Duck *TRIM14* transcript is not differentially expressed in lung samples at 1 and 3 dpi but is upregulated at 1 dpi in spleen.

Quantitative real-time (qPCR) shows that *TRIM14* at 1 dpi and 3 dpi in mock, low pathogenic (BC500) and highly pathogenic (VN1203) IAV infected (A) lung tissue; there is fairly consistent expression, regardless of infection. In highly pathogenic (VN1203) IAV infected (B) spleen at 1 dpi, I do observed increased expression - even though there is variability within the mock and low pathogenic IAV (BC500) samples. By 3 dpi in VN1203 infected spleen, this upregulation is abrogated. Statistical analysis was performed using a one-way ANOVA test for variance with Tukey's multiple comparison post-hoc test with an α of 0.05, comparisons of the samples of the same dpi compared to mock were not significant.

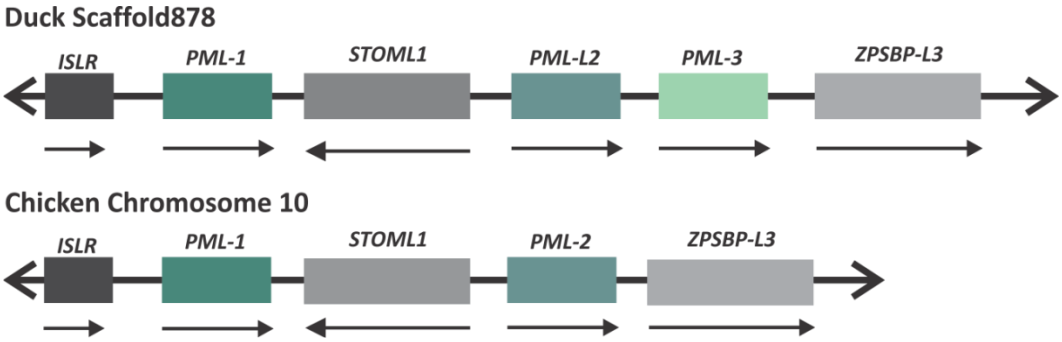

Figure 3-7. Duck scaffold878 contains three predicted *PML* coding regions.
In scaffold878 of the draft White Pekin genome, three separate *PML* (or *TRIM19*) ORFs are predicted. This is a schematic of the PML region, but the scaffold878 non-*TRIM* genes is syntenic with the chicken chromosome 10 region. Immediately upstream of the first *PML* prediction (Apl_10900) is immunoglobulin superfamily containing leucine-rich repeat (ISLR). Immediately downstream of *PML-1* is *stomatin (EPB72)-like 1*(*STOML1*). Downstream of *PML-L2* (Apl_10902) and *PML-L3* (Apl_10903) is *zona pellucida sperm-binding protein 3-like* (*ZPSBP-L3*).

74

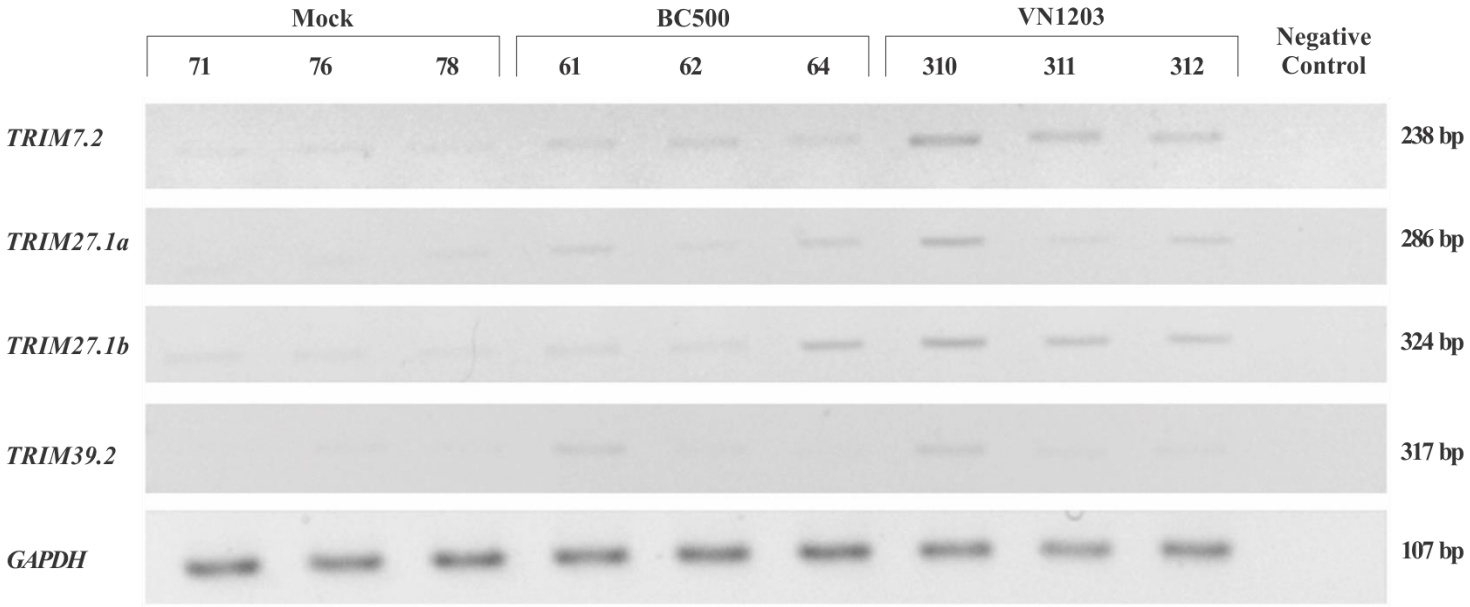

Figure 3-8. *TRIM7.2, TRIM27.1a, TRIM27.1b* and *TRIM39.2* are upregulated in 1 dpi lung tissue.
RT-PCR using Platinum taq (Invitrogen) enzyme at 25 cycles shows increased band intensity for all four TRIM genes examined. *TRIM7.2* is upregulated in both low pathogenic IAV (BC500) and in highly pathogenic IAV (VN1203) infected lung tissues for all 6 ducks as compared to the lower level of expression (lighter band intensity) for mock samples. *TRIM27.1a* is upregulated in VN1203 infected lung as compared to the near absence in the mock samples. *TRIM27.1b* is highly upregulated in VN1203 infected samples and in duck 61 and 64 of the BC500 infected lung samples. *TRIM39.2* is also upregulated in VN1203 samples and in duck 61 infected with BC500. GAPDH measures cDNA quality and the endogenous control is stable across all cDNA samples.

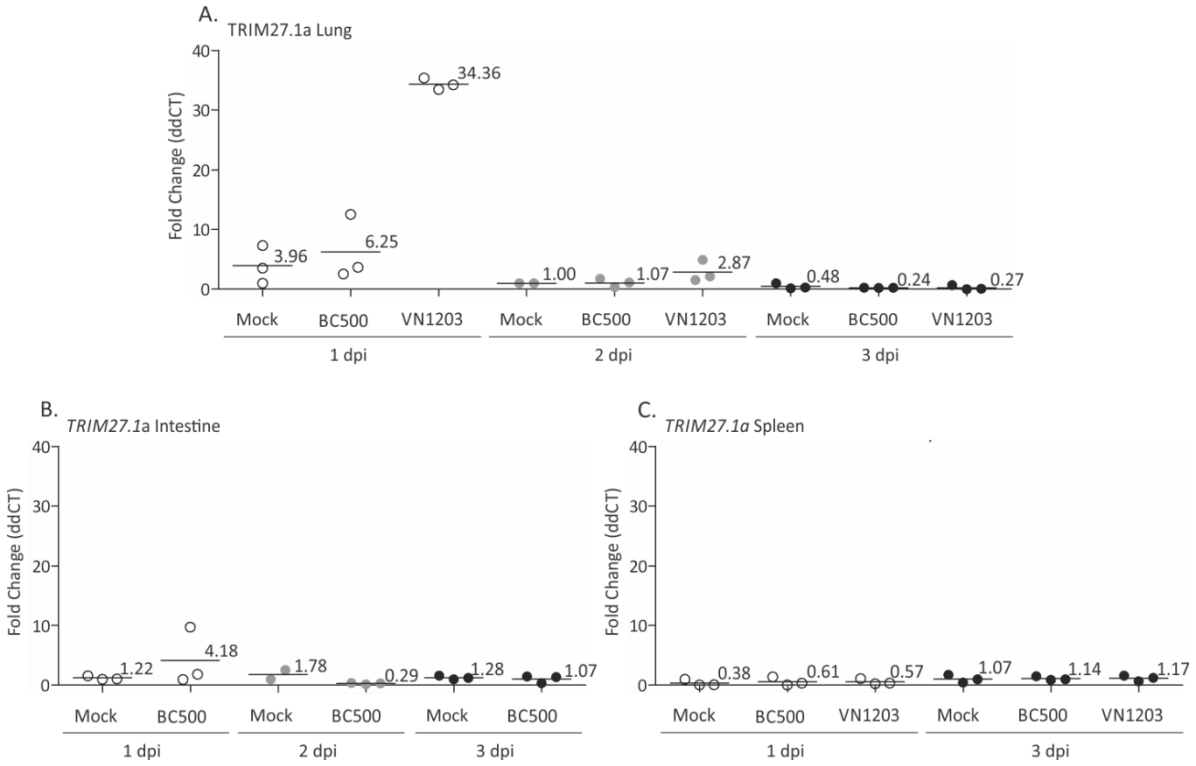

Figure 3-9. Expression of *TRIM27.1a* in infected lung tissue is higher in VN1203 infected tissues.
TRIM27.1a is most highly upregulated in (A) highly pathogenic IAV (VN1203) infected lung tissue at 1 dpi. Expression rapidly drops off and returns to the level of mock by 2 dpi. In (B) Intestine samples, *TRIM27.1a* is very slightly upregulated (mean of 4.18 fold over the level of mock) during low pathogenic IAV (BC500) infection at 1 dpi, but no expression changes are observed on 2 or 3 dpi. There is no change in expression (C) in spleen of *TRIM27.1a* during the course of an early infection with either BC500 or VN1203.

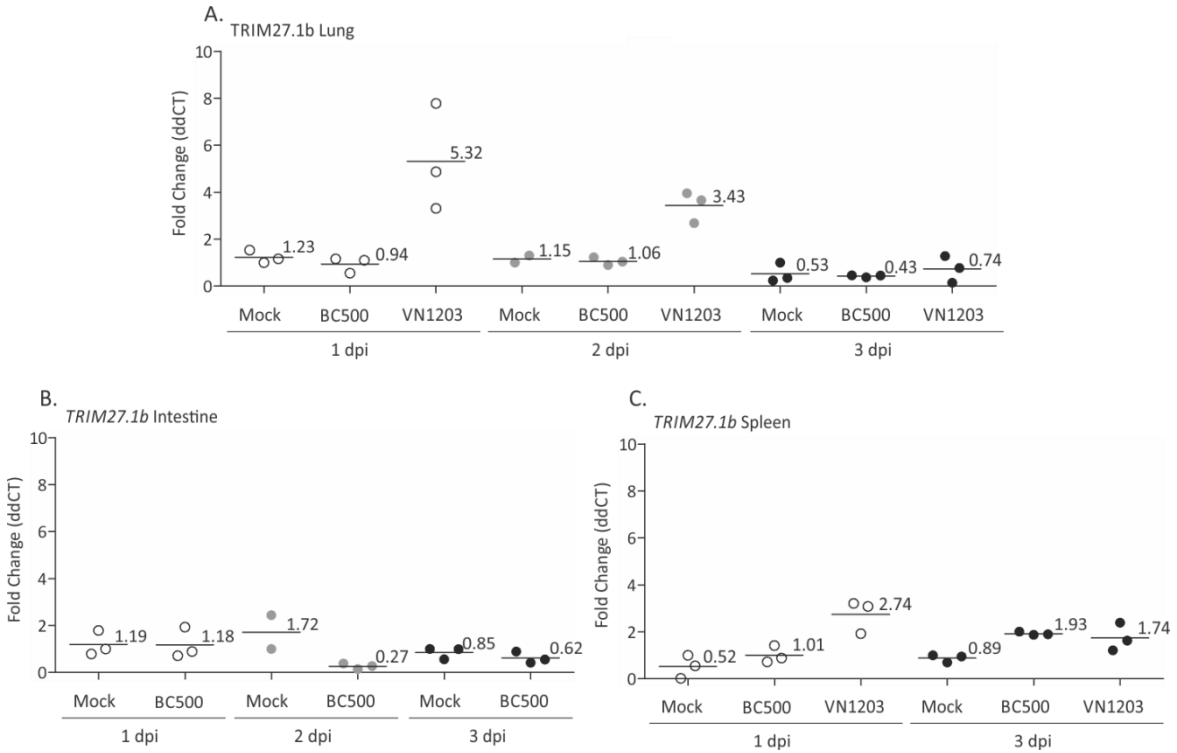

Figure 3-10. Expression of *TRIM27.1b* in infected lung tissue is higher in VN1203 infected lung and spleen tissues.
TRIM27.1b is upregulated in (A) highly pathogenic IAV (VN1203) infected lung tissue at 1 dpi. Expression drops off slowly and returns to the level of mock by 3 dpi. In (B) Intestine samples, *TRIM27.1b* expression is consistent across all samples and days. There is a slight increase in expression (C) in spleen of *TRIM27.1b* at 1 dpi with VN1203.

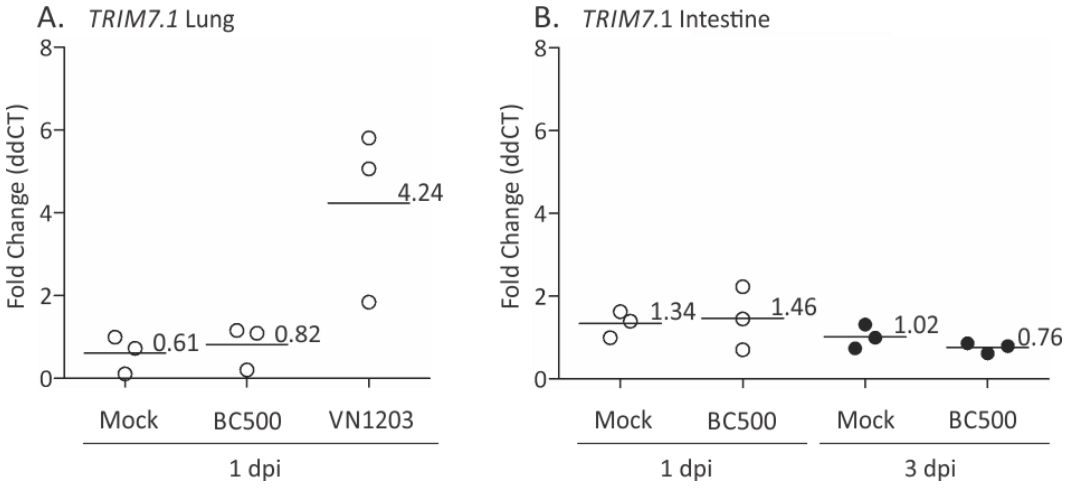

Figure 3-11. *TRIM7.2* is upregulated in highly pathogenic IAV infected duck lung at 1 dpi.

Quantitative real-time (qPCR) shows that *TRIM7.2* is (A) slightly upregulated in 1 dpi in highly pathogenic IAV (VN1203) infected lung tissue. The mean expression level of the three ducks is 4.24 above the level of mock samples. However, in (B) intestine samples infected with the low pathogenic IAV (BC500) expression level of *TRIM7.2* does not change at either 1 dpi or 3 dpi as compared to mock. Statistical analysis was performed using a one-way ANOVA test for variance with Tukey's multiple comparison post-hoc test with an α of 0.05, comparisons of the samples compared to mock are shown with an asterisk denoting significance, * is $p < 0.05$.

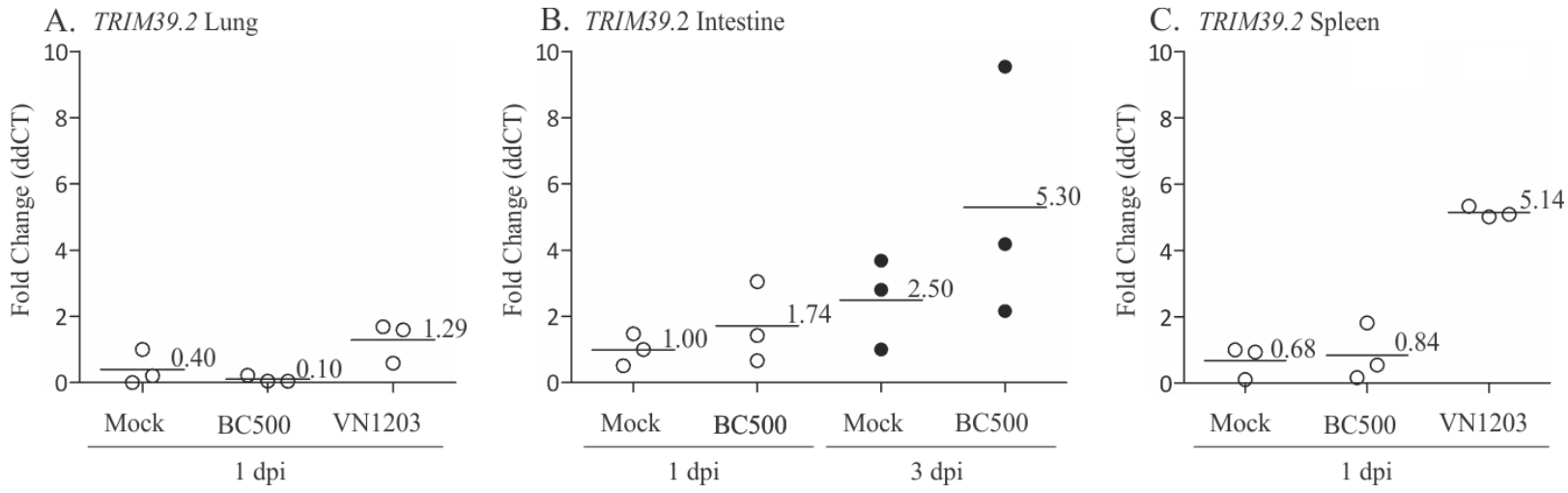

Figure 3-12. *TRIM39.2* is upregulated in low pathogenic IAV infected duck intestine at 3 dpi and VN1203 infected spleen tissue at 1 dpi.

Quantitative real-time (qPCR) shows that *TRIM39.2* is (A) slightly upregulated in 1 dpi in highly pathogenic IAV (VN1203) infected lung tissue, but (B) more highly upregulated in low pathogenic IAV (BC500) infected intestine 3 dpi. The increase seems to be more gradual and sustained in intestine than in lung tissue. (C) At 1 dpi in the spleen *TRIM39.2* is upregulated 5.14-fold during high path infection.

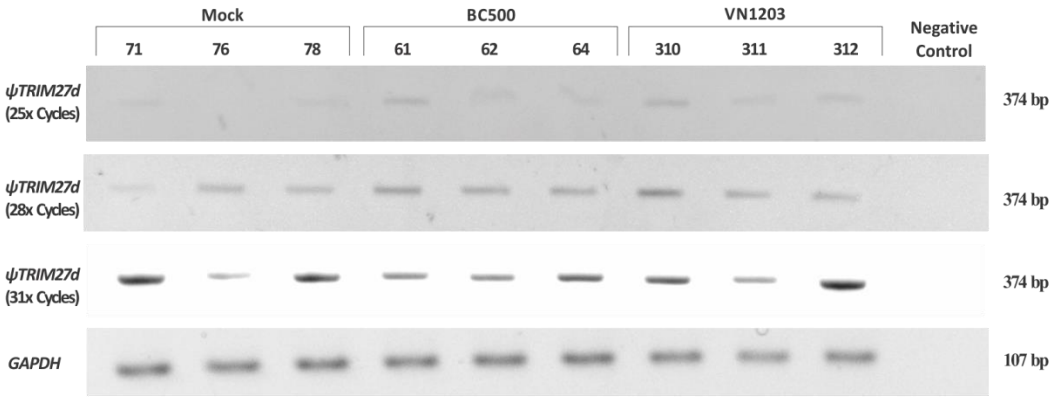

Figure 3-13. RT-PCR amplification of duck *pTRIM27d* (*TRIM27-L/BTN*) transcript to determine relative expression level in infected tissue samples at 1 dpi.
RT-PCR using platinum taq enzyme at 25, 28 and 31 cycles demonstrates the consistent level of expression of *pTRIM27d* over lung tissue regardless of infection. RT-PCR was conducted before a thorough analysis of the genome region around *pTRIM27d* was conducted and before the conclusion of *pTRIM27d* as a member of the butryrophilin family was made and I renamed this gene product *TRIM27-L/BTN*.

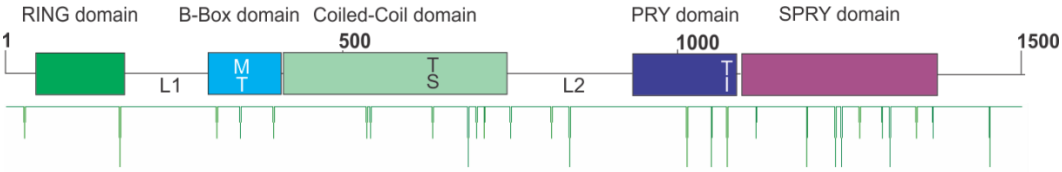

Figure 3-14. SNP substitution heat map in the protein domains of TRIM27.1a and the corresponding amino acid changes.
A total of 27 SNP sites occur within the length of *TRIM27.1a*. This corresponds to only 3 amino acid substitutions in the B-box, coiled-coil and PRY domains.

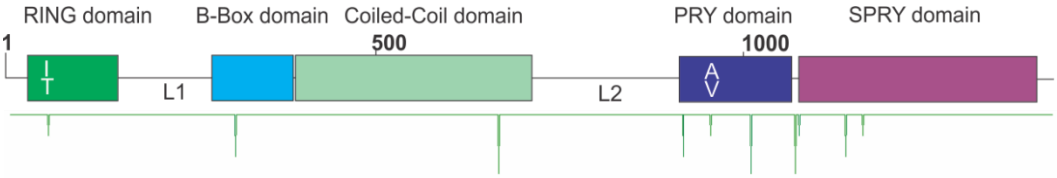

Figure 3-15. SNP substitution heat map of *TRIM27.1b* and the corresponding amino acid substitutions.
A total of 10 SNP sites occur within the length of *TRIM27.1b* which corresponds to only 2 amino acid substitutions in the RING and PRY domain.

Chapter 4. RESULTS AIM 3

4.1 Characterization of TRIM27.1a and TRIM27.1b

Our aim was to search for a duck TRIM that was unique from chickens which could play a role in differential susceptibility to IAV infection. By using the information obtained from genomic annotations, expression analysis and the literature, I narrowed our focus on two TRIMs located within the TRIM-rich MHC region of ducks – *TRIM27.1a* and *TRIM27.1b*. These two genes fit our criteria as a candidate duck specific immune-relevant TRIM for a number of reasons; 1. they are located within the duck MHC region which is the immune centre of the genome, 2. the expression of both of these *TRIM*s is upregulated early in the innate immune response of ducks to highly pathogenic IAV (VN1203) infection, 3. they appear to be a duplication which is duck specific (as *TRIM27.1b* is absent in both the chicken and turkey MHC locus predictions), and 4. human TRIM27 (Ret-finger protein) is known to interact with members of the IKK-family of proteins which are integral signaling components of the intracellular innate immune pathway (Zha *et al.* 2006). As such, I focused our efforts on these two genes and pursued functional characterization of *TRIM27.1a* and *TRIM27.1b* in transfected cells.

4.1.1 *TRIM27.1a* and *TRIM27.1b* are likely the product of gene duplication

TRIM27.1b appears to be a duck specific gene product which is absent in the chicken and turkey genomes. As the genes for *TRIM27.1a* and *TRIM27.1b* appear adjacent to one another in scaffold618 (Figure 3-2) and their ORF reads in the same direction I predicted that *TRIM27.1a* and *TRIM27.1b* are products of a duck specific gene duplication event. TRIM27.1a and TRIM27.1b have the same conserved domain architecture (Figure 4-1) including the typical TRIM characteristics of RING, B-box and coiled-coil domains and a C-terminal PRY/SPRY domain. Although the domain

architecture is conserved between the two TRIM27.1 proteins, the two TRIM27.1 gene products have low amino acid sequence identity; TRIM27.1a and TRIM27.1b share only 51% identity to each other.

Because TRIM27 and TRIM39 are homologs (Homologene, NCBI) and to ensure correct annotation of the novel duck gene as *TRIM27.1b*, I aligned the amino acid sequences from all TRIM27s and TRIM39s located within scaffol618 (Table 4-1). TRIM27.1b shares the highest identity with TRIM27.1a (51% identity). In the RBCC motif, TRIM27.1a and TRIM27.1b are 53% identical and in the PRY/SPRY domain they are 51% identical. As this is the highest overall homology to any of the other paralogous genes I am hypothesizing that *TRIM27.1a* and *TRIM27.1b* are the products of a duplication event of an ancestral TRIM27.1 gene in the duck which has since diverged in sequence and possibly functionally.

As human TRIM27 is known to be involved in immune regulation in cells (Dho & Kwon 2003; Zha *et al.* 2006) I hypothesized that one, or both, of the duck TRIM27.1 proteins may play a similar role in the intracellular innate immune response pathway. I assessed if structural and amino acid similarity exists between the human TRIM27 and either of the duck TRIM27.1 genes. The percent identity of TRIM27.1a and TRIM27.1b is 41% and 38% identity with human TRIM27, respectively (Figure A-8 and Figure A-9). This is not unusually low when one compares homologous gene products from humans and avian species.

4.1.2 *TRIM27.1b* is distinct from *TRIM27.1* of chickens and turkeys

To understand the origins of *TRIM27.1a* and *TRIM27.1b* in ducks, alignments of the chicken and the turkey TRIM27.1 and TRIM27.2 amino acid sequences were completed and phylogenetic trees assembled from the amino acid sequence alignment (Figure 4-2). As predicted, TRIM27.2 proteins from duck (EOB02164.1) chicken

(NP_001092829.1) and turkey (ACA64760.1) group together and TRIM27.1a aligns very strongly with chicken TRIM27.1 (NM_001030671.2) and turkey TRIM27.1 (ACA64758.1). Although TRIM27.1b groups more strongly with chicken and turkey TRIM27.1, it is certainly distinct and diverges early from the TRIM27.1 alignment (Figure 4-2). For this alignment, I included duck TRIM7.1 amino acid sequence as a closely related outgroup.

4.2 Functional characterization of *TRIM27.1a* and *TRIM27.1b* through transient co-transfection in DF1 cells

As human TRIM27 has been shown in interact with members of the IKK-family (Zha *et al.* 2006) which are signaling components downstream of the retinoic acid-inducible gene I (RIG-I) pathway, I sought to express the duck *TRIM27.1a* and *27.1b* genes in RIG-I activated cells. A well characterized and robust system for measuring innate intracellular immune responses of DF1 (chicken embryonic fibroblast) cells has been established in our lab (Miranzo-Navarro, unpublished) (Barber *et al.* 2010). I employed the use of a constitutively active RIG-I construct composed of a Glutathione S-Transferase (GST) fused to the two tandem duck caspase recruitment domains (d2CARD) from duck RIG-I (Miranzo-Navarro, unpublished), and co-transfection of TRIM genes to determine what, if any, role *TRIM27.1a* and *TRIM27.1b* play in the antiviral response of ducks.

As we do not currently have a duck derived cell line, we employ the use of chicken DF1 cells to examine interactions of RIG-I, IAV and the downstream effectors. Although an imperfect system to examine this interaction, chicken DF1 cells do have a number of advantages as well as the obvious disadvantages. RIG-I and another cytoplasmic retinoic acid-inducible gene family member, Melanoma Differentiation-

Associated protein 5 (MDA5) share the same downstream cytoplasmic signaling components; as chickens do not have the gene for RIG-I but do have the MDA5 gene, the signaling components downstream of RIG-I are intact and functional. Our lab has previously demonstrated this functionality of chicken DF1 cells transfected with duck RIG-I (Barber *et al.* 2010). In addition, as there is no endogenous RIG-I in DF1 cells, transient or stable transfections of duck RIG-I expression constructs will not have any confounding endogenous expression to contend with. By using this system of transient transfection of a constitutively active d2CARD construct we eliminate the need to turn on the signaling cascade through the use of exogenous ligand, such as 5'-triphosphate single-stranded RNA. This, therefore, eliminates an additional step which could increase the amount of experimental variability between different experiments while resulting in a robust and predictable stimulation of innate immune effectors in the transfected cells.

Another concern about using chicken DF1 cells is the cell type the line is derived from. Although chicken DF1 cells are derived from embryonic fibroblasts, and avian influenza is typically either a respiratory (highly pathogenic IAV infecting respiratory epithelial cells) or gastrointestinal (low pathogenic IAV replicating in the duck intestine) virus, the response to influenza infection may not be representative of the natural progression of infection in an *in vivo* duck model. However, 9 to 10 day old embryonated chicken eggs are used in order to propagate influenza virus. As such, chicken DF1 cells and embryonated chicken eggs do allow for influenza replication and are therefore a good ex vivo system to examine innate immune responses to active IAV infections.

As previously mentioned, RIG-I is a cytoplasmic sensor that binds to 5'-triphosphate single-stranded RNA produced during viral infection. RIG-I is composed of a helicase domain (which binds to the 5'-triphosphate end of single stranded viral RNA ligand) and 2 tandem CARD domains, RIG-I induces a signaling cascade which

culminates in the production of genes downstream of RIG-I (or the antiviral program) (Trowsdale & Parham 2004). Signaling is initiated through E3-ligase dependent ubiquitination of the CARD domains (Gack *et al.* 2007) which can function independently of the helicase domain (Glusman *et al.* 2000). The GST-d2CARD construct is constitutively active because the construct lacks the N-terminal helicase domain of RIG-I so there is no dependence on the native ligand to bind and allow for the conformational change which exposes the CARD domains to the E3-ligases which modify it, though still requires ubiquitination to become active.

RIG-I is present in ducks but absent in chickens (Barber *et al.* 2010), which allows the use of the GST-d2CARD construct in a chicken cell lines where no endogenous RIG-I exists. I expressed this construct transiently in chicken embryonic fibroblast (DF1) cells in order to induce the antiviral program in the transfected cells and increase production of the RIG-I bioset genes. This was integral to assessing the roles *TRIM27.1a* and *TRIM27.1b* could play in the pathway. I used an indirect measure of immune activation to assess involvement in the signaling cascade by using qPCR probes and primer sets for relative quantification of two genes downstream of the RIG-I pathway (Barber *et al.* 2013); interferon beta (*IFN-β*) and myxovirus resistance gene 1 (*MX1*).

In activated cells, where the GST-d2CARD construct was transiently transfected into the DF1 cells, a sharp increase in the total transcript of both *IFN-β* and *MX1* was observed. For the relative quantification purposes, I assigned this d2CARD sample as the calibrator ($22 \geq$ Ct value ≥ 24) (1.00-fold) in order to use a value for which the target gene of interest is clearly present (Ct value >35). All expression levels were therefore represented as fold-change respectively to the activated cell expression level. When transiently transfected into DF1 cells, in the absence of d2CARD (or resting cells), relative to the active cells and control cells transfected with just the control GST

construct, cells transfected with *TRIM27.1a* alone did not express either antiviral gene at 24 hours post-transfection (PT) (Figure 4-3 and Figure 4-5) or 48 hours PT (Figure 4-11). In the same way, *TRIM27.1b* alone did not affect transcription of *IFN-β* or *MX1* when transfected into cells at 24 hours PT (Figure 4-7 and Figure 4-9) nor at 48 hours PT (Figure 4-12).

When we analysed the three experimental replicates and observed a consistent trend of suppression of both anti-viral genes (Figure 4-4 and Figure 4-6). This is in line with our hypothesis that duck TRIM27.1 may perform a similar function as human TRIM27, in transiently co-transfected cells expression of the *TRIM27.1a* construct significantly decreased expression of our two antiviral genes; *IFN-β* ($p < 0.001$, $n = 3$) (Figure 4-4) and *MX1* ($p < 0.001$, $n = 3$) (Figure 4-6). On average, a decrease of 0.65-fold below the level of constitutively active cells (d2CARD transfected) was observed for *IFN-β* expression (Figure 4-4). Congruently, overexpression of *TRIM27.1a* in activated cells also decreased the expression level of *MX1* in co-transfected cells (Figure 4-6), although to a lesser extent than observed for *IFN-β* expression. On average, a decrease of 0.60-fold below the level of constitutively active cells (d2CARD transfected) was observed for *MX1* expression (Figure 4-6).

Contrary to our hypothesis, in transiently co-transfected cells expression of the *TRIM27.1b* construct increases expression of our two antiviral genes; *IFN-β* (Figure 4-7) and *MX1* (Figure 4-9). Consistently observed, an increase in *IFN-β* expression between 3.85-fold (Figure 4-7B) and 7.34- fold (Figure 4-7A) above the level of constitutively active cells (transfected with d2CARD) was observed. The same trend was observed for MX1 expression; with between 1.56-fold (Figure 4-9B) and 4.23-fold (Figure 4-9C) increase in expression.

When we analysed the three experimental replicates and observed a consistent trend of enhancement of both anti-viral genes (Figure 4-8 and Figure 4-10). This is in line contrary to our hypothesis that a duck TRIM27.1 may perform a similar function as human TRIM27, in transiently co-transfected cells expression of the *TRIM27.1b* construct increased expression of our two antiviral genes; *IFN-β* ($p < 0.001$, $n = 3$) (Figure 4-8) and *MX1*, although not signifcantly ($p > 0.05$, $n = 3$) (Figure 4-10). On average, an increase of 6.02-fold above the level of constitutively active cells (d2CARD transfected) was observed for *IFN-β* expression (Figure 4-8). And on average, an increase of 2.69-fold above the level of constitutively active cells (d2CARD transfected) was observed for *MX1* expression (Figure 4-6).

4.2.1 Transcriptional regulation effect of *TRIM27.1a* and *TRIM27.1b* at 48 hours PT is weaker than at 24 hours.

In the initial experiment, I sought to determine antiviral gene expression after 48 hours PT in order to determine the most effective time point for our experiments. Antiviral gene expression was counter intuitive at 48 hours PT. Although, *TRIM27.1a* suppressed expression of *IFN-β* and *MX1* at 24 hours PT in chickens cells (approximately 60% of the level of expression observed in the d2CARD constitutively activated cells) (Figure 4-3), at 48 hours PT the expression of *IFN-β* increased with expression *TRIM27.1a* and so was the expression of *MX1* (Figure 4-11). This observation was inconsistent with the previous observation at 24 hours PT of *TRIM27.1a* in that expression was increased for *IFN-β* (approximately 1.85-fold to 1.02-fold) and *MX1* (1.85-fold) after 48 hours of transfection (Figure 4-11). As *TRIM27.1a* is a short lived expression in infected lung tissues (Figure 3-9) with the peak at 1 dpi in highly

pathogenic IAV (VN1203) infected ducks the most reliable, and biologically relevant time point is 24 hours PT.

TRIM27.1b co-transfection at 48 hours (Figure 4-12) was also contrary to what was observed at 24 hours PT (Figure 4-7 and Figure 4-9). At 48 hours PT, both *IFN-β* and *MX1* expression was decreased to 50% of the expression level in d2CARD constitutively activated cells (0.5-fold across the board). Based on these results I opted to run all subsequent experiments at 24 hours PT.

4.2.2 TRIM27.1aV5 and TRIM27.1bV5 proteins are highly expressed at 24 hours PT and have the same transcriptional effects on antiviral genes.

To determine if the transfected TRIM27.1 genes were expressed at 24 hours PT, I performed a co-transfection experiment with the V5-tagged constructs, extracted the protein and ran an SDS-page gel and western blot with an anti-V5 epitope antibody to the whole cell lysate (WCL) (Figure 4-13). By 24 hours PT expression of the TRIM27.1aV5 and TRIM27.1bV5 in the WCL is high.

To ensure our experimental data was consistent with the new constructs, I ran the quantitative real-time experiment with the V5-tagged constructs to verify that the transcriptional modulation roles of *TRIM27.1aV5* and *TRIM27.1bV5* were not altered. The same pattern of *IFN-β* and *MX1* expression was observed, where *TRIM27.1aV5* suppresses expression (Figure 4-14) and *TRIM27.1bV5* increases expression of our downstream antiviral genes (Figure 4-15). As the results of our cotransfection assays with both the untagged versions and V5-tagged versions of our *TRIM27.1* genes yielded the same effects on *MX1* and *IFN-β* expression, and I have shown that both TRIM27.1aV5

and TRIM27.1bV5 are highly expressed on the protein level at 24 hr PT, I continued all subsequent work with these V5-tagged constructs.

4.2.3 TRIM27.1bV5 does not directly interact with RIG-I d2CARD to enhance activation of the antiviral pathway

We have now observed that *TRIM27.1aV5* and *TRIM27.1bV5* play a role in depressing and enhancing the antiviral program in a cell when the RIG-I pathway is active. As TRIM proteins have a RING-domain that can act as an E3-ligase, it is possible that TRIM27.1b modulates expression of antiviral genes by directly interacting with the CARD domains of RIG-I. Direct interaction with RIG-I is observed for TRIM25 during ubiquitination of RIG-I to activate downstream signaling components (Glusman *et al.* 2000). It is also possible that TRIM27.1b interacts with a downstream signaling component as is observed with human TRIM27 (Zha *et al.* 2006). However, we do not have the reagents or a system in place to examine interactions with the components of the RIG-I signaling cascade in ducks or in chicken cells. We do have a system currently in place to examine direct interactions of RIG-I d2CARD domains and specific tagged proteins of interest. By co-expressing the constructs, extracting the proteins and using glutathione-coated sepharose beads I can pull down the GST-d2CARD fused protein and anything that is interacting directly with it. Although, previous research has suggested that human TRIM27 interacts with downstream signaling components (Zha *et al.* 2006), as we had the system in place, I attempted to demonstrate the interaction or absence of interaction with the duck RIG-I CARD domains. Although I was unable to cleanly conduct a full experiment with controls, I was able to demonstrate the absence of a physical interaction with TRIM27.1b and the GST-d2CARD construct in the course of an

optimization experiment (Figure A-10). I used the V5-tagged *TRIM27.1b* construct to run an optimization SDS-page experiment and western blot with the GST-d2CARD and TRIM27.1bV5. If there is direct interaction between GST-d2CARD and TRIM27.1bV5, when I pull down the GST-d2CARD with the sepharose beads, I will get a signal in the same lane with both the anti-GST antibody and the anti-V5 antibody blots. I used three different conditions for the pull down, least stringent (conventional extraction using lysis buffer), moderately stringent (using TIF buffer which contains glycerol to decrease non-specific binding) and most stringent (pre-blocking the beads with 5% w/v BSA in TIF buffer) conditions.

Under more stringent conditions (TIF+BSA) lane, I lost the signal from the anti-V5 antibody blot meaning that under our most stringent conditions, TRIM27.1bV5 does not pull down with the constitutively active GST-d2CARD construct. Under stringent conditions, where beads were blocked with BSA overnight and washed with a TIF buffer (which contains glycerol) there is an absence of V5 reactive protein product (TRIM27.1bV5). If a specific interaction between the GST-d2CARD construct and TRIM27.1bV5 was occurring I would see bands corresponding to the TRIM27.1bV5 protein of interest in the same pull down as GST-d2CARD domain fusion protein when I blot with anti-V5 and anti-GST, respectively. I also observed evidence of non-specific binding of the TRIM27.1bV5 protein to the beads or GST-I only (DOG109 or the plasmid containing the N-terminal glutathione-S-transferase gene without the d2CARD domains), as evident by the presence of a band corresponding to the molecular weight of TRIM27.1bV5 when co-transfected with the GST-I only control plasmid under somewhat stringent conditions, the TIF wash (Figure A-10).

We were unable to generate a full scale experiment with no interfering background binding in the controls. This suggests that perhaps there an interaction between the TRIM27.1bV5 and TRIM27.1aV5 and the GST-I component of the fusion protein. Further work would be necessary in order to confirm the absence of an interaction by generating differentially tagged constructs and performing co-immunoprecipitation.

4.2.4 Absolute copy number qPCR demonstrates TRIM27.1aV5 and TRIM27.1bV5 modulate antiviral gene expression

As I confirmed overexpression of our two V5-tagged proteins in cells transfected with our *TRIM27.1aV5* and *TRIM27.1bV5* constructs, I sought the most effective way to demonstrate the immunomodulatory roles with a construct that I have shown to be both transcriptionally expressed and translated at 24 hours PT. Representation of fold change in expression relative to d2CARD constitutively active cells did not effectively communicate the vast difference in gene expression I were observing. Compared to resting GST-I control cells, d2CARD active cells were increasing expression by as much as 10 cycles in the qPCR assays; theoretically this could be as much as 1000-fold change in expression which I were representing as 1.00-fold in the relative quantification assays (Figure 4-3 to Figure 4-10 and Figure 4-14 to Figure 4-15). So in order to best demonstrate the changes in transcription observed with *TRIM27.1aV5* depression and *TRIM27.1bV5* enhancement of antiviral gene expression, I employed the use of a standard curve based absolute quantification real-time PCR analysis (abqPCR).

To use copy number quantification to represent the data, I needed to first clone our two target antiviral genes into a vector to generate a standard curve for amplification.

I amplified the complete chicken *IFN-β* gene and cloned it into pCR2.1 vector (Figure A-11) from the previously used cDNA samples, and a fragment of the *MX1* gene (*MX1 fragment*) that contains the region where our chMX1 probe binds (Figure A-12).

Consistent with our observations for relative quantification, the abqPCR demonstrated immumodulatory roles for both duck *TRIM27.1* genes. *TRIM27.1aV5* consistently decreased transcription of *IFN-β* in all 4 replicate experiments (Figure 4-16). There is some variability in the copy number of *IFN-β* expressed in the different experiments, which is not unusual given the type of assay employed. All experiments were conducted from separate populations of cells, using different midi-preps of constructs and lot numbers of lipofectamine. Transfection efficiency will vary between experiments and RNA isolation quality will vary as well. Although our pDsRed-N1 transfection controls were relatively consistent, there will always be variability in this transient system. However, the same trend is observed for each replicate of the experiments. A reduction of 49.6 and 60.8% of *IFN-β* copies was observed with the co-transfection of d2CARD and *TRIM27.1aV5* (Figure 4-16).

In order to assess this intrinsic variability, I plotted the copy numbers of all 4 experimental replicates in a single dot plot graph that shows the mean of copies (represented by the bar) against spread of data (dot plots) and ran a 1 way analysis of variance test (ANOVA) with a Tukey's post-test between d2CARD samples (constitutively activated cells) and our co-transfected d2CARD+TRIM27.1aV5 copy number (Figure 4-17). Due to the variability observed in all 4 experimental replicates, the decrease in expression of *IFN-β* (from average of 226.82 copies to 126.65 copies in TRIM27.1aV5 transfected cells) was not a statistically significant decrease in expression (n.s. represents $p > 0.05$, $n = 4$). Co-transfection of d2CARD and TRIM27.1aV5 also decreased expression of the other antiviral gene *MX1* (Figure 4-18) although variability in

depression of *MX1* was observed. A very wide range of *MX1* expression was observed in the four experimental replicates. Reduction of MX1 transcript compared to d2CARD expression ranged from as little as between 97.7% to as low as 0.09% was observed when TRIM27.1aV5 was co-transfected with d2CARD. Variability in *MX1* gene expression is not surprising as levels will be influenced greatly by the production of type 1 interferons in transfected cells as well as surrounding cells in the population. However, between experiments the variability in expression level was vastly different. In order to determine if the changes were significant across all experimental samples, plotted the copy numbers of all 4 experimental replicates in a single dot plot graph that shows the mean of copies (represented by the bar) against spread of data (dot plots) and ran a 1 way analysis of variance test (ANOVA) with a Tukey's post-test between d2CARD samples (constitutively activated cells) and our co-transfected d2CARD+TRIM27.1aV5 copy number to determine significance (Figure 4-19). The data was not significant due to spread of the data (n.s. represents $p > 0.05$, $n = 4$). High variability within the samples aside, the general trend still displayed an immunosuppressive role for *TRIM27.1aV5*.

Expression of *TRIM27.1bV5* consistently increased transcription of *IFN-β* in all 4 replicate experiments (Figure 4-20). There is, again, some variability in the copy numbers of *IFN-β* expressed in the different experiments, but the same trend is observed for each replicate in the experiment. Between 330.5 and 774.3% increase in *IFN-β* copies was observed with the co-transfection of d2CARD and TRIM27.1bV5 (Figure 4-20A to D). Additionally, in replicate #4 I added another experimental group wherein equivalent amounts of *TRIM27.1aV5* (250 ng) and *TRIM27.1bV5* (250 ng) constructs were co-transfected with d2CARD (Figure 4-20D). Enhanced transcriptional regulation of *IFN-β* was observed (from 377.42 copies in d2CARD to 3034.78 copies in the d2CARD+TRIM27.1aV5+TRIM27.1bV5 samples; a 804.1% increase in expression).

This suggests the immunostimulatory ability of *TRIM27.1bV5* overrides the immunosuppressive activity of *TRIM27.1aV5* when overexpressed in cell culture.

When I plotted the 4 experimental replicates together, the increase in expression of *IFN-β* (from average of 226.82 copies to 1259.46 copies in TRIM27.1bV5 co-transfected cells) was statistically significant ($p < 0.01$) (Figure 4-21). I also plotted the single experimental results of d2CARD+ 27.1aV5+ 27.1bV5 here, and the difference between average constitutively active d2CARD samples and both TRIMs was significant.

Co-transfection of d2CARD and *TRIM27.1bV5* also increased expression of the other antiviral gene, *MX1* (Figure 4-22). An increase in expression level between 149.3 to 190.7% of d2CARD expression levels was observed when TRIM27.1bV5 was present. When all experimental replicates were plotted and mean calculated (Figure 4-23) the increase in expression of *MX1* with *TRIM27.1bV5* was not significant as compared to the d2CARD level of expression (n.s represents $p > 0.05$, $n = 4$).

4.2.5 Modulation of the ChIFN-2 promoter by duck TRIM27.1 genes

In order to complement our observations with qPCR and abqPCR, I wanted to demonstrate immunomodulatory effects of duck *TRIM27.1a* and *TRIM27.1b* on the activity of a type I interferon promoter. I used a dual-luciferase reporter system, which was previously used to demonstrate activation of the RIG-I pathway (Barber *et al.* 2010), to show that *TRIM27.1aV5* and *TRIM27.1bV5* depress and increase the response of ChIFN-2 promoter (the chicken *IFN-β* promoter), respectively. In this experiment, the amount of d2CARD construct (5 ng) remains consistent in all activated samples, and the varying amounts of *TRIM27.1aV5* and *TRIM27.1bV5* construct is normalized with addition of empty vector (pcDNA3.1/Hygro+) in order to maintain a constant amount of exogenous DNA transfected into the cells. Four replicates of this experiment were

conducted with different pools of DF1 cells, and different *TRIM27.1aV5* and *TRIM27.1bV5* construct preparations.

To determine if a dose-dependent relationship exists between the suppression of ChIFN-2 promoter activity and amount of the immunosuppressive *TRIM27.1aV5* construct added into the system, a gradient of increasing amounts of *TRIM27.1aV5* was transfected into d2CARD activated cells (from 25 ng of *TRIM27.1aV5* to 500 ng) (Versteeg *et al.* 2013) (Figure 4-24). Experimental replicate #1 demonstrated a beautiful dose-dependent suppression of firefly luciferase reporter indicating a dose dependent suppression of the ChIFN-2 promoter (Figure 4-24A). The ratio of fold-induction of ChIFN-2 driven firefly luciferase normalized to GST-I induction decreased from 55.72 with d2CARD down to 27.82 with d2CARD+500 ng of *TRIM27.1aV5*. As predicted, our control constructs did not influence firefly luciferase expression (empty vector, *GST-I* and *TRIM27.1aV5* constructs). Variability in the promoter suppression of *TRIM27.1aV5* was observed in experimental replicate #2, and there appears to be no obvious dose-dependent relationship (from 15.43 in d2CARD to 14.56 in d2CARD+27.1aV5(500ng) sample) to firefly reporter expression and amount of *TRIM27.1aV5* (Figure 4-24B), but in experimental replicate #3 addition of *TRIM27.1aV5* does supress ChIFN-2 promoter activity (Figure 4-24C) from the normalized ratio of 87.81 in d2CARD down to 45.616 in d2CARD+27.1aV5 (500ng) sample. Replicate #4 shows a very strong dose dependent relationship with firefly luciferase response suppression with increasing amounts of TRIM27.1aV5 (Figure 4-24D) supressing firefly response from 19.62 in d2CARD down to 5.16 in d2CARD+27.1aV5(500ng). When I plotted the results on a single graph to look at mean ratio of normalized firefly:renilla expression compared to spread, the general trend is with increasing amounts of TRIM27.1aV5, increased suppression of ChIFN-2 promoter is observed (Figure 4-25) supressing the normalized *IFN-β* fold induction by

nearly half (from an average of 44.64 down to 23.18). There is however, no statistical significance observed and no clear peak in suppression observed using the 1 way ANOVA with Tukey's post-test (n.s. represents $p > 0.05$, $n = 4$) (Figure 4-25).

Consistent to our observations of *TRIM27.1bV5* as an immunostimulatory TRIM, our dual luciferase reporter system demonstrated a significant influence of *TRIM27.1bV5* on level of *IFN-β* promoter activity. All three experimental replicates show a dose-dependent increase in ChIFN-2 promoter activity with increasing amounts of *TRIM27.1bV5* present in the system (Figure 4-26). The peak of activation of *TRIM27.1bV5* seems to be at around 100 ng to 250 ng of *TRIM27.1bV5* in RIG-I constitutively activated cells. In replicate #1, the peak of activation is observed at 250 ng of TRIM27.1bV5 with a ratio of 503.34 to 55.72 in d2CARD only activated cells (Figure 4-26A). This is 903.3% increase in activity over constitutively active cells. In replicate number 2, the peak of activation is at 100 ng of TRIM27.1bV5, with a ratio of 327.50 to 15.43 in d2CARD only constitutively active cells (Figure 4-26B). This is a 2122.5% increase in activity of the ChIFN-2 promoter with 100 ng of TRIM27.1bV5. In experimental replicate #3, the peak of activation of the ChIFN-2 promoter is with 250 ng of TRIM27.1bV5 (Figure 4-26C). Here, a ratio of 486.24 to 87.81 in d2CARD cells corresponds to a 553.7% increase in activity over constitutively active cells. In the final replicate #4, the peak of activation is at 100 ng of TRIM27.1bV5, with a ratio of 311.25 to 19.62 in d2CARD only constitutively active cells (Figure 4-26D). This is a 1586.4% increase in activity of the ChIFN-2 promoter with 100 ng of *TRIM27.1bV5*. In these experiments I also co-expressed 250 ng of *TRIM27.1aV5* and 250 ng of *TRIM27.1bV5* in d2CARD activated cells, and I consistently saw significant promoter activation when I added equivalent amounts of both immunomodulatory TRIMs. Enhancement of ChIFN-2

promoter ranged between 200 and 500% of constitutively activated d2CARD cells, with 460.3% in rep #1, 528.4% in rep #2, 346.2% in rep #3 and 199.3% in rep #4.

Even with the variability in the ratio of expression, when I plot the average and the spread of the three separate experiments on a single graph, the increase in promoter activity with each increasing amount of *TRIM27.1bV5* is statistically significant with the addition of 100 ng ($p < 0.001$, $n = 4$) and 250 ng ($p < 0.001$, $n = 4$) of *TRIM27.1bV5* (Figure 4-27). The peak of activation is at 100 ng of *TRIM27.1bV5*, with a ratio of 360.87 to 44.64 in d2CARD only constitutively active cells (Figure 4-27). This is an average 808.4% increase in activity of the ChIFN-2 promoter with 100 ng of *TRIM27.1bV5*. Due to the variability between replicates, the co-expression of equivalent amounts of *TRIM27.1aV5* and *TRIM27.1bV5* was not a significant difference, although the average increase in promoter activity was 381.5% higher than the d2CARD constitutively activated cells.

4.2.6 Immunostimulatory effect of *TRIM27.1bV5* is dominant over the immunosuppressive effect of *TRIM27.1aV5*

Out of curiosity, I conducted a single experiment to look at the dose-dependent relationship of increasing amounts of *TRIM27.1bV5* in concert with the standard inhibitory 250 ng of *TRIM27.1aV5*. Although this full experiment was only conducted once, it is likely worth repeating. Consistent with our previous observations that equivalent amounts of *TRIM27.1aV5* and *TRIM27.1bV5* had an immunostimulatory effect on the *ChIFN-2* promoter, increasing amounts of the *TRIM27.1bV5* immunostimulatory construct overrode the inhibitory effects of *TRIM27.1aV5* (250 ng) (Figure 4-28). Even at 50 ng of *TRIM27.1bV5* with 250 ng of *TRIM27.1aV5*, an increase in firefly luciferase response was observed, a ratio of 26.41 to 19.62 in the d2CARD constitutively active cells; this corresponds to a 134.6% increase over control. The peak

of activity, although less robust than previously observed (Figure 4-26), was observed with 100 ng of TRIM27.1bV5 in addition to the 250 ng of TRIM27.1aV5. Here, I saw a ratio of 42.28 to 19.62 in the d2CARD control which corresponds to a 215.5% increase in *ChIFN-2* promoter activity.

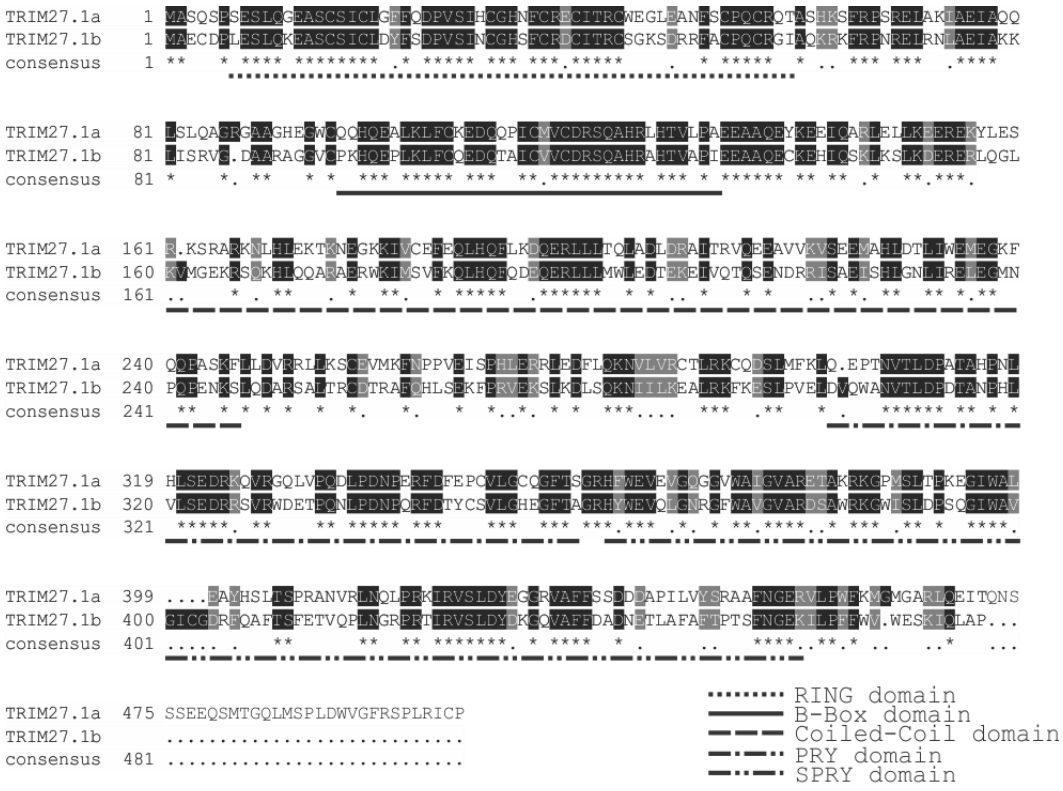

Figure 4-1. Alignment of TRIM27.1a and TRIM27.1b with annotated domains. This alignment of the protein sequences of TRIM27.1a and TRIM27.1b demonstrates the conserved domain architecture of the two proteins and the divergence of the coiled-coil domain. Overall percent identity between TRIM27.1 and TRIM27.1b is 51%. This alignment was made using the online MultAlin interface and the BoxShade server. Consensus conservation is indicated with an asterisk.

Table 4-1. Percent identity of domains of TRIM27 and TRIM39 proteins from scaffold618.

A blastp alignment of the specified regions of each query TRIM protein was aligned to each subject using standard settings. Percent identity was recorded for each alignment. Start and end of each domain was determined by blastp protein domain specified on NCBI. The highest percent identity score for TRIM27.1b in domain and overall amino acid sequence homology is to the gene immediately upstream, TRIM27.1a.

Query	Subject	Domains Analyzed	Percent Identity
27.1b	27.1a	RBCC	53%
		PRY/SPRY	51%
		Overall	51%
27.1b	27.2	RBCC	50%
		PRY/SPRY	45%
		Overall	46%
27.1b	39.1-L/BR	PRY/SPRY	43%
		Overall	43%
27.1a	27.2	RBCC	49%
		PRY/SPRY	53%
		Overall	51%
39.1-L/BR	27.1a	PRY/SPRY	55%
		Overall	45%
39.1-L/BR	27.2	PRY/SPRY	48%
		Overall	41%
39.1-L/BR	39.2	PRY/SPRY	40%
		Overall	40%
39.2	27.1a	RBCC	41%
		PRY/SPRY	36%
		Overall	29%
39.2	27.1b	RBCC	38%
		PRY/SPRY	34%
		Overall	29%
39.2	27.2	RBCC	34%
		PRY/SPRY	27%
		Overall	31%

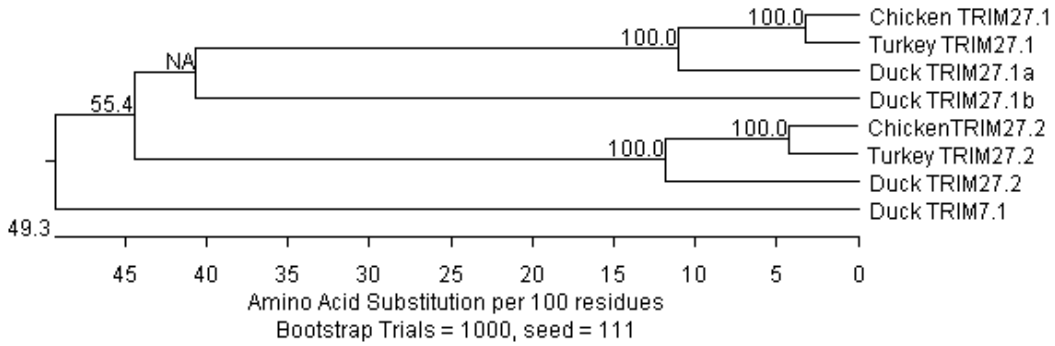

Figure 4-2. Phylogenetic tree of avian TRIM27.1 and TRIM27.2 proteins clusters TRIM27.1b with chicken, turkey and duck TRIM27.1.

Phylogenetic tree is structured as a phenogram based on the ClustalW alignment of the avian TRIM27.1 and TRIM27.2 proteins using MegAlign program (DNAstar, Version10 suite). TRIM27.2s and TRIM27.1s from all species group together as predicted. Bootstrapping was performed using default settings of 1000 trials and 111 seeds. Duck TRIM27.1b is most closely related to chicken and turkey TRIM27.1 and duck TRIM27.1a. Included in this analysis is duck TRIM7.1, as TRIM7, -27 and -39 are homologs. Duck TRIM7.1 is the outlier of the group and the alignment demonstrates that TRIM7.1 is the least closely related to the TRIM27s.

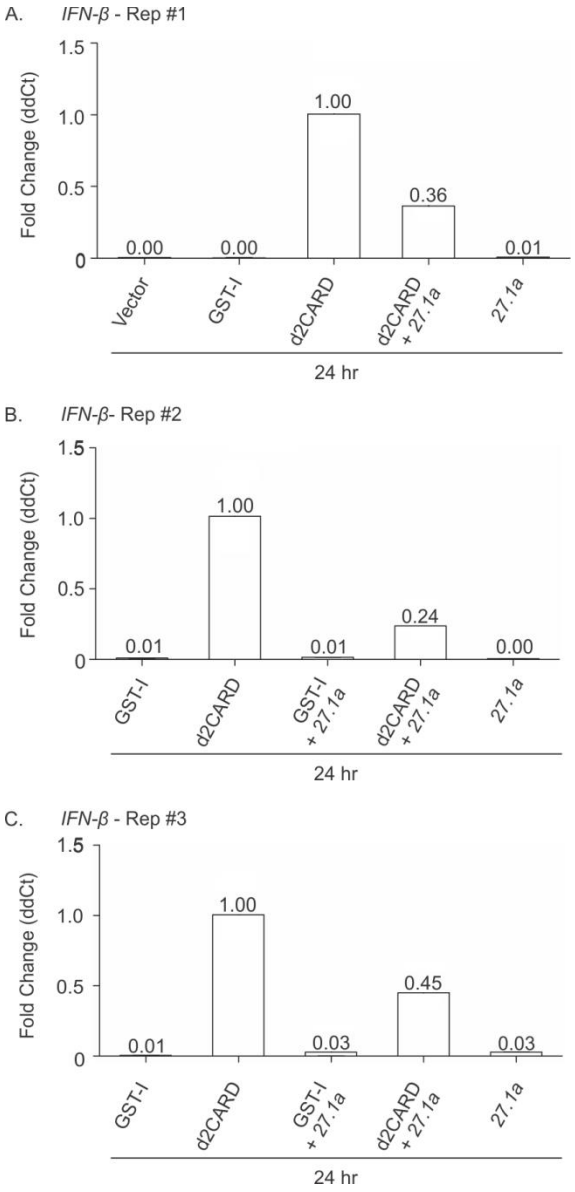

Figure 4-3. Expression of *TRIM27.1a* in activated cells depresses expression of *IFN-β* but has no effect in resting cells.

Three experimental replicates are represented here. In each experiment, 24 hours PT (PT), total RNA was extracted using TRIzol® reagent from a DF1 cell monolayer. The triplicate experiments varied in cell passage numbers, population and midiprep stocks used for the experiment. Bars represent the calculated RQ average of the triplicate wells with respect to an endogenous control (GAPDH, which expression level remains consistent) for a single experiment. Spread of the RQ values are not represented. Co-transfection of *TRIM27.1a* in activated cells decreases expression of *IFN-β* to less than half of activated cells expression levels. (A) Replicate number 1 I observed a 64% decrease in fold expression of *IFN-β*, (B) in replicate 2, a 76% decrease in *IFN-β* transcription levels and (C) in replicate 3 a 55% decrease in *IFN-β* levels was observed. *IFN-β* transcript levels was not affected by expression of *TRIM27.1a* alone in DF1 cells

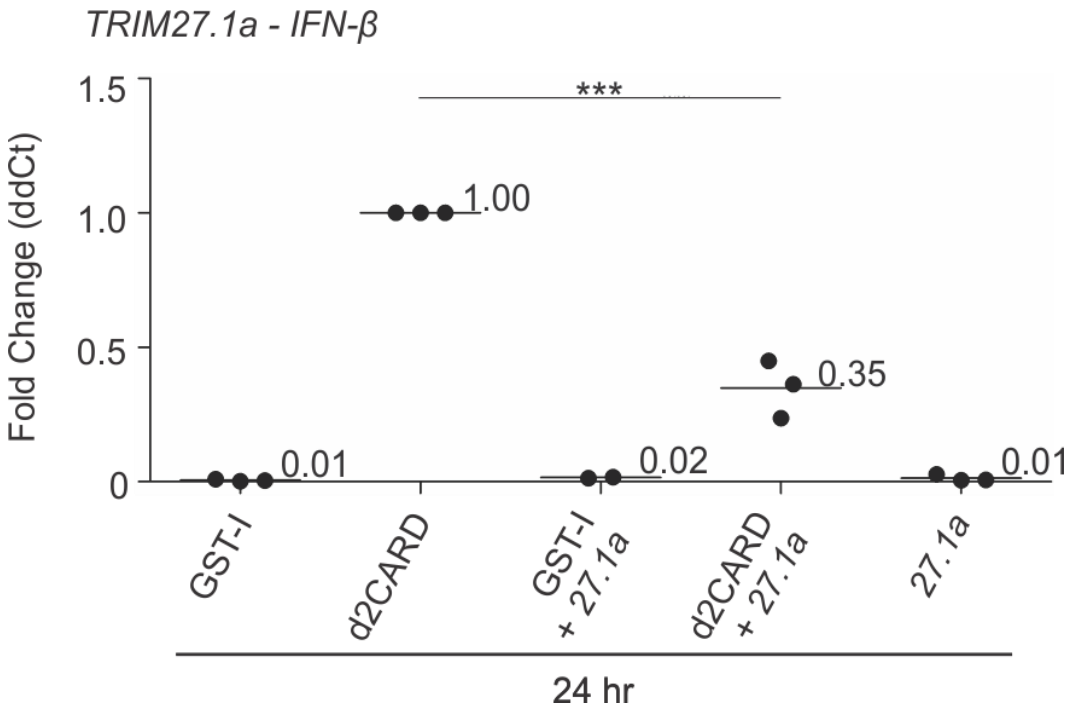

Figure 4-4. Co-expression of d2CARD and *TRIM27.1a* significantly decreases the relative expression level of *IFN-β* in DF1 cells.
The three experimental replicates from figure 4-3 are represented in a single dot plot. Each dot represents a single experimental replicate of each sample. Horizontal bars indicate the calculated RQ average of the three experimental replicates. Spread of the RQ values within each experiment are not represented. Co-transfection of *TRIM27.1a* in activated cells significantly ($p < 0.001$) decreases expression of *IFN-β* to an average of 0.35-fold less than the d2CARD activated cells expression levels, a reduction of 0.65-fold. *IFN-β* transcript levels was not affected by expression of *TRIM27.1a* alone in DF1 cells. Statistical significance was calculated using a one-way ANOVA and a Tukey's post-test using GraphPad version 5.0 software by Prism.*** represents $p < 0.001$, $n = 3$.

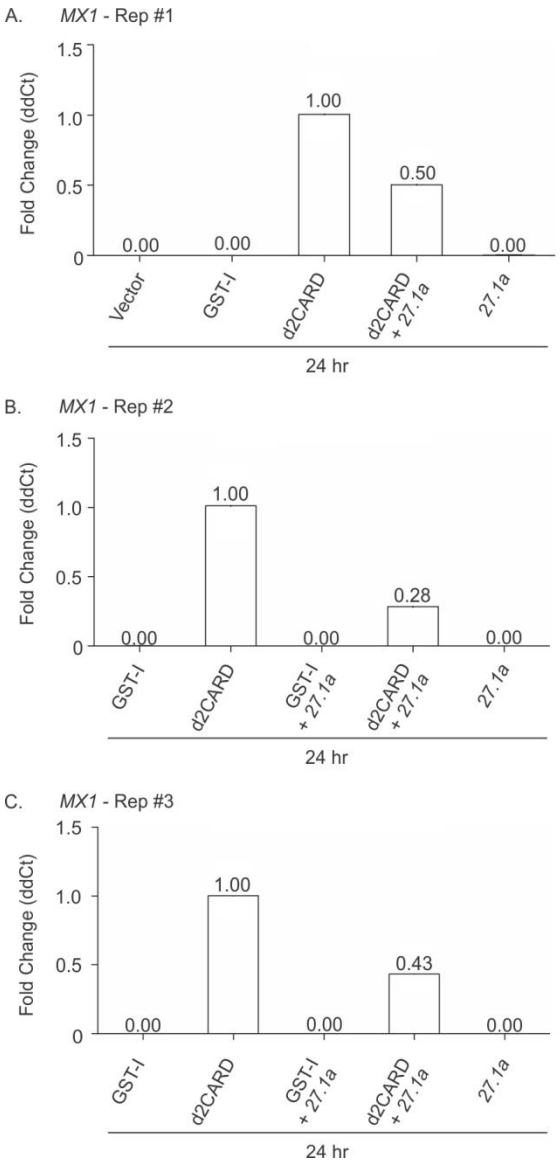

Figure 4-5. Expression of *TRIM27.1a* in activated cells depresses expression of *MX1* but has no effect on resting cells.

Three experimental replicates are represented here. In each experiment, 24 hours PT (PT), total RNA was extracted using TRIzol® reagent from a DF1 cell monolayer. The triplicate experiments varied in cell passage numbers, population and midiprep stocks used for the experiment. These are representative data of samples run in duplicate for each experiment. Bars represent the calculated RQ average of the triplicate wells with respect to an endogenous control (GAPDH, which expression level remains consistent) for a single experiment. Spread of the RQ values are not represented. Co-transfection of TRIM27.1a in activated cells decreases expression of *MX1* to less than half of activated cells expression levels. (A) Replicate number 1 I observed a 50% decrease in fold expression of *MX1*, (B) in replicate 2, a 72% decrease in *MX1* transcription levels and (C) in replicate 3 a 57% decrease in *MX1* levels was observed. *MX1* transcript level was not affected by expression of *TRIM27.1a* alone in DF1 cells.

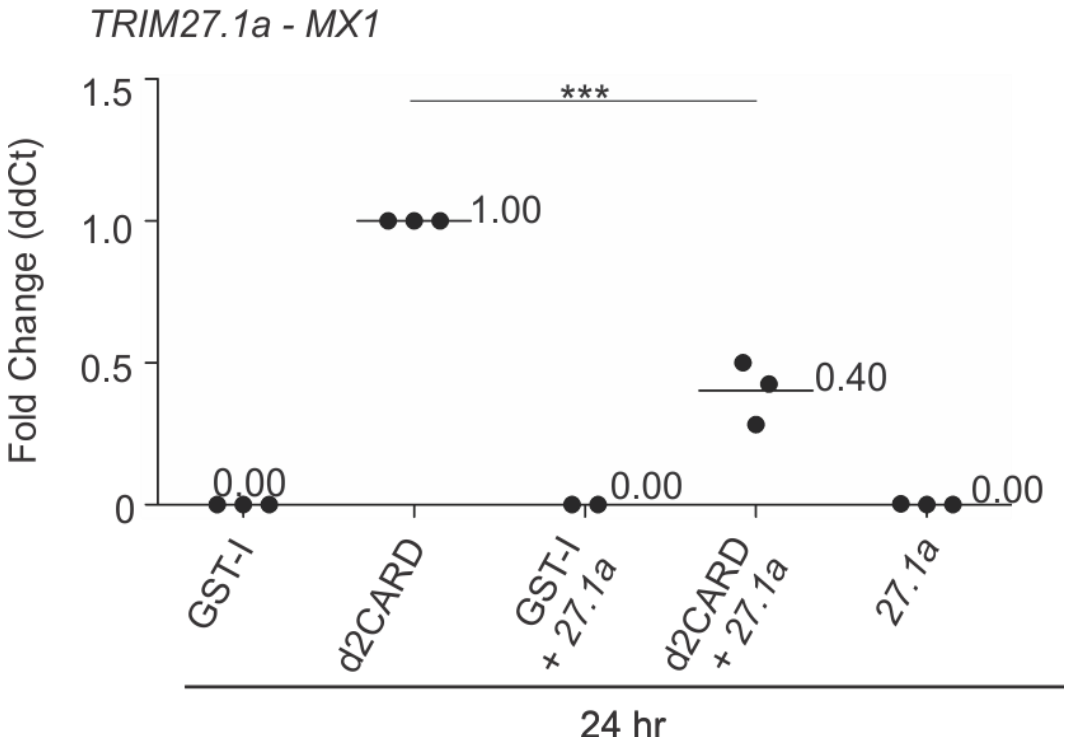

Figure 4-6. Co-expression of d2CARD and *TRIM27.1a* significantly decreases the relative expression level of *MX1* in DF1 cells.
The three experimental replicates from figure 4-3 are represented in a single dot plot. Each dot represents a single experimental replicate of each sample. Horizontal bars indicate the calculated RQ average of the three experimental replicates. Spread of the RQ values within each experiment are not represented. Co-transfection of TRIM27.1a in activated cells significantly ($p < 0.001$) decreases expression of *MX1* to an average of 0.40-fold less than the d2CARD activated cells expression levels, a reduction of 0.60-fold. *MX1* transcript level was not affected by expression of *TRIM27.1a* alone in DF1 cells. Statistical significance was calculated using a one-way ANOVA and a Tukey's post-test using GraphPad version 5.0 software by Prism. *** represents $p < 0.001$, $n = 3$.

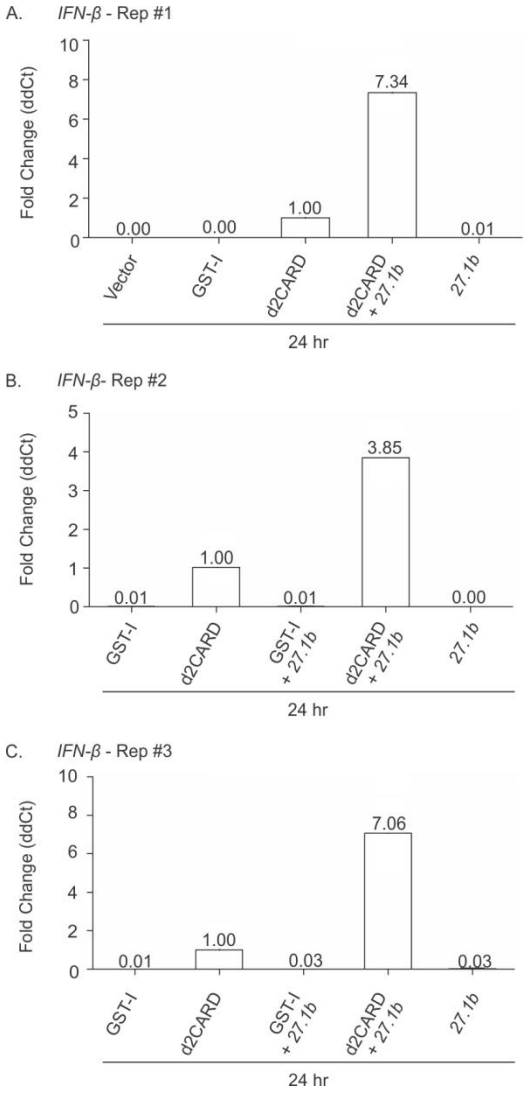

Figure 4-7. Expression of *TRIM27.1b* in activated cells enhances expression of *IFN-β* but has no effect on resting cells.

Three experimental replicates are represented here. In each experiment, 24 hours PT (PT), total RNA was extracted using TRIzol® reagent from a DF1 cell monolayer. The triplicate experiments varied in cell passage numbers, population and midiprep stocks used for the experiment. These are representative data of samples run in duplicate for each experiment. Bars represent the calculated RQ average of the triplicate wells with respect to an endogenous control (GAPDH, which expression level remains consistent) for a single experiment. Spread of the RQ values are not represented. Co-transfection of *TRIM27.1b* in activated cells increases expression of *IFN-β* more than 3.5-fold of activated cells expression levels. (A) Replicate number 1 I observed a 7.34-fold increase in expression of *IFN-β*, (B) in replicate 2, a 3.85-fold increase in *IFN-β* transcription levels and (C) in replicate 3 a 7.06-fold increase in *IFN-β* levels was observed. *IFN-β* transcript level was not affected by expression of *TRIM27.1b* alone in DF1 cells.

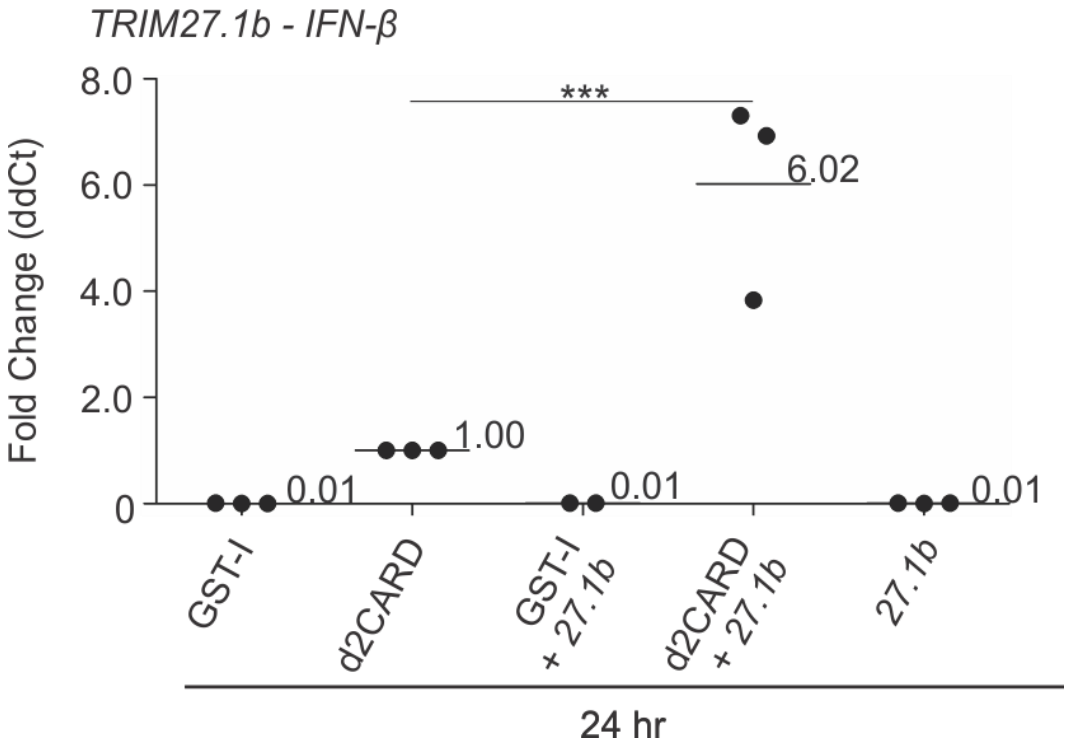

Figure 4-8. Co-expression of d2CARD and *TRIM27.1b* significantly increases the relative expression level of *IFN-β* in DF1 cells.
The three experimental replicates from figure 4-3 are represented in a single dot plot. Each dot represents a single experimental replicate of each sample. Horizontal bars indicate the calculated RQ average of the three experimental replicates. Spread of the RQ values within each experiment are not represented. Co-transfection of *TRIM27.1b* in activated cells significantly ($p < 0.001$) increases expression of *IFN-β* to an average of 6.02-fold higher than the d2CARD activated cells expression levels. *IFN-β* transcript level was not affected by expression of *TRIM27.1b* alone in DF1 cells. Statistical significance was calculated using a one-way ANOVA and a Tukey's post-test using GraphPad version 5.0 software by Prism.*** represents $p < 0.001$, $n = 3$.

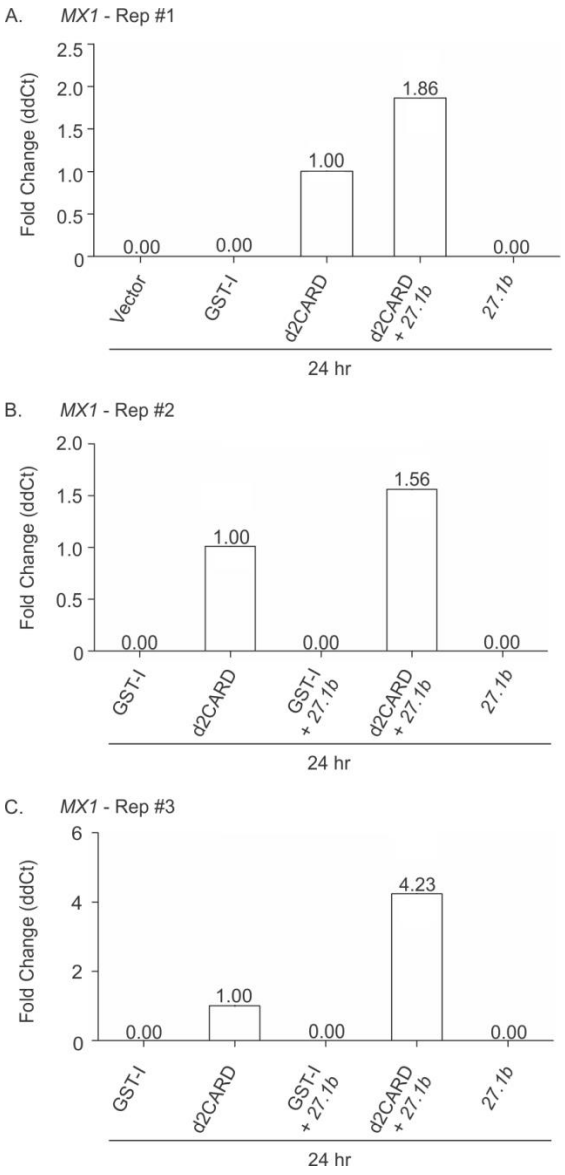

Figure 4-9. Expression of *TRIM27.1b* in activated cells enhances expression of *MX1* but has no effect on resting cells.

Three experimental replicates are represented here. In each experiment, 24 hours PT (PT), total RNA was extracted using TRIzol® reagent from a DF1 cell monolayer. The triplicate experiments varied in cell passage numbers, population and midiprep stocks used for the experiment. These are representative data of samples run in duplicate for each experiment. Bars represent the calculated RQ average of the triplicate wells with respect to an endogenous control (GAPDH, which expression level remains consistent) for a single experiment. Spread of the RQ values are not represented. Co-transfection of *TRIM27.1b* in activated cells increases expression of *MX1* to more than 1.5-fold than that of activated cell expression levels. (A) Replicate number 1 I observed a 1.86-fold increase in fold expression of *MX1*, (B) in replicate 2, a 1.56-fold increase in *MX1* transcription levels and (C) in replicate 3 a 4.23-fold increase in *MX1* levels was observed. *MX1* transcript level was not affected by expression of *TRIM27.1b* alone in DF1 cells.

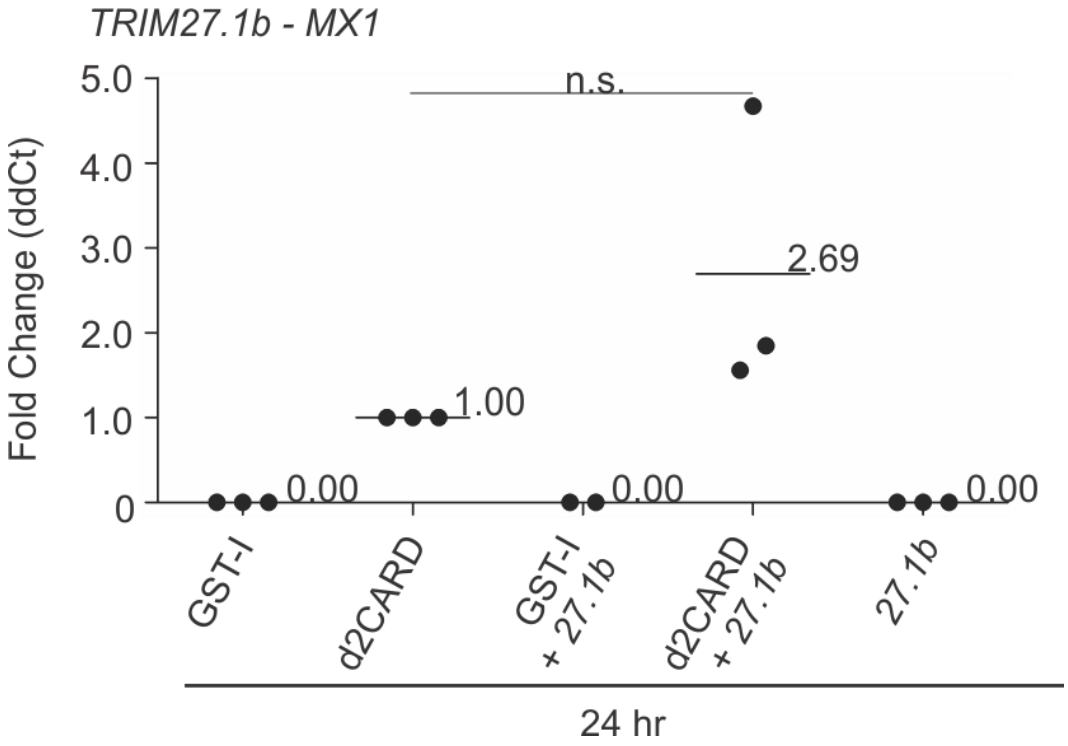

Figure 4-10. Co-expression of d2CARD and *TRIM27.1b* does not significantly increase the relative expression level of *MX1* in DF1 cells .
The three experimental replicates from figure 4-3 are represented in a single dot plot. Each dot represents a single experimental replicate of each sample. Horizontal bars indicate the calculated RQ average of the three experimental replicates. Spread of the RQ values within each experiment are not represented. Co-transfection of *TRIM27.1b* in activated cells increases expression of *MX1* to an average of 2.69-fold less than the d2CARD activated cells expression levels. However, the change is not statistically significant. *MX1* transcript level was not affected by expression of *TRIM27.1b* alone in DF1 cells. Statistical significance was calculated using a one-way ANOVA and a Tukey's post-test using GraphPad version 5.0 software by Prism. n.s. represents $p > 0.05$, $n = 3$.

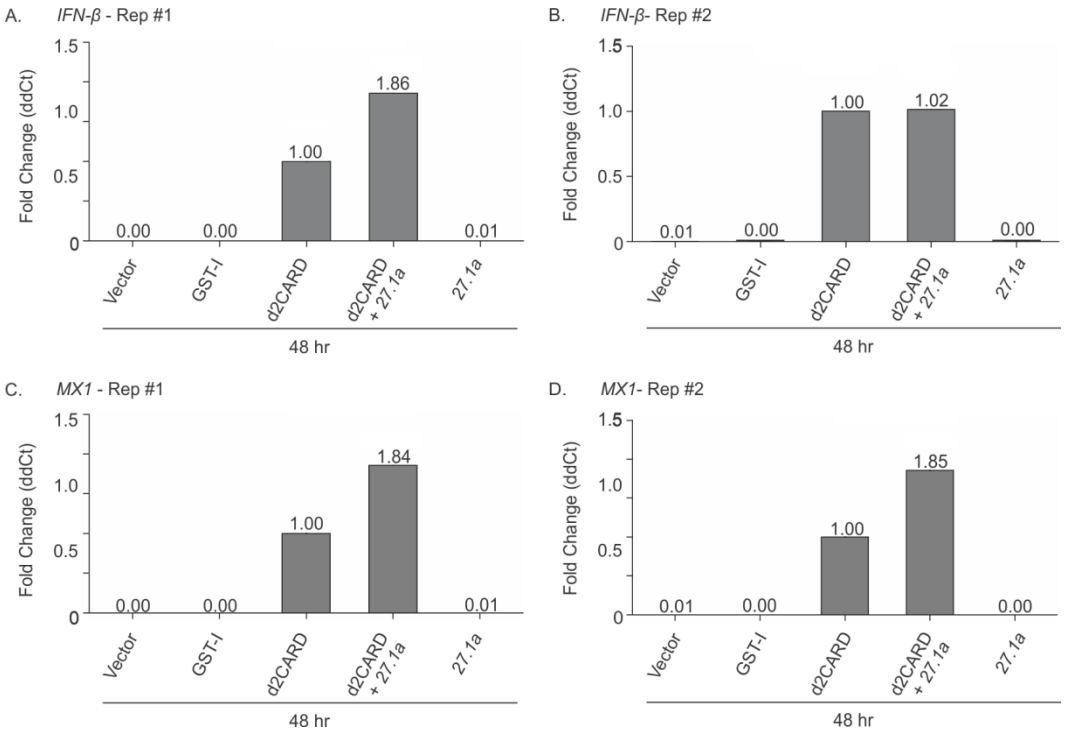

Figure 4-11. Modulation of antiviral gene expression after 48 hours PT of *TRIM27.1a* in activated cells is less dramatic than at 24 hr PT.
Data presented here are two replicate transfections within a single experiment. Bars represent the calculated RQ average of the triplicate wells for a single experiment. Spread of the RQ values are not represented. Co-transfection of *TRIM27.1a* in activated cells decreases expression of *IFN-β* and *MX1* by185%. *IFN-β* expression in (A) replicate 1 increased by 186% of activated cells, and (B) in replicate 2 a 2% increase was observed. *MX1* expression was also enhanced at 48 hours PT where in (C) in replicate 1 a 184% increase and (D) in replicate 2 a 185% increase was observed. *IFN-β* or *MX1* transcript level was not affected by expression of *TRIM27.1b* alone in DF1 cells for 48 hours.

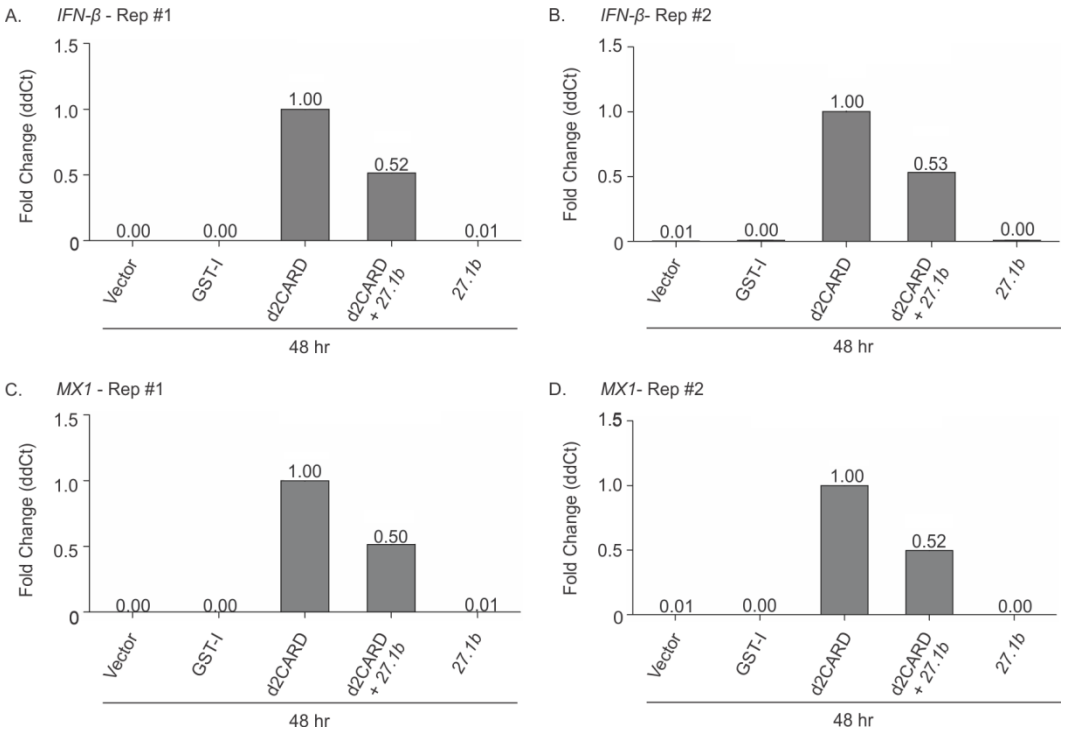

Figure 4-12. Modulation of antiviral gene expression after 48 hours PT of *TRIM27.1b* in activated cells is less dramatic than at 24 hr PT.
Data presented here are two replicate transfections within a single experiment. Bars represent the calculated RQ average of the triplicate wells for a single experiment. Spread of the RQ values are not represented. Co-transfection of *TRIM27.1b* in activated cells decreases expression of *IFN-β* and *MX1* by 50%. *IFN-β* expression in (A) replicate 1 decreased by 48% of activated cells, and (B) in replicate 2 a 47% decrease was observed. MX1 expression was also depressed at 48 hours PT where in (C) in replicate 1 a 50% decrease and (D) in replicate 2 a 48% decrease was observed. *IFN-β* or *MX1* transcript level was not affected by expression of *TRIM27.1b* alone in DF1 cells for 48 hours.

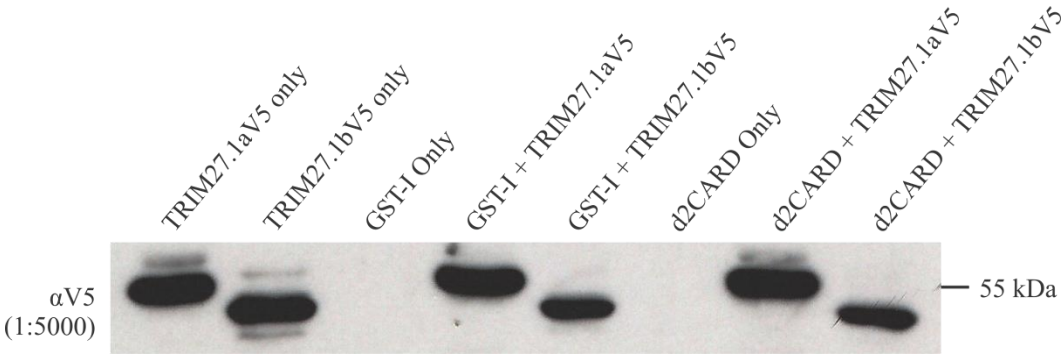

Figure 4-13. 24 hours PT TRIM27.1aV5 and TRIM27.1bV5 tagged proteins are highly expressed in DF1 cells

Both TRIM27.1aV5 and TRIM27.1b V5 are abundantly produced in DF1 cells just 24 hours PT. Proteins extracted are the whole cell lysate (WCL) and the two sizes are 59 kDa for TRIM27.1aV5 and 56 kDa for TRIM27.1bV5. The concentration of the SDS-page gel that was used is 0.8% and protein ladder marker is indicated by a dash on the right.

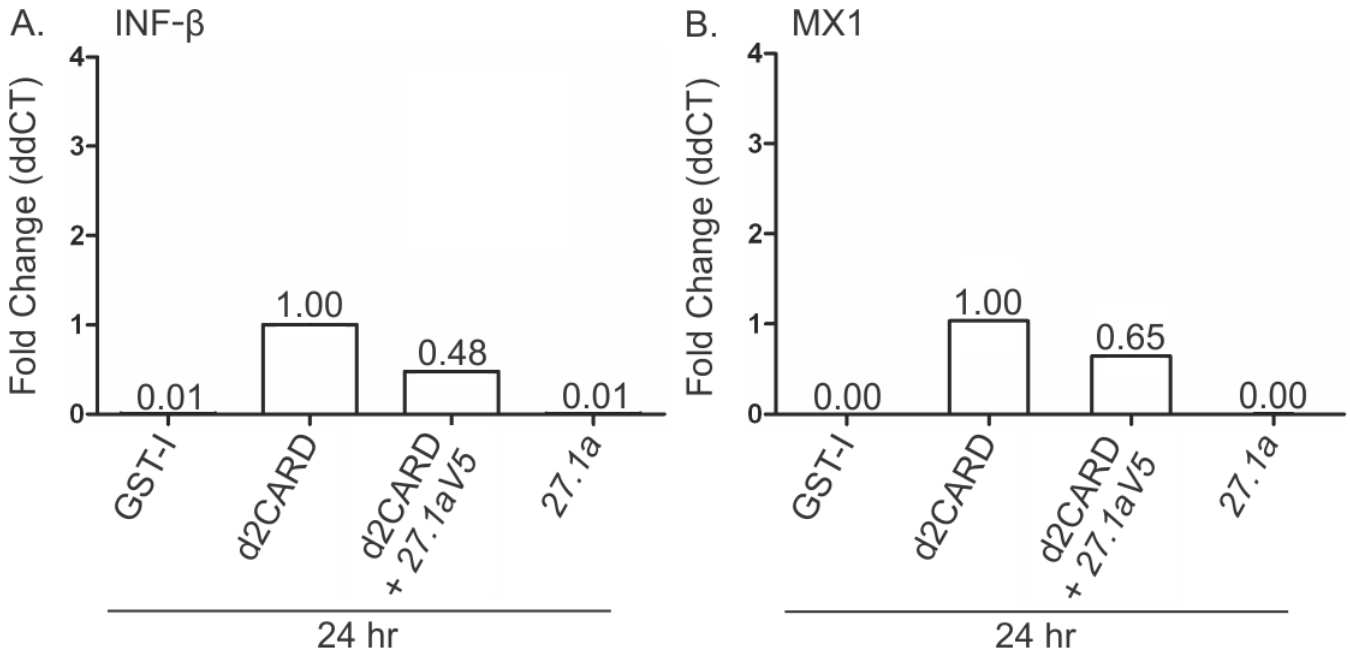

Figure 4-14. Decreased expression of both *IFN-β* and *MX1* in cells co-transfected with *TRIM27.1aV5* and d2CARD constructs. In order to determine if the *TRIM27.1aV5* construct has a consistent effect on expression of *IFN-β* and *MX1* as the untagged *TRIM27.1a* construct, we conducted a single relative expression experiment using the *TRIM27.1aV5* construct. Transient co-transfection of chicken DF1 cells with d2CARD (RIG-I) constitutively activated cells and our *TRIM27.1aV5* construct were cultured for 24 hrs PT. RNA was isolated using the TRIzol method at 24 hours PT. Data presented here is the qPCR data for *IFN-β* and *MX1* expression in a single experimental transfection within a single experiment (n = 1) in order to demonstrate the transcriptional modulation effect is conserved between tagged and untagged constructs. Bars represent the calculated RQ average of the triplicate wells for a single experiment. Spread of the RQ values are not represented. Relative qPCR shows that expression of (A) *IFN-β* transcription levels are decreased by 70% of the level of the constitutively active (RIG-I^{++}) cells and (B) *MX1* is decreased by to 57% as compared to the activated cells.

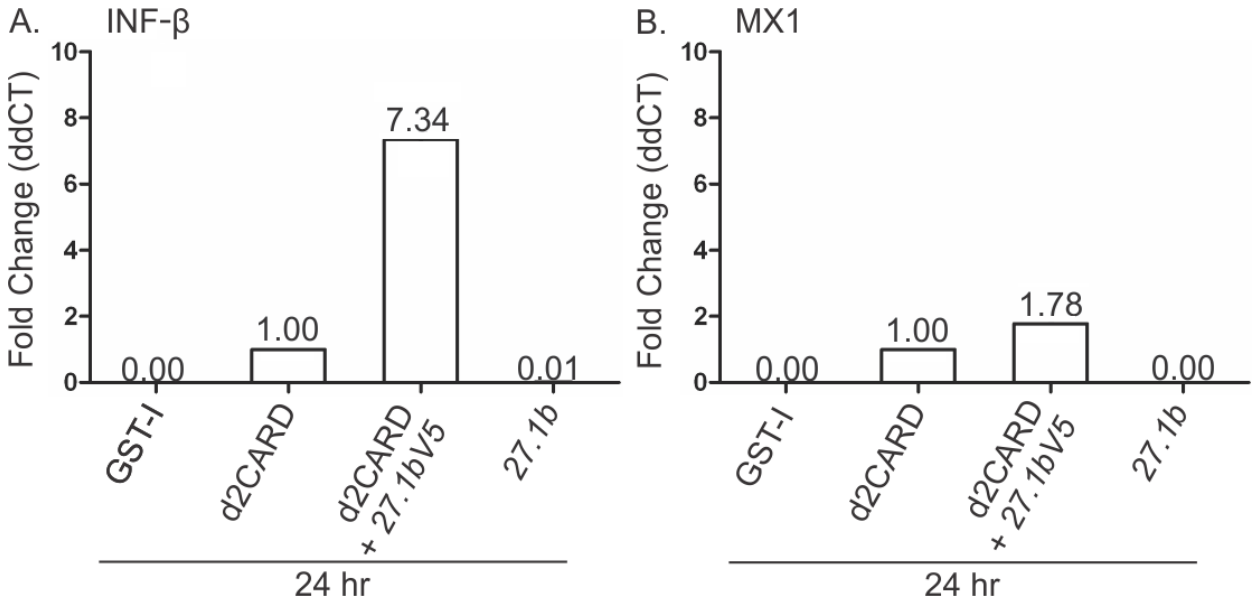

Figure 4-15. Increased expression of both *IFN-β* and *MX1* in cells co-transfected with *TRIM27.1bV5* and d2CARD constructs. In order to determine if the *TRIM27.1bV5* construct has a consistent effect on expression of *IFN-β* and *MX1* as the untagged *TRIM27.1b* construct, we conducted a single relative expression experiment using the *TRIM27.1bV5* construct. Transient co-transfection of chicken DF1 cells with d2CARD (RIG-I) constitutively activated cells and our *TRIM27.1bV5* construct were cultured for 24 hrs PT. RNA was isolated using the TRIzol method at 24 hours PT. Data presented here is the qPCR data for *IFN-β* and *MX1* expression in a single experimental transfection within a single experiment (n = 1) in order to demonstrate the transcriptional modulation effect is conserved between tagged and untagged constructs. Spread of the RQ values are not represented. Relative qPCR shows that expression of (A) *IFN-β* transcription levels are increased by 8-fold above of the level of the constitutively active (d2CARD) cells and (B) *MX1* is increased to 4-fold as compared to the activated cells. This relative expression qPCR was completed just to ensure the V5-tagged constructs perform in the same manner as the untagged constructs prior to the absolute quantification experiments to follow. Data represented here is from a single experiment, n = 1.

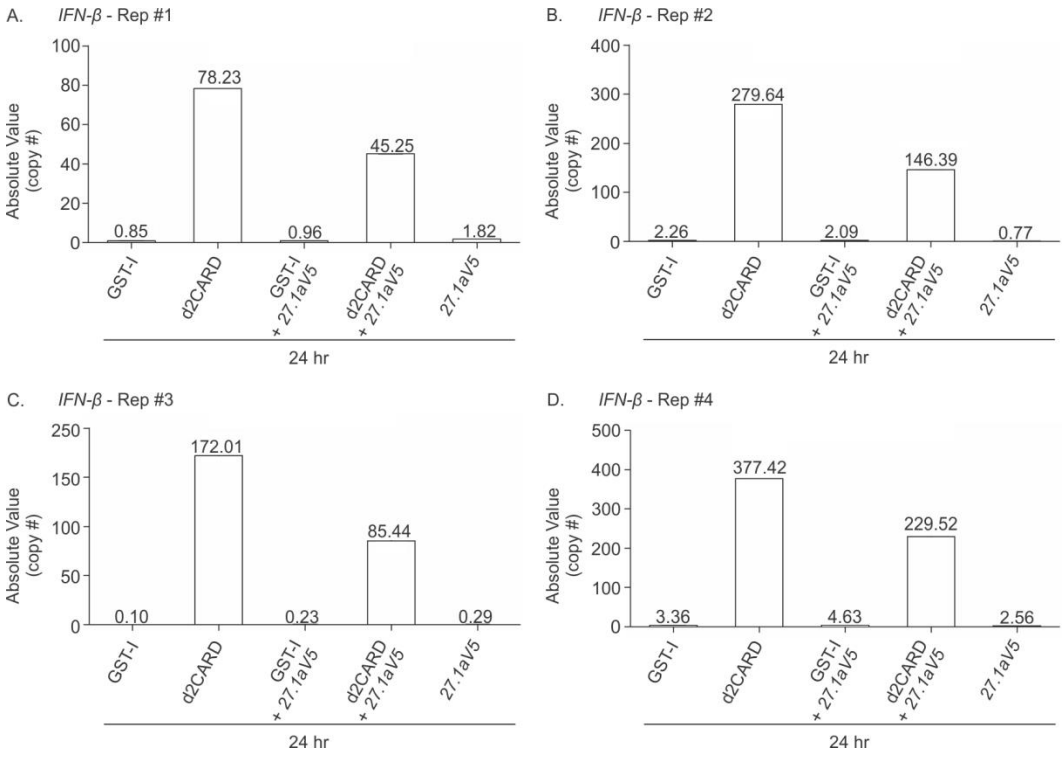

Figure 4-16. *TRIM27.1aV5* decreases the absolute value of expression of *IFN-β*. Transient co-transfection of chicken DF1 cells with d2CARD (RIG-I) constitutively activated cells and our *TRIM27.1aV5* construct were cultured for 24 hrs PT. RNA was isolated using the TRIzol method at 24 hours PT. Absolute value of expression was determined by ten-fold dilution series (from 10^8 copies to 10^1 copies) of *IFN-β* in pCR2.1 vector. Samples were run in triplicate wells, and the average Ct was used to calculate copy number based on standard curve intercept and slope. The four independent experimental replicates shown here complement the luciferase experiments. (A) Replicate #1, experiment #8 co-transfection of *TRIM27.1aV5* decreases *IFN-β* expression to 57.8% of d2CARD. (B) Replicate #2, experiment #9 co-transfection of *TRIM27.1aV5* decreases *IFN-β* expression to 52.3% of d2CARD. (C) Replicate #3, experiment #10 co-transfections decreases *IFN-β* expression to 49.6% of d2CARD. (D) Replicate #4, experiment #11 co-transfection decreases *IFN-β* expression to 60.8% of d2CARD.

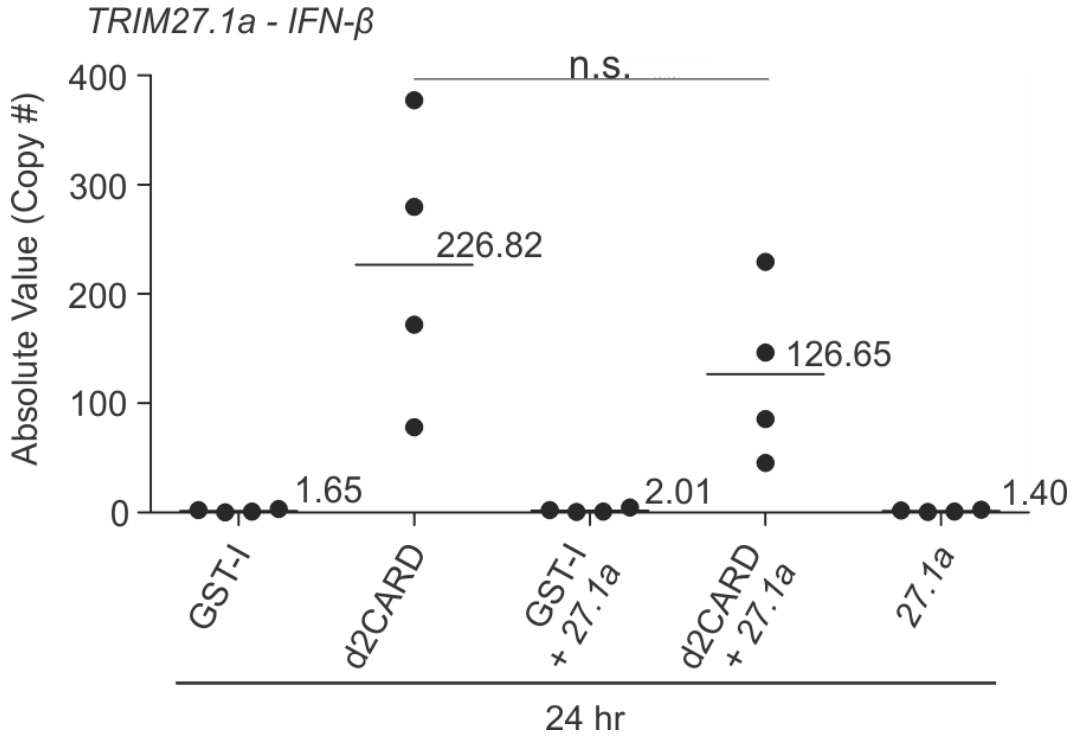

Figure 4-17. Average reduction of expression of *IFN-β* in four replicate co-transfection experiments with d2CARD and *TRIM27.1aV5* is not significant.
The copy number results of all 4 experimental replicates of *TRIM27.1aV5* co-transfection assays (figure 4-12) were plotted as mean and range. The reduction of average expression of *IFN-β* in cells co-transfected with d2CARD and *TRIM27.1aV5* is 55.8% below d2CARD. Statistical significance was calculated using a one-way ANOVA and a Tukey's post-test using GraphPad version 5.0 software by Prism. n.s. represents $p > 0.05$, $n = 4$.

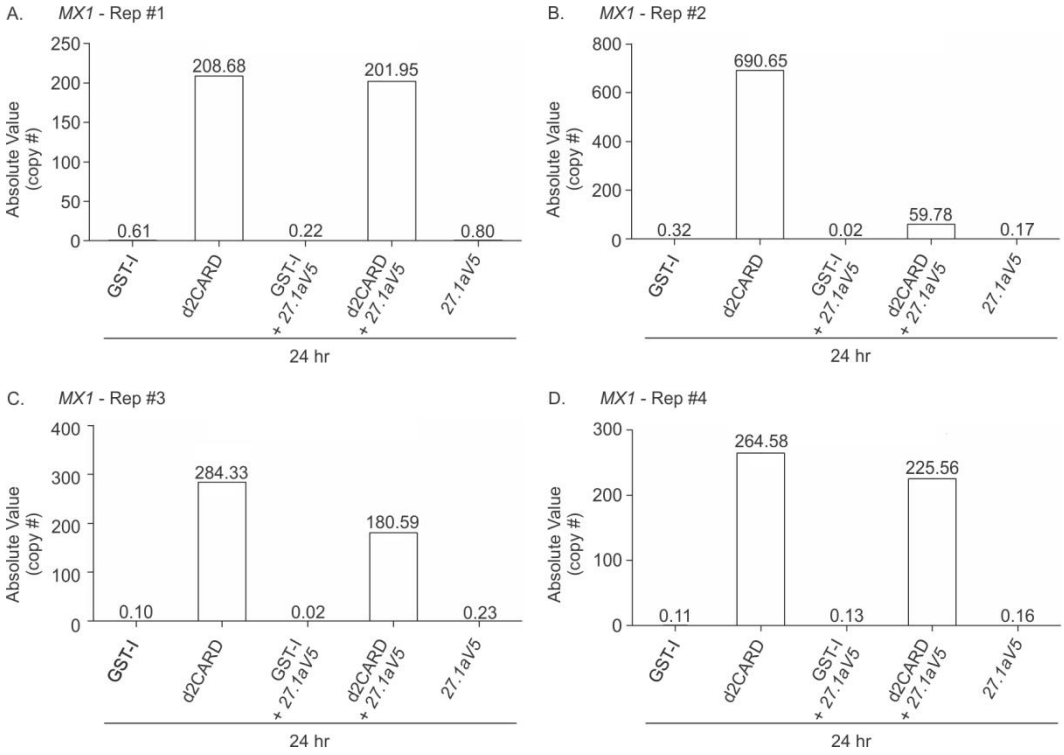

Figure 4-18. *TRIM27.1aV5* decreases the absolute value of expression of *MX1*. Transient co-transfection of chicken DF1 cells with d2CARD (RIG-I) constitutively activated cells and our *TRIM27.1aV5* construct were cultured for 24 hrs PT. RNA was isolated using the TRIzol method at 24 hours PT. Absolute value of expression was determined by ten-fold dilution series (from 10^8 copies to 10^1 copies) of *MX1 fragment* in pCR2.1 vector. Samples were run in triplicate wells, and the average Ct was used to calculate copy number based on standard curve intercept and slope. The four independent experimental replicates shown here complement the luciferase experiments. (A) Replicate #1, experiment #8 co-transfection of *TRIM27.1aV5* decreases *MX1* expression to only 97.7% of d2CARD. (B) Replicate #2, experiment #9 co-transfections decreases *MX1* expression to 0.09% of d2CARD. (C) Replicate #3, experiment #10 co-transfection of *TRIM27.1aV5* decreases *IFN-β* expression to % of d2CARD. (D) Replicate #4, experiment #11 co-transfection decreases *IFN-β* expression to 63.5% of d2CARD. In each independent graph, the n = 1.

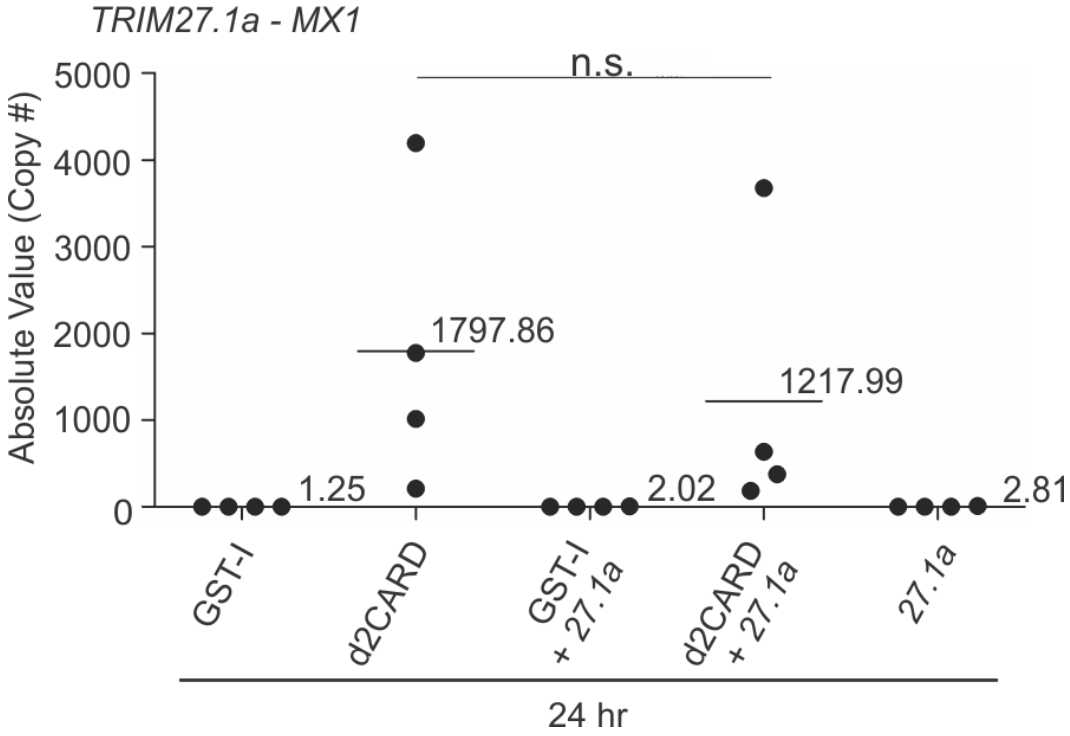

Figure 4-19. Average reduction of expression of *MX1* in four replicate co-transfection experiments with d2CARD and *TRIM27.1aV5* is not significant.
The copy number results of all 4 experimental replicates of *MX1* qPCR in the *TRIM27.1aV5* co-transfection assays (figure 4-14) were plotted as mean and range. Average expression of *MX1* in cells co-transfected with d2CARD and *TRIM27.1aV5* is 46.1% below d2CARD. Because of the high variability in the replicates, this result is not significant. Statistical significance was calculated using a one-way ANOVA and a Tukey's post-test using GraphPad version 5.0 software by Prism. n.s. represents $p > 0.05$, $n = 4$.

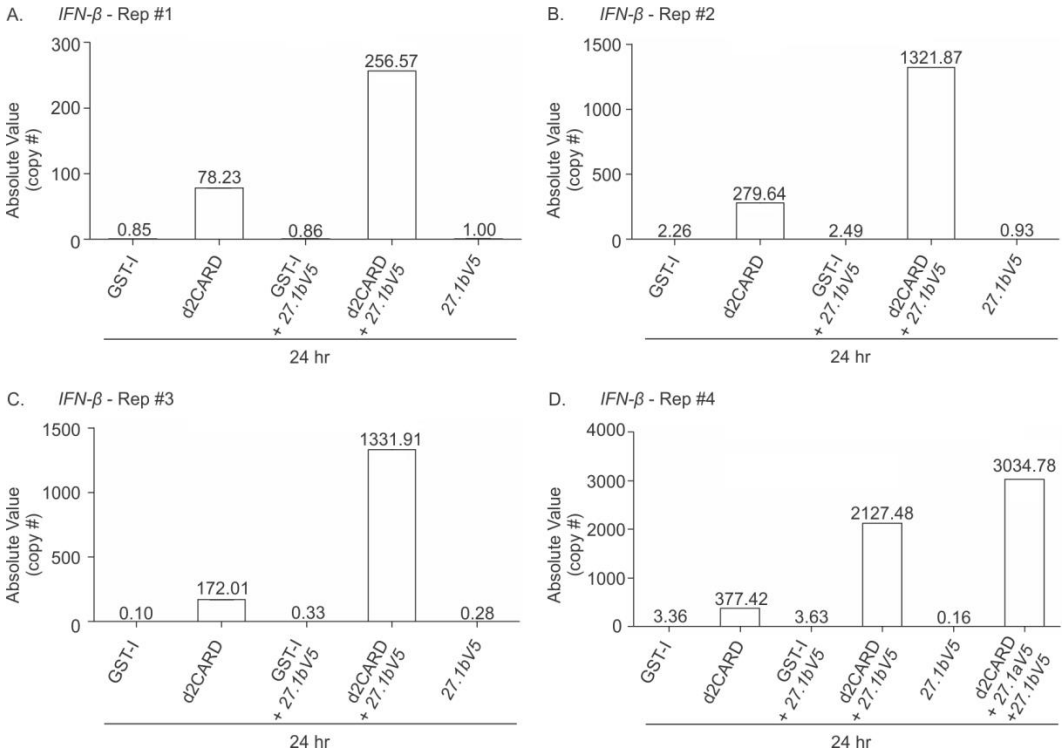

Figure 4-20. *TRIM27.1bV5* increases the absolute value of expression of *IFN-β* in d2CARD constitutively activated cells.

Transient co-transfection of chicken DF1 cells with d2CARD (RIG-I) constitutively activated cells and our *TRIM27.1bV5* construct were cultured for 24 hrs PT. RNA was isolated using the TRIzol method at 24 hours PT. Absolute value of expression was determined by ten-fold dilution series (from 10^8 copies to 10^1 copies) of *IFN-β* in pCR2.1 vector Samples were run in triplicate wells, and the average Ct was used to calculate copy number based on standard curve intercept and slope. The four independent experimental replicates shown here complement the luciferase experiments. (A) Replicate #1, experiment #8 co-transfection of *TRIM27.1bV5* increases *IFN-β* expression to 330.5% of d2CARD. (B) Replicate #2, experiment #9 co-transfections increases *IFN-β* expression to 472.7% of d2CARD. (C) Replicate #3, experiment #10 co-transfection of *TRIM27.1bV5* increases *IFN-β* expression to 774.3% of d2CARD. (D) Replicate #4, experiment #11 co-transfection increases *IFN-β* expression to 563.7% of d2CARD. I also co-expressed *TRIM27.1aV5* and *TRIM27.1bV5* with the d2CARD construct in the same cells in rep #4 to determine if one effect overshadows the other, and a dramatic increase in *IFN-β* expression was observed, 804.1% above the level of d2CARD. In each independent graph, the n = 1.

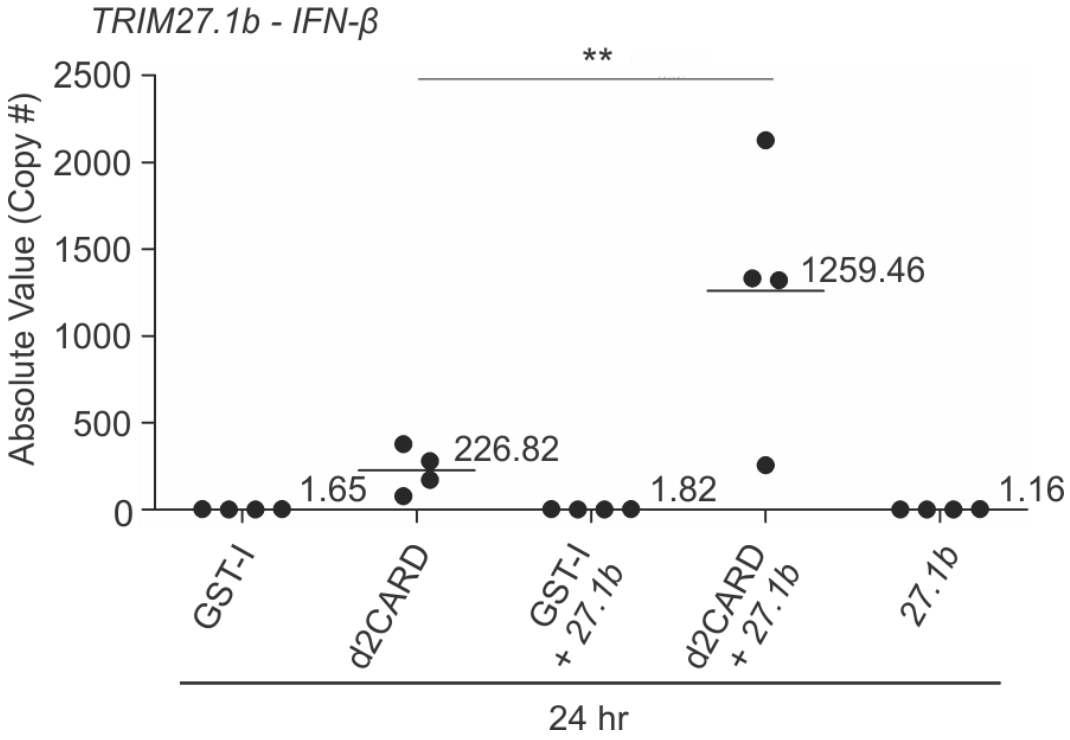

Figure 4-21. Average increase of expression of *IFN-β* in four replicate co-transfection experiments with d2CARD and *TRIM27.1bV5* is statistically significant. The copy number results of all 4 experimental replicates of *TRIM27.1bV5* co-transfection assays (figure 4-16) were plotted as mean and range. The increase of average expression of *IFN-β* in cells co-transfected with d2CARD and TRIM27.1bV5 is 555.3% above d2CARD. The increase is significant ($p < 0.001$). Statistical significance was calculated using a one-way ANOVA and a Tukey's post-test using GraphPad version 5.0 software by Prism. ** represents $p < 0.01$, $n = 4$.

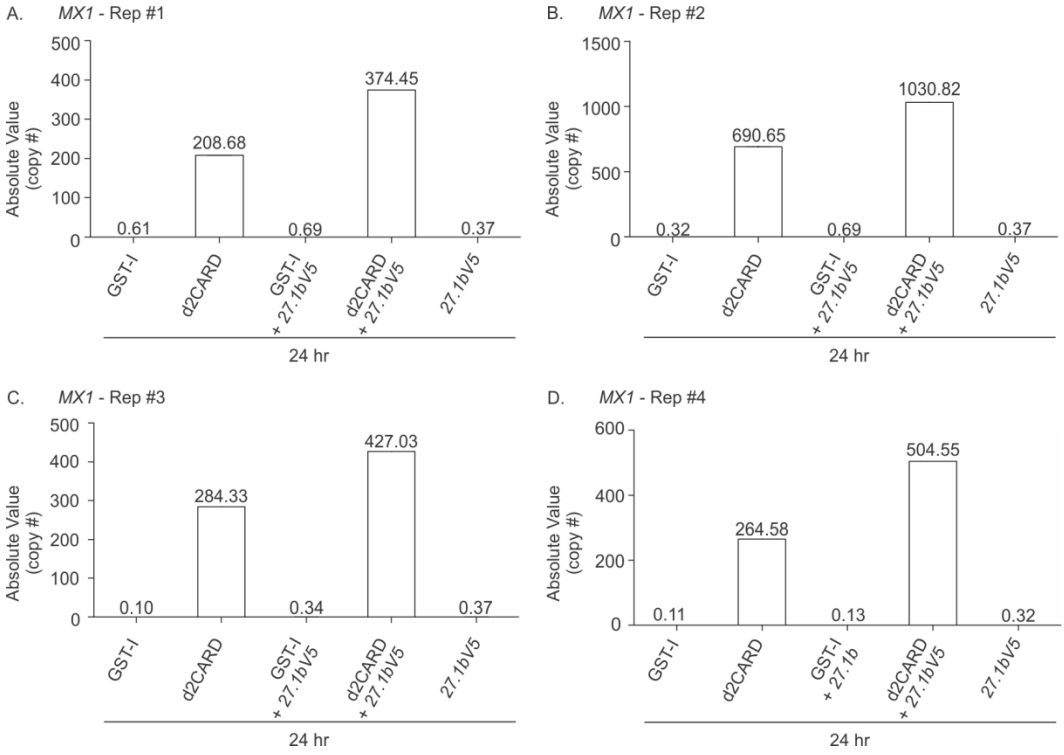

Figure 4-22. *TRIM27.1bV5* increases the absolute value of expression of *MX1*. Transient co-transfection of chicken DF1 cells with d2CARD (RIG-I) constitutively activated cells and our *TRIM27.1bV5* construct were cultured for 24 hrs PT. RNA was isolated using the TRIzol method at 24 hours PT. Absolute value of expression was determined by ten-fold dilution series (from 10^8 copies to 10^1 copies) of *MX1* fragment in pCR2.1 vector. Samples were run in triplicate wells, and the average Ct was used to calculate copy number based on standard curve intercept and slope. The four independent experimental replicates shown here complement the luciferase experiments. (A) Replicate #1, experiment #8 co-transfection of *TRIM27.1bV5* increases *MX1* expression to only 181.2% of d2CARD. (B) Replicate #2, experiment #9 co-transfection of *TRIM27.1bV5* increases *MX1* expression to 149.3% of d2CARD. (C) Replicate #3, experiment #10 co-transfections increases *MX1* expression to 150.2% of d2CARD. (D) Replicate #4, experiment #11 co-transfection increases *MX1* expression to 190.7% of d2CARD. In each independent graph, the n = 1.

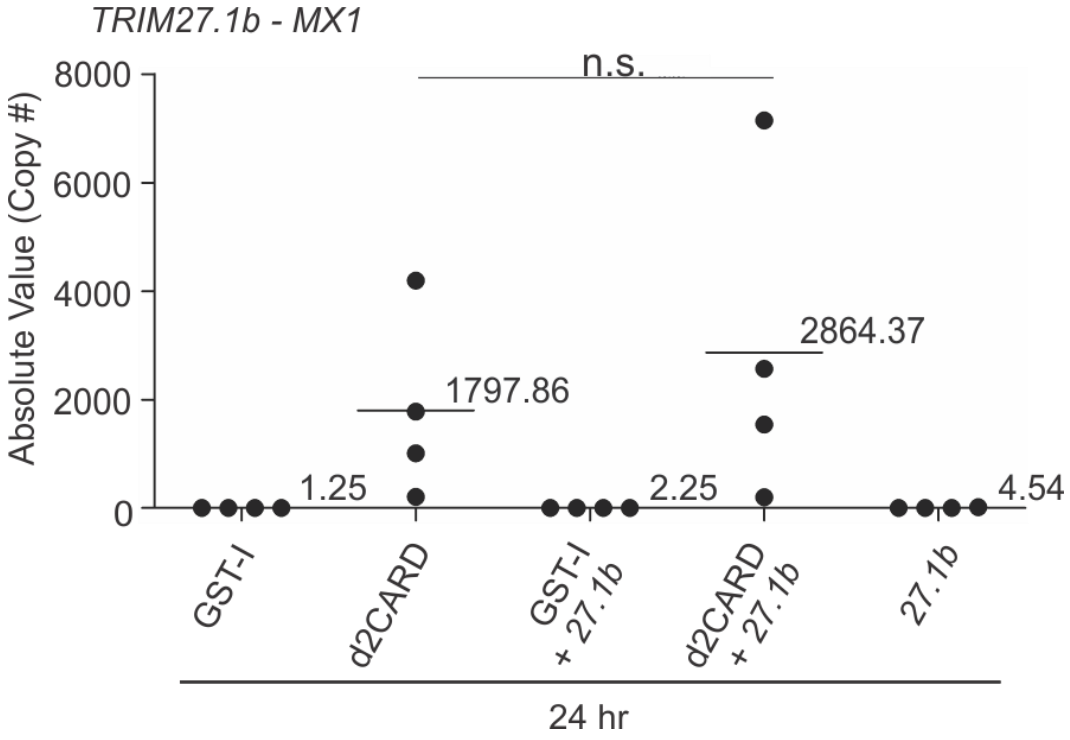

Figure 4-23. Average increase in expression of *MX1* in four replicate co-transfection experiments with d2CARD and *TRIM27.1bV5* is not statistically significant.
The copy number results of all 4 experimental replicates of *MX1* qPCR in the *TRIM27.1aV5* co-transfection assays (figure 4-18) were plotted as mean and range. Average expression of *MX1* in cells co-transfected with d2CARD and *TRIM27.1aV5* is 161.4% above d2CARD. Statistical significance was calculated using a one-way ANOVA and a Tukey's post-test using GraphPad version 5.0 software by Prism. n.s. represents $p > 0.05$, $n = 4$.

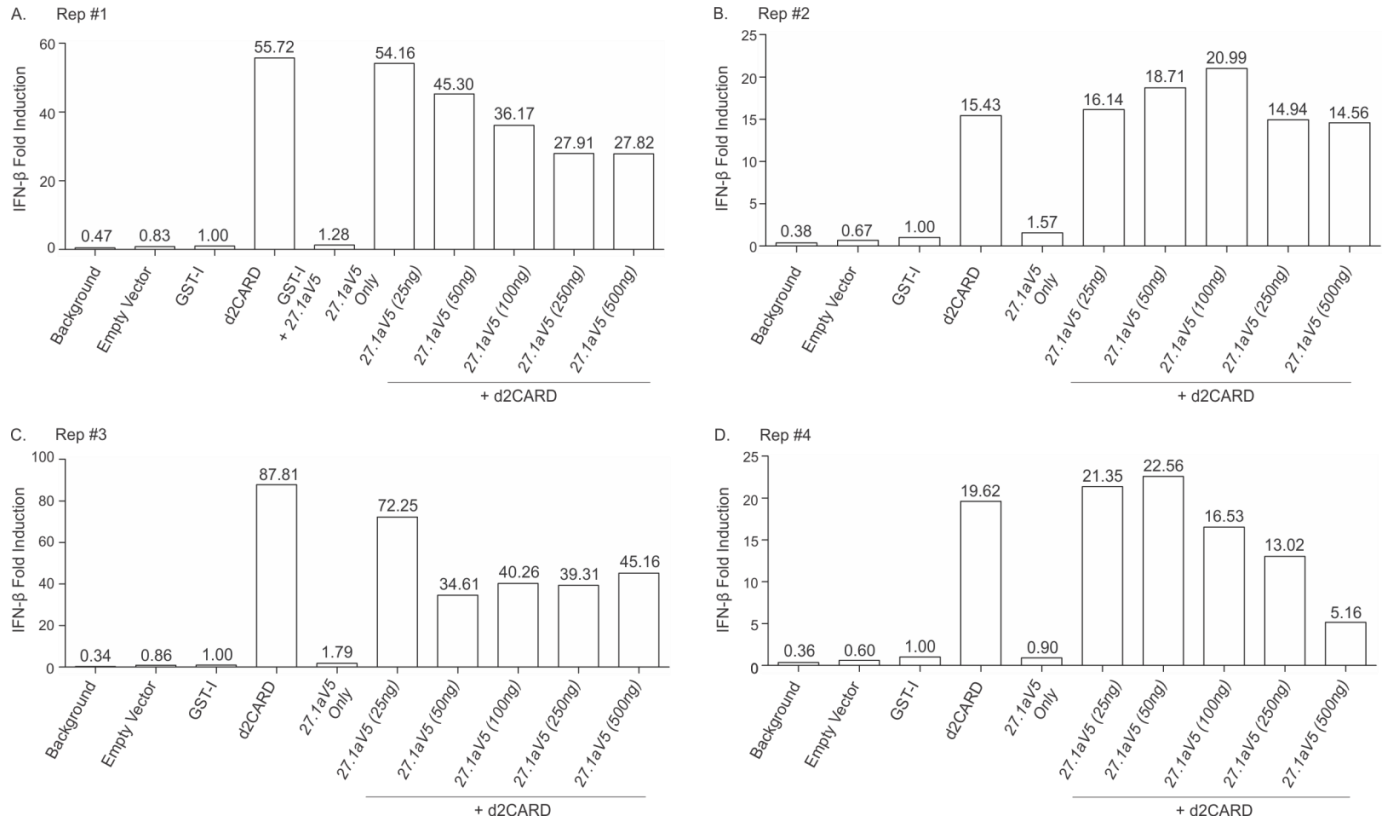

Figure 4-24. ChIFN-2 promoter activation is decreased with increasing amounts of *TRIM27.1aV5* plasmid.
A dual reporter assay shows a dose dependent response of the ChIFN-2 promoter to increasing amounts of *TRIM27.1aV5* construct. The overall trend observed is a reduced activity of the ChIFN-2 promoter which drives the firefly luciferase as increasing amounts of *TRIM27.1aV5* is transfected. There is no obvious peak of suppression, but the results complement the immunosuppressive observations using qPCR. Values are expressed as the ratio of firefly luciferase to renilla luciferase activity and are normalized to GST-I control vector ChIFN-2 induction levels. Shown here in A, B, C and D are four replicate experiments. In each independent graph, the n = 1.

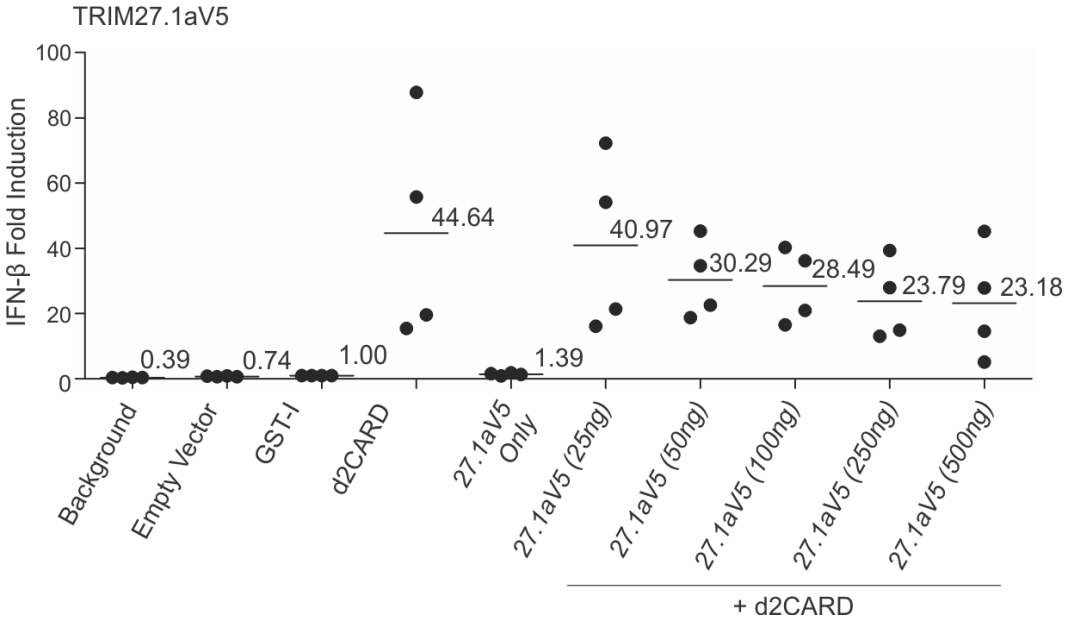

Figure 4-25. Suppression of ChIFN-2 promoter activity by *TRIM27.1aV5* in the average of four replicate co-transfection experiments with d2CARD and *TRIM27.1bV5* is not statistically significant but demonstrates a clear suppressive trend.

To determine if there is a significant relationship to the amount of ChIFN-2 promoter suppression to increasing amounts of *TRIM27.1aV5* construct, I plotted the average and the range of the three replicates. The overall trend observed is a reduced activity of the ChIFN-2 promoter which drives the firefly luciferase as increasing amounts of *TRIM27.1a* is added. There is no significant change due to a high degree of variability. There is also no obvious peak of suppression. Values are expressed as the average ratio of firefly luciferase to renilla luciferase activity and each value used to calculate average normalized to the GST-I control vector ChIFN-2 induction levels. Statistical significance was calculated using a one-way ANOVA and a Tukey's post-test using GraphPad version 5.0 software by Prism. n.s. represents $p > 0.05$, $n = 4$.

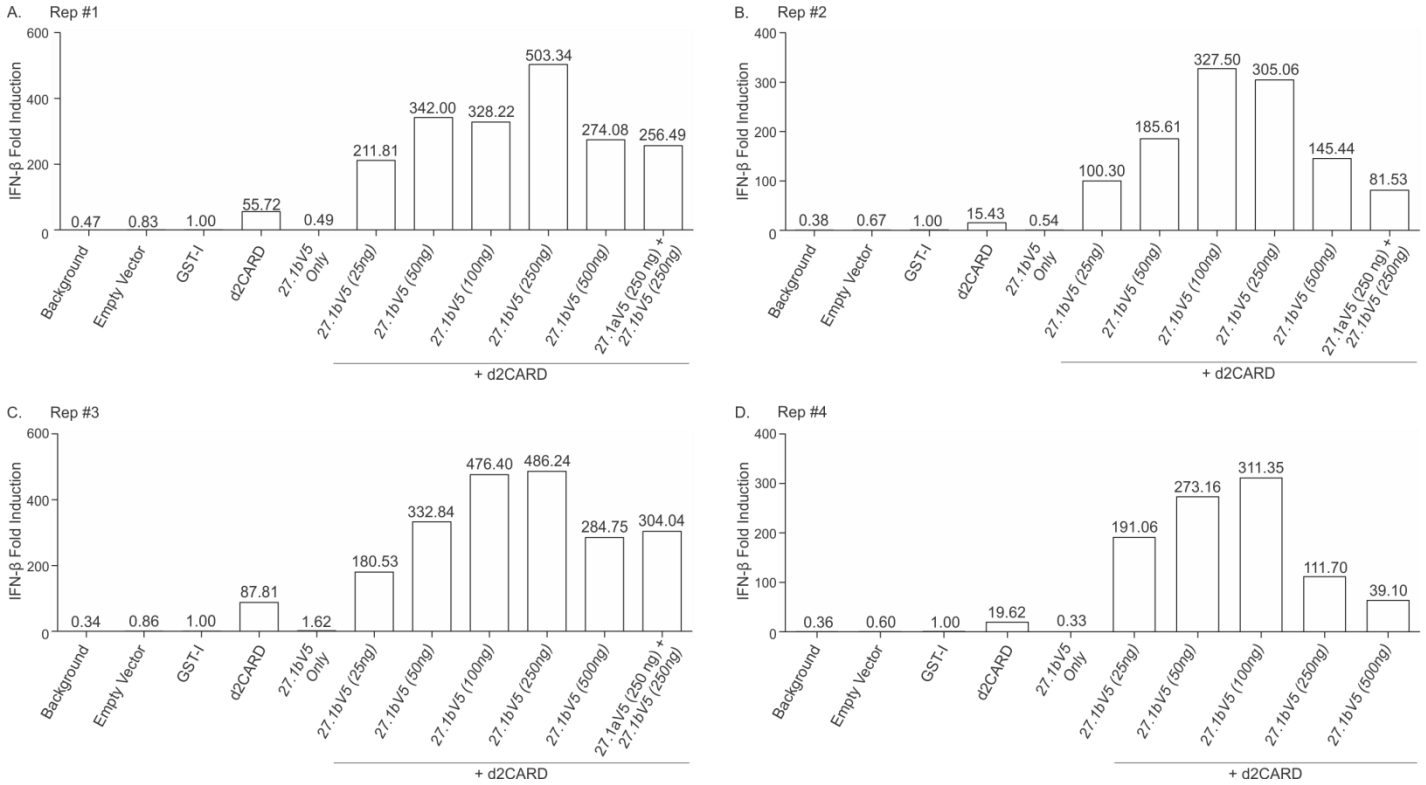

Figure 4-26. ChIFN-2 promoter activation is increased with increasing amounts of *TRIM27.1bV5* plasmid.
A dual reporter assay shows a dose dependent response of the ChIFN-2 promoter to increasing amounts of *TRIM27.1bV5* construct. The overall trend is increased activation of the ChIFN-2 promoter with increasing amounts of transfected *TRIM27.1bV5*. The observed peak of activation is between 100 ng and 250 ng of vector, the results complement the immunostimulatory observation using qPCR. Values are expressed as the ratio of firefly luciferase to renilla luciferase activity and are normalized to GST-I control vector ChIFN-2 induction levels. When *TRIM27.1aV5* and *TRIM27.1bV5* are co-transfected together at equivalent amounts (250 ng) enhancement of the ChIFN-2 promoter is observed. Shown here in A, B, C and D are four replicate experiments. In each independent graph, the n = 1.

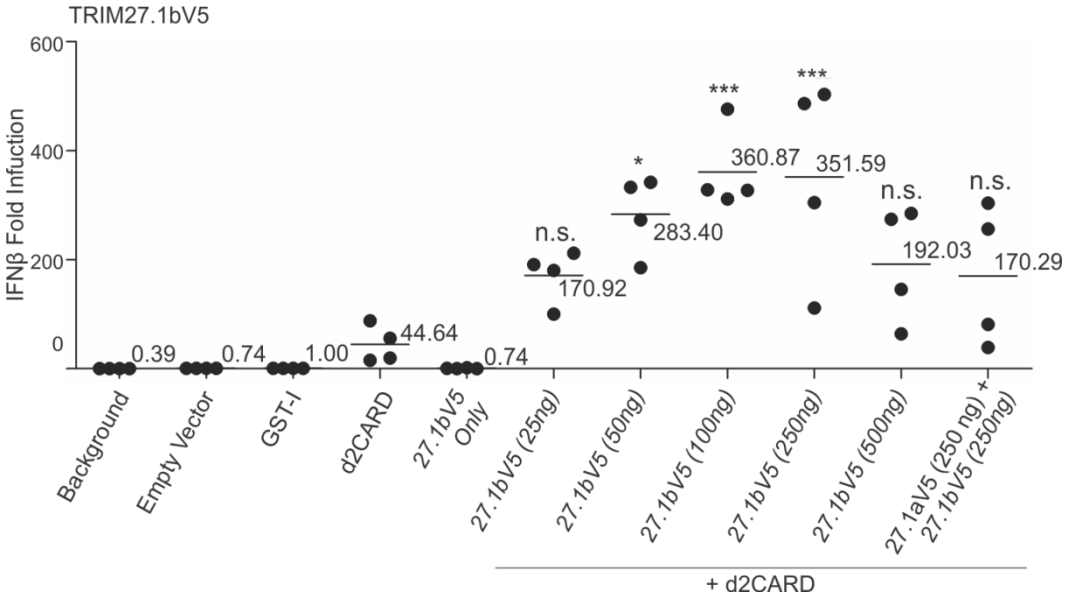

Figure 4-27. Activation of ChIFN-2 promoter by *TRIM27.1bV5* in the average of four replicate co-transfection experiments with d2CARD and *TRIM27.1bV5* is statistically significant and peaks at 100 ng of *TRIM27.1bV5*.

To determine if there is a significant relationship to the amount of ChIFN-2 promoter suppression to increasing amounts of *TRIM27.1bV5* construct, I plotted the average and the range of the three replicates. The overall trend observed is a dramatically enhanced and statistically significant increase in activity of the ChIFN-2 promoter which drives the firefly luciferase as increasing amounts of *TRIM27.1b* is added. The peak of activation seems to be at 250 ng of *TRIM27.1bV5* vector. In addition, co-expressing *TRIM27.1a* and *TRIM27.1b* significantly increases ChIFN-2 promoter activity which suggests the immunostimulatory activity of *TRIM27.1bV5* has a stronger effect than the immunosuppressive activity of *TRIM27.1a*. When *TRIM27.1aV5* and *TRIM27.1bV5* are co-transfected together at equivalent amounts (250 ng) enhancement of the ChIFN-2 promoter is observed as indicated by the mean, but due to variability in the replicates, this is not a statistically significant increase over constitutively active d2CARD transfected cells. Values are expressed as the average ratio of firefly luciferase to renilla luciferase activity and each value used to calculate average normalized to the GST-I control vector ChIFN-2 induction level in each replicate. Statistical significance was calculated using a one-way ANOVA and a Tukey's post-test using GraphPad version 5.0 software by Prism. n.s. represents $p > 0.05$, * is $p < 0.05$, ** is $p < 0.01$ and *** is a $p < 0.001$, ($n = 4$).

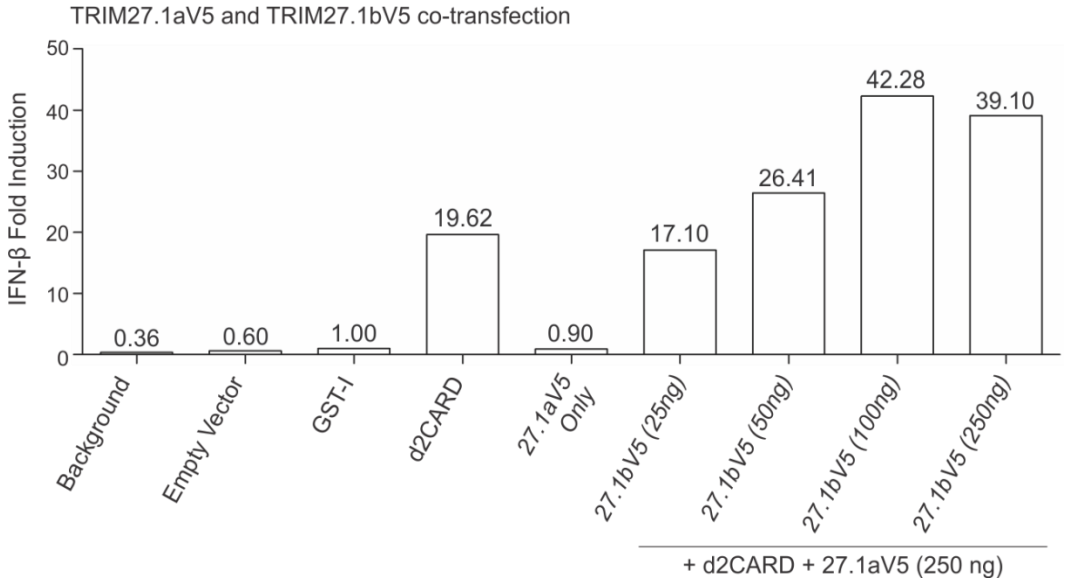

Figure 4-28. Immunostimulatory activity of *TRIM27.1bV5* is more potent than the immunosuppressive activity of *TRIM27.1aV5*.
To determine what effect co-expression of the two *TRIM27.1* constructs would have on activity on the ChIFN-2 promoter, I co-expressed a standard amount of *TRIM27.1aV5* (250ng) with increasing amounts of the *TRIM27.1bV5* construct. This graph is the only replicate of this experiment conducted thus far. The overall trend observed is that even low concentrations of the immunostimulatory *TRIM27.1bV5* construct (50 ng) counteract the immunosuppressive *TRIM27.1aV5* and modestly increases expression of firefly luciferase above the constitutively activated cells (d2CARD). The peak of activity for *TRIM27.1bV5* in addition to *TRIM27.1aV5* appears to be with the addition of 100 ng of *TRIM27.1bV5*. All vectors were normalized to a standard 500 ng with addition of pcDNA3.1/Hygro+ empty vector. Values are expressed as the average ratio of firefly luciferase to renilla luciferase activity and each value used to calculate average normalized to the GST-I control vector ChIFN-2 induction levels. This is a graph of a single experiment, due to time constraints this dose dependent experiment was conducted only once, (n = 1).

Chapter 5. DISCUSSION

In our investigation of the repertoire of duck TRIMs, I sought to determine if ducks have *TRIM*s which would confer a unique, species-specific advantage to survival and propagation of IAV. As ducks are the natural host of IAV (Kim *et al.* 2009; Jourdain *et al.* 2010), I hypothesized that one or a number of TRIMs may be playing a unique role in controlling either replication of the virus, or the immune responses to IAV infection. I wanted to first determine what *TRIM*s ducks have, and if there were any unique characteristics about the duck repertoire. By comparison of the duck repertoire with the chicken repertoire, an IAV susceptible species, I narrowed down the *TRIM*s to a manageable set of candidates within the MHC locus. From these duck *TRIM*s I determined four are differentially expressed in an immune or IAV relevant organ. I next sought to resolve what role, if any, TRIMs are likely to be playing in controlling replication of IAV and what potential implications could the differences in *TRIM* gene repertoire have on survival of chickens and ducks. Here, I showed that ducks do have a unique *TRIM* gene, that is expressed during highly pathogenic IAV infection, is absent in chickens and that is immunostimulatory.

5.1 Ducks have a diverse repertoire of TRIMs

Key to understanding the differences in the duck and chicken *TRIM* repertoire, the first hurdle was determining what *TRIM*s were present and recognizable in the duck. I determined that there is a wide array of *TRIM* family members that are recognizable in the duck genome, but the total list (Table 3-1) likely underestimates the duck repertoire. As mentioned previously, although coverage of genetic material is enough for 64-passes, gaps in the genome remain and regions of unresolved sequence and discontiguous scaffolds still remain. Before I can develop a thorough understanding of the duck TRIM

repertoire relationship and co-evolution as it relates to influenza virus, the genome must be elucidated as clearly as possible. As there are currently still gaps in the genome assembly and our prediction of the TRIM family members, there are likely still duck specific *TRIM*s to be elucidated. This is also a family of genes, with conserved domain architecture, so read assembly problems may come into play. The recognizable *TRIM*s in the draft genome consist mainly of group 1 TRIMs (evolutionarily conserved, with variable C-terminal domains, section 1.5, Table 1-1 and Table 3-1) (Sardiello *et al.* 2008; Marin 2012) with 32 predicted *TRIM*s (Table 3-1) corresponding to 25 of the representative group 1 members. The representatives of group 2 *TRIM*s (Marin 2012) are far less robust, as duplicated representatives of 6 of the group 2 *TRIM*s exist (Table 3-1), corresponding to 15 different group 2 *TRIM* genes predicted. The vast majority of the recognizable group 2 *TRIM*s in the current repertoire are located within scaffold618. Also, because the duck genome was annotated using available EST databases and synteny analysis with the chicken genome, duck specific TRIMs may be missed in the first draft. I therefore believe there is likely to be several of unannotated group 2, PRY/SPRY containing *TRIM* genes in the duck genome that are as yet unapparent. As the group 2 *TRIM*s are the more rapidly evolving subset (section 1.5), there is a very real possibility that the duck group 2 repertoire could be unique or expanding in a species-specific manner.

5.1.1 Scaffold618 *TRIM*s are likely IAV and immune relevant

Although little work on *TRIM39.2* and *TRIM7.2* in scaffold618 was done – both of these genes hold potential for some immune involvement which will require further investigation. *TRIM7.2* is upregulated at 1 dpi in highly pathogenic IAV (VN1203) infected lung tissue (Figure 3-11) and although there is nothing currently known about the role of TRIM7 in avian or mammalian immune responses there is still an enduring

possibility for *TRIM7.2* to contribute directly to IAV restriction or another signaling role in intracellular immune responses. Additionally, *TRIM39.2* is slightly upregulated at 3 dpi in intestine (Figure 3-12), the site of replication of low pathogenic IAV infections, and in 1 dpi VN1203 spleen, where chicken *TRIM39.2* has been shown to be most highly expressed (Pan *et al.* 2011), duck *TRIM39.2* expression is increased 5-fold over mock infected tissue. Expression in the spleen does not indicate involvement in direct IAV restriction, but may indicate a role in signaling or in general immunomodulation. Although I did not pursue functional analysis of these genes it is possible that there may be a yet to be determined role in immune modulation. As both *TRIM7* and *TRIM39* are homologs of *TRIM27* (HomoloGene, NCBI), elaboration of the repertoire within the avian MHC may indicate duplication and, although they are all conserved in the three avian species discussed here, these two candidates are worth pursuing functionally.

5.1.2 *TRIM27.1a* and *TRIM27.1b* are likely functionally divergent polymorphic paralogs in the MHC

Although the repertoire presented here is far from exhaustive, the duck TRIM family is still well developed from our early vantage point. From the list of 47 putative recognizable *TRIM* or *TRIM* fragments (Table 3-1), I pursued only a small fraction of the full list. Scaffold618 and the 8 putative *TRIM* genes within this contig have strong evidence to suggest their location within the duck MHC locus. As the conservation of *TRIM*s and non-*TRIM* genes alike, between the duck and those found in the chicken and turkey MHC suggests that scaffold618 will reside telomeric to the previously mapped duck MHC locus (Mesa *et al.* 2004; Moon *et al.* 2005). Given the long (90 my) divergence of chickens and ducks, very little has changed within this MHC located TRIM-rich region outside of the duplication. Given that TRIM7, -27 and -39 are known homologs of one another (HomoloGene, NCBI) and all belong to the group 2, rapidly

evolving TRIM family members (Table 1-1), genes within scaffold618 probably originated from a single ancestral *TRIM*, as is observed with the *TRIM5* locus in humans, mice, cows and dogs (Sawyer *et al.* 2007) (section 1.5). Although our bioinformatic analysis is not robust, assigning *TRIM27.1b* as a paralog of *TRIM27.1a* is reasonable. Considering that the highest percent identity of TRIM27.1b to any TRIM in scaffold618 is to TRIM27.1a (51% identity, Table 4-1), the direction and position of the ORF in scaffold 618 (Figure 3-2) and considering that avian TRIM27 proteins aligns TRIM27.1b most closely with duck TRIM27.1a and TRIM27.1 from chicken and turkey (Figure 4-2), I believe the two genes to be the result of an ancient duplication event. Granted, I have presented no evidence here to suggest that perhaps *TRIM27.1b* is not ancestral and was lost from the chicken and turkey genomes. In the course of this work, I did not pursue a thorough and concise search for evidence of a residual *TRIM27.1b* in either of the published galliform genomes, what I can say is that in our pursuit of assigning accurate nomenclature to *TRIM27.1b,* I saw no evidence of a putative homolog in either the chicken or turkey genomes. Of note as well is the absence of a zebra finch (*Taeniopygia guttata*) prediction for duck TRIM27.1b. I have tried to identify a homolog of TRIM27.1b in the available zebra finch genome through blast with protein sequence, genomic sequence, coding sequence and intron sequences. There is no annotated or sequenced hit from the zebra finch to duck TRIM27.1b. Additionally, I have yet to identify a zebra finch scaffold that is syntenic with duck scaffold618. Elucidating the zebra finch, or even another avian genome more closely related to the duck than the chicken and turkey, would help to clarify the origins of duck *TRIM27.1b* as ancient duplication that was lost in the Galliforms order or as a duck specific duplication event. Indeed, as duck *TRIM27.1b* interacts with and modulates the downstream components of

the RIG-I pathway, and RIG-I is lost in chickens, there is an absence of selective pressure to retain a gene that confers no additional benefit to the chicken.

What our work does demonstrate is that the two adjacent *TRIM27.1* genes located within the duck MHC have opposing functions in modulation of intracellular immune signaling (Figure 5-1). I showed that *TRIM27.1a* is immunosuppressive, consistently depressing production of *IFN-β* and *MX1* by approximately 50% of the level of constitutively active d2CARD cells. In addition, *TRIM27.1a* was highly expressed in highly pathogenic (VN1203) infected duck lung (Figure 3-9) at 1 dpi indicating an important role in expression during the early innate response of ducks to IAV. Initially, the immunosuppressive nature of *TRIM27.1a* on the antiviral gene expression was counterintuitive to what I know to be important in the duck immune response to IAV. An immediate (1 dpi), robust (multigene ISG expression) and profound (1000-fold increase in ISG expression) (Barber *et al.* 2010; Vanderven *et al.* 2012; Barber *et al.* 2013) activation of the antiviral program is of great importance in the duck response to highly pathogenic IAV. As such, a 30-fold increase in an immunosuppressive *TRIM* seems to contradict the robust nature of the duck immune response. As our luciferase results indicate, a large amount of *TRIM27.1aV5* construct (500 ng) was required to suppress *IFN-β* promoter activation (Figure 4-24), and even so the suppression was incomplete and variable (Figure 4-25). However, perhaps the expression of this immunosuppressive *TRIM27.1a* could help in providing a balanced intracellular activation response to be beneficial to the duck. Elaborating on the point, the hallmark of the pathology associated with IAV is over activation of immune responses (Kobasa *et al.* 2007). Perhaps a contributing role of *TRIM27.1a* is to maintaining short lived dramatic responses and that after 1 dpi, expression of *TRIM27.1a*, along with other anti-inflammatory mediators help to quell the responses in ducks. This may be why I find *TRIM27.1a* homologs in ducks,

chickens and turkeys. Further investigation would be warranted once a duck cell line could be obtained, targeted knockdown of endogenous *TRIM27.1a* could help determine if pathological effects associated with the absence of *TRIM27.1a* expression occurs.

We also demonstrate that the unique duck TRIM27.1b consistently and dramatically increasing production of *IFN-β* and *MX1* by approximately 10-fold higher than the expression level of constitutively active d2CARD cells (Figure 4-7 and Figure 4-9). The potent immunostimulatory effect of *TRIM27.1b* on IFN-β promoter activity (Figure 4-26 and Figure 4-27) and on expression of downstream RIG-I antiviral genes (Figure 4-20 and Figure 4-22) was definitely unexpected, and also warrants speculation on its role in a highly pathogenic IAV infection. Although there was a relatively small upregulation of *TRIM27.1b* in highly pathogenic IAV infected lung tissue at 1 dpi (5-fold) I have demonstrated that even a small amount of the immunostimulatory *TRIM27.1bV5* was able to counteract the immunosuppressive effects of its paralog, *TRIM27.1aV5* (Figure 4-28). As I have no samples from earlier on in the *in vivo* IAV infections, perhaps the 5-fold expression of *TRIM27.1b* is not the peak. If there was immediate upregulation and expression of *TRIM27.1b* in highly pathogenic IAV infected lung tissue there may be a contributory role in initiating the robust innate immune responses characteristic of duck IAV responses through enhanced production of IFN-β. What is very interesting about the interplay of these two immunomodulatory TRIMs is that *TRIM27.1b* is absent from the published genomes of the members of the galliform order. huTRIM27 is often described in roles that are immunosuppressive (section 1.6) so the unexpected immunostimulatory effect of duck TRIM27.1b leaves a large number of open ended questions about how it functions. Zha *et al.* (2006) described a direct effect for huTRIM27 on the NFκB signaling pathway, but perhaps duck TRIM27.1b does not have the same binding partners nor physical interaction function as the huTRIM27. As

the ChIFN-2 promoter has consensus binding sites for both NFκB and the IRF family (Sick *et al.* 1998), there is a possibility that *TRIM27.1b* modifies a member of the IRF family directly in order to enhance activation, this will be discussed below. However, without further investigation as to the functional roles of *TRIM27.1a* or *TRIM27.1b* in the pathway this is all just speculation. The interplay of all aspects of PRRs, PAMPs, cell signaling components, cross-talk, viral virulence factors, strain type and general fitness of the host in addition to species-specific genetic components will all contribute to the development of pathology or clearance of a highly pathogenic IAV viral infection.

5.1.3 Allelic polymorphisms are likely not contributing to phenotypic differences

From our SNP analysis I can ascertain that, although these two genes are polymorphic, the low amino acid substitution rate compared to the number of SNPs in the genes indicates negative selection is occurring. Perhaps due to location within the rapidly evolving avian MHC, the observed polymorphisms in both genes may simply be piggybacking along. Although two SNPs that correspond to amino acid substitutions do occur in the PRY domains of TRIM27.1a and TRIM27.1b, the consequences of those substitutions are likely negligible to function. In the PRY domain of TRIM27.1a, a substitution occurring in duck 312 at position T356I could cause a functional change; polar threonine to the hydrophobic isoleucine could cause a conformational change in the PRY domain. However, both of these amino acids are bulky Cβ branched amino acids which are restricted in movement (Betts & Russell 2003). Similarly, the single amino acid change within the PRY domain of TRIM27.1b at position A320V would likely be of little consequence as both of these amino acids have aliphatic side chains. Again, the Cβ branched nature of valine could alter the flexibility of the position (Betts & Russell 2003), as discussed above but further work with constructs containing both substitutions

would need to be done in order to determine if allelic differences between ducks and substitutions in the PRY domain could influence function.

5.1.4 Elucidating the roles of TRIM27.1a and TRIM27.1b will require further investigation

Further interpretations of function could be determined from domain deletion mutants of the TRIM27.1a and TRIM27.1b proteins. Zha *et al.* (2006) reported that the C-terminal PRY/SPRY domains of huTRIM27 were responsible for the interaction with IKKε. As TRIM27.1a seems to function in a similar manner as huTRIM27, having an immunosuppressive role and depressing the production of type I interferons and ISGs, if the functional domain of TRIM27.1a is in the C-terminus there may be conserved interactions with the duck TRIM27.1a and duck IKK family members. Conversely, TRIM27.1b has an immunostimulatory role in the activated cell, opposite to what is observed for huTRIM27 and TRIM27.1a, so there may be no direct interaction with the IKK family. As huTRIM27 has been shown to have both a ubiquitin E3-liagase capability (Napolitano *et al.* 2011) and a SUMOylating E3-ligase capability(Chu & Yang 2011) it is conceivable to think that TRIM27.1b enhances transcriptional activation of *IFN-β* through modifying signaling component(s) of the RIG-I pathway. I have shown that TRIM27.1b does not likely interact with RIG-I directly (Figure A-10) and does not function in the absence of intracellular immune activation (Figure 4-7, Figure 4-8, Figure 4-20 and Figure 4-22), so increased *IFN-β* and *MX1* transcription may be through modification of or interaction with a downstream component. Where in the pathway the enhanced activation occurs is unknown. In addition, I did not explore here which domains of TRIM27.1a and TRIM27.1b are responsible for their immunomodulatory functions. Interestingly, TRIM28 has been shown to depress IRF7 activation through the E3-ligase activity of the RING domain (Liang *et al.* 2011), perhaps TRIM27.1b has a

similar function resulting in an immunostimulatory activity through the alternate or secondary arm of RIG-I activation, IRF7 (section 1.3). Or the contrary may be true, where E3-ligase activity is not required for the immunostimulatory abilities of TRIM27.1b. I cannot rule out direct interaction with an inhibitory component, enhancing activity of a downstream signaling component to amplify the cascade or to modify a transcription factor to enhance transcriptional activation, such as IRF7.

5.2 Duck TRIMs outside of the MHC locus are interesting candidate genes

Duck TRIM19 (or PML) is a promising avenue of exploration as it would seem that, in avian species, more than 1 homolog of TRIM19 are present. Although TRIM19 is a well-known and well-studied transcription factor (Cheng & Kao 2012; Ohgiya *et al.* 2012; Berscheminski *et al.* 2013) I predict two separate TRIM19 genes are present in the duck, but I did not determine through sequencing how many TRIM19 homologs are present in the duck nor chicken genomes. As the involvement of mammalian TRIM19 in cell cycle regulation, cancer development, signaling has been so well studied (section 1.4.2) TRIM19 is definitely a worthy pursuit. TRIM19 is a member of the group 1 TRIMs which are evolutionarily conserved and which lacks a PRY/SPRY domain. As such, there may be no IAV duck host coevolution occurring with TRIM19 but it is interesting that both the duck and chicken predict more than one homolog of TRIM19. Perhaps there is an avian specific function to TRIM19 homologs/paralogs that is absent or yet to be observed in the mammalian system.

Our initial pursuit of TRIM14 as a differentially expressed TRIM was perhaps less fruitful that originally thought. Our EST and differential map to gene analysis based on the draft duck genome and 454 deep sequencing suggested that TRIM14 was expressed

during IAV infections. Our qPCR results suggest a less than profound involvement for this gene. However, the recent association between TRIM14 and hepatitis C restriction (Metz *et al.* 2012) and the observations that duck TRIM14 is slightly upregulated in 3 dpi infected lung and spleen samples (Figure 3-5 and Figure 3-6B) suggests that this TRIM family member may be worth further investigation. Structurally, TRIM14 lacks the RING domain, in the C-uncategorized group (Sardiello *et al.* 2008), so it is unlikely that there is a role in E3-ligase activities.

5.3 Future directions

The first step in pursuing further functional characterization of TRIM27.1a and TRIM27.1b would to be to construct domain deletion constructs and look at which domains are responsible for immunomodulation. As the question of the role of E3-ligase activity is still unanswered the deletion mutants will provide valuable information into the validity of creating tagged ubiquitin and SUMO constructs. If the RING-domain of either of the TRIM27.1 proteins confers either immunomodulatory effects, co-immnoprecipitation with tagged modifier constructs would indicate which E3-ligase capability is of importance to the avian TRIM27.1s. However, if the C-terminal PRY/SPRY domain is the important domain in immunomodulation, as is observed with the huTRIM27 and the IKK interactions (Zha *et al.* 2006), then construction of epitope-tagged IKK duck family members would be the next logical step in elucidating the interactions. However, there are many downstream signaling components of the RIG-I pathway, and as duck TRIM27.1a and huTRIM27 share less than 50% identity it is possible that duck TRIM27.1a acts in a completely different and novel manner. In addition, immunomodulation may not be the sole role of duck TRIM27.1a and

TRIM27.1b. As mentioned previously, TRIMs have been shown to have many different roles in different contexts; TRIM5α directly restricts replication of HIV (Stremlau *et al.* 2006) and has been shown to have a role that involves the E3-ligase activity as well (Lienlaf *et al.* 2011). One unique method to analyze cellular activation that may be of great interest to the immunostimulatory function of TRIM27.1b is a nuclear translocation assay using NFκB. As type I interferons have an autocrine and paracrine stimulatory effect on NFκB nuclear translocation, if I employed the use of a fluorescently labelled TRIM construct and a nuclear translocation assay with confocal microscopy and/or with flow cytometry could assess the activation of the whole cell population on the whole versus in individually transfected cells. As a control, production of avian IFN-β and exogenous addition to an untransfected cell population could be used to compare the activation of DF1 cells to type I interferons alone. This could help to elucidate if the enhanced output of *IFN-β* and *MX1* are the result of intracellular signaling enhancement (if more cells are double positive for the transfected gene, and trasnlocated NFκB), the result of increased response to enhanced IFN-β production in the population (more cells which are single positive for NFκB translocation in the absence of the construct reporter) or a combination of the two.

An interesting characteristic of duck primary cells is that they are more likely to apoptose during IAV infection than primary chicken cells (Kuchipudi *et al.* 2012). A more rapid apoptotic phenotype was observed with both low and highly pathogenic IAV infections as compared to the primary chicken cells. Although this is speculation, huTRIM27 has been shown to induce apoptosis through the N-terminal RBCC motif when over expressed (Dho & Kwon 2003). Although no evidence for increased apoptosis phenotype in chicken DF1 cells overexpressing TRIM27.1a or TRIM27.1b was observed, our work here was conducted independent of IAV infection. In the future, over

expression studies using TUNEL assays could indicate or dismiss a similar role of duck TRIM27.1s in induction of apoptosis. Additionally, activation of the NFκB transcription factor can push a cell towards the NFκB survival pathway, so perhaps TRIM27.1b could have an anti-apoptotic phenotype. Both ducks and chickens possess the *TRIM27.1a* homolog, which is immunosuppressive (Figure 4-3 to Figure 4-6), results in decreased ISRE and NFκB responsive promoter activation (Figure 4-24 and Figure 4-25), and seems to function similarly to huTRIM27 (Zha *et al.* 2006) so overexpression of *TRIM27.1a* in the context of an IAV infection could result in more rapid apoptosis in chicken DF1 cells. Although this is interesting to speculate about, it does not answer – and indeed confounds the question as to why duck cells – which have an extra immunostimulatory TRIM27.1b absent in chickens, yet apoptose more rapidly than chicken cells. However, if enhanced apoptosis is observed in either overexpression system when DF1 cells are infected with low pathogenic IAV, apoptosis assays may provide some valuable and quantifiable insight.

Another very interesting avenue to pursue would be to use confocal fluorescence microscopy to look at localization of TRIM27.1a and TRIM27.1b in the cells. As huTRIM27 and huTRIM19 have been shown to co-localize together in perinuclear structures called PML NBs (section 1.4.2), employing the use of advanced fluorescent microscopy to look at localization in the cell may demonstrate divergent phenotypes compared to human TRIM27. However, in order to pursue work such as this, transient transfection overexpression studies will likely be of little use due to variability in the population. What may be of great use to future studies would be stable transfectants of tagged constructs under an inducible promoter.

Although, the most valuable resource for the study of interactions of *TRIM27.1a* and *TRIM27.1b* in the context of an infection would be with a duck derived cell line. If a duck cell line were available, the valuable resources of knockdowns and endogenous signaling components could provide valuable insights into the interplay in the context of the duck background. I could use direct ligand stimulation instead of the use of co-transfection with the constitutively active d2CARD construct which could decrease transfection variability and expression of the endogenous genes would be more representative versus overexpression studies conducted here. And although TRIM27.1b is absent from the chicken genome, and therefore absent from DF1 cells, background levels of TRIM27.1a expression and artificiality of transiently transfected cells may cloud the endogenous functions.

5.4 Conclusions

The first aim of this study was to use the newly available draft duck genome to determine the duck *TRIM* gene repertoire and compare it to the available chicken genome. To achieve this, I first had to generate a list of potential immune relevant TRIMs recognizable in the draft duck genome. Annotated from the draft duck genome are 47 predicted *TRIM* genes of which scaffold618 contain 9 *TRIM* or *TRIM*-like genes that is syntenic with other avian MHC loci. Two genes within this scaffold618 TRIM-rich region of the duck MHC appear to be a unique duck duplication, *TRIM27.1a* and *TRIM27.1b*. This list will be by no means exhaustive; the duck genome, although coverage of genetic material is enough for 64-passes, gaps in the genome remain (Huang *et al.* 2013). I performed gene synteny analysis against the published chicken and turkey genomes for loci that were deemed to be important due to concentration of *TRIM* genes

(which indicates expansion in a single region) or because previous data suggested upregulation during IAV infection or immunomodulatory abilities. I identified a single scaffold where a high concentration of TRIM genes were located (scaffold618) and determined that the scaffold maps to the chicken TRIM-rich region of the MHC BF/BL locus. Finally, I determined that one apparently divergent duplication of *TRIM27.1* to two *TRIM27.1a* and *TRIM27.1b* genes had occurred and is unique in ducks.

Our second aim was to confirm whether the candidate TRIMs were relevant to IAV infection. Based on the previous expression analyses, ESTs, 454 deep sequencing, SSH and microarray data I could better predict the TRIMs which are likely to be upregulated during IAV infection. I determined that the two *TRIM27.1* genes are upregulated at 1 dpi in highly pathogenic (VN1203) IAV infected duck lung tissue, 30-fold and 5-fold, respectively. Two other genes in the locus are upregulated during highly pathogenic IAV infection in duck lung tissue. The two *TRIM27.1* genes are polymorphic but amino acid substitutions are low compared to the number of SNPs in the coding sequence (27 SNPs versus 3 amino acid substitutions in TRIM27.1a and 12 SNPs versus 2 amino acid substitutions in TRIM27.1b).

Our final aim was to determine if the identified *TRIM*s played a role in altering expression of antiviral effectors in cell culture. As previously mentioned, huTRIM27 is known to interact with key members of the innate intracellular signaling cascade (Figure 1-3A). I hypothesized that one or both genes of the *TRIM27.1*duplication may play a similar role in modulating intracellular innate immune responses (Figure 1-3B). I measured immune activation through quantitative PCR (Figure 1-3C) and luciferase assay to show that ducks possess two immunomodulatory *TRIM27.1* genes, one that is unique to the duck, and that the two genes have opposite transcriptional modulatory

effects on *IFN-β* and *ISG*s. Both duck *TRIM27.1* genes are immunomodulatory but have opposite effects on antiviral gene expression in cell culture. *TRIM27.1a* is immunosuppressive, decreasing transcription of type I interferons and an ISG by approximately half. *TRIM27.1b* is immunostimulatory; increasing expression of type I interferons and an ISG by as much as 10-fold above constitutively activate cells. *TRIM27.1a* and *TRIM27.1b* expression has the same oppositional effects on the chicken IFN-β promoter activation, suggesting a role in modulating the NFκB or IRF7 signaling pathways.

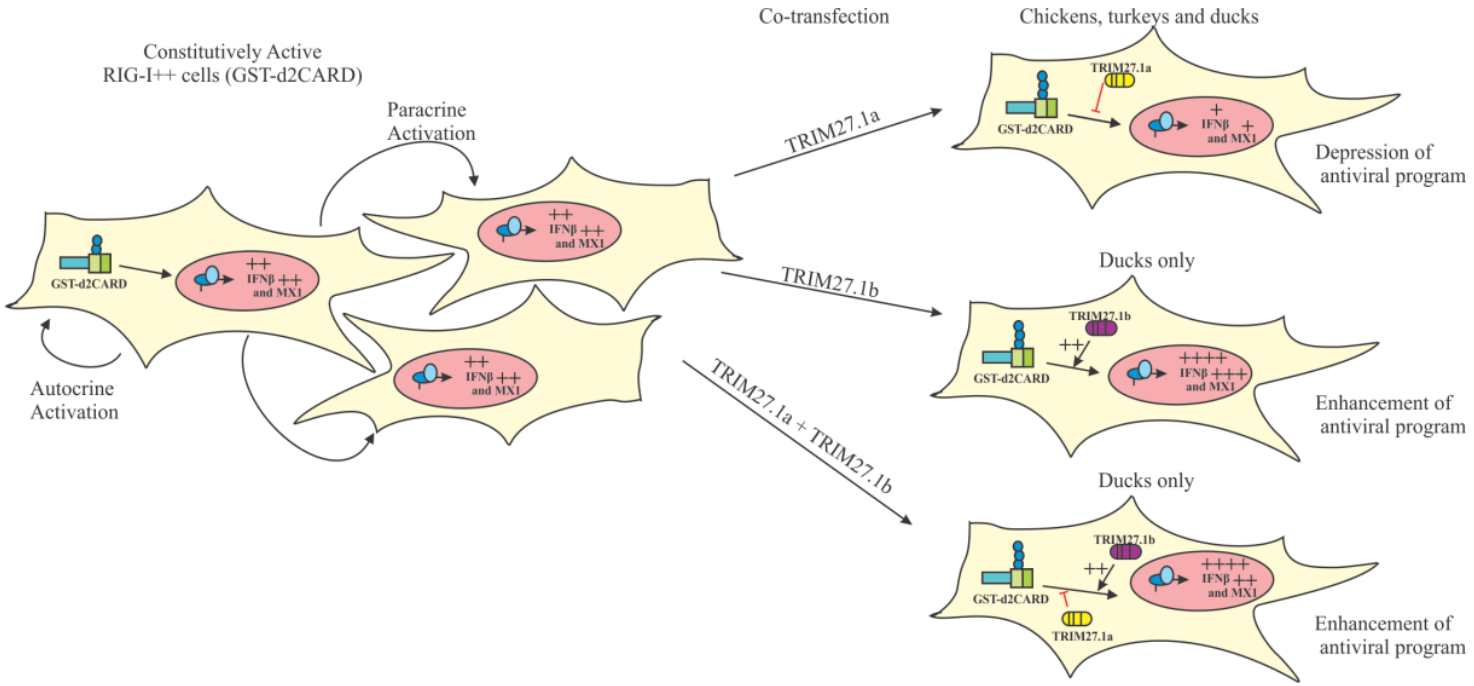

Figure 5-1. Model of antiviral suppression and enhancement with co-transfection of duck *TRIM27.1a* and *TRIM27.1b*. In cell culture, when I activate and turn on the antiviral program using the transfected constitutively active d2CARD construct, the downstream products of the RIG-I signaling pathways are produced and robust activation of the antiviral program is initiated. I can measure increased transcription of type I interferons (*IFN-β*) and interferon stimulated genes (ISGs, like *MX1*) in the activated cell population through qPCR. Constitutively activated d2CARD transfected cells (robust cell activation in constitutively active cells is indicated by ++) will produce *IFN-β* which will affect neighboring cells activated through paracrine IFN-β activation. When I co-expressed *TRIM27.1a* in activated cells, I observed a depression of expression of *IFN-β* and *MX1*. As chickens, turkeys and ducks all have homologs of *TRIM27.1a*, this is likely a conserved feature of avian *TRIM27.1a*-like homologs. When I co-expressed *TRIM27.1b* in activated cells, a dramatic increase in production of *IFN-β* and *MX1* was

observed. The enhancement of the antiviral program is downstream of RIG-I, but at an unknown component in the cascade. *TRIM27.1b* is only found in ducks, and as such *TRIM27.1b* in ducks may enhance their ability to respond so profoundly to a highly pathogenic IAV infection. I also demonstrated that the immunostimulatory effect of *TRIM27.1b* has a greater effect on antiviral gene transcription than the immunosuppressive effect of *TRIM27.1a*. As *TRIM27.1b* is unique to ducks, interplay of these two genes in the RIG-I signaling pathway is duck specific.

Chapter 6. REFERENCES

Alexopoulou, L., A. C. Holt, R. Medzhitov and R. A. Flavell (2001). "Recognition of double-stranded RNA and activation of NF-kappaB by Toll-like receptor 3." Nature **413**(6857): 732-738.

Ando, A., A. Shigenari, J. K. Kulski, C. Renard, P. Chardon, T. Shiina and H. Inoko (2005). "Genomic sequence analysis of the 238-kb swine segment with a cluster of TRIM and olfactory receptor genes located, but with no class I genes, at the distal end of the SLA class I region." Immunogenetics **57**(11): 864-873.

Arimoto, K.-i., K. Funami, Y. Saeki, K. Tanaka, K. Okawa, O. Takeuchi, S. Akira, Y. Murakami and K. Shimotohno (2010). "Polyubiquitin conjugation to NEMO by triparite motif protein 23 (TRIM23) is critical in antiviral defense." Proceedings of the National Academy of Sciences of the United States of America **107**(36): 15856-15861.

Barber, M. R., J. R. Aldridge, Jr., X. Fleming-Canepa, Y. D. Wang, R. G. Webster and K. E. Magor (2013). "Identification of avian RIG-I responsive genes during influenza infection." Molecular Immunology **54**(1): 89-97.

Barber, M. R. W., J. R. Aldridge, R. G. Webster and K. E. Magor (2010). "Association of RIG-I with innate immunity of ducks to influenza." Proceedings of the National Academy of Sciences of the United States of America **107**(13): 5913-5918.

Barr, S. D., J. R. Smiley and F. D. Bushman (2008). "The interferon response inhibits HIV particle production by induction of TRIM22." PLoS Pathogens **4**(2).

Baskin, C. R., H. Bielefeldt-Ohmann, T. M. Tumpey, P. J. Sabourin, J. P. Long, A. Garcia-Sastre, A.-E. Tolnay, R. Albrecht, J. A. Pyles, P. H. Olson, L. D. Aicher, E. R. Rosenzweig, K. Murali-Krishna, E. A. Clark, M. S. Kotur, J. L. Fornek, S. Proll, R. E. Palermo, C. L. Sabourin and M. G. Katze (2009). "Early and

sustained innate immune response defines pathology and death in nonhuman primates infected by highly pathogenic influenza virus." Proceedings of the National Academy of Sciences of the United States of America **106**(9): 3455-3460.

Bazzigher, L., A. Schwarz and P. Staeheli (1993). "No enhanced influenza virus resistance of murine and avian cells expressing cloned duck Mx protein." Virology **195**(1): 100-112.

Bell, J. L., A. Malyukova, J. K. Holien, J. Koach, M. W. Parker, M. Kavallaris, G. M. Marshall and B. B. Cheung (2012). "TRIM16 Acts as an E3 Ubiquitin Ligase and Can Heterodimerize with Other TRIM Family Members." PLoS One **7**(5): e37470.

Bernasconi, D., U. Schultz and P. Staeheli (1995). "The interferon-induced Mx protein of chickens lacks antiviral activity." Journal of Interferon and Cytokine Research **15**(1): 47-53.

Berscheminski, J., P. Groitl, T. Dobner, P. Wimmer and S. Schreiner (2013). "The adenoviral oncogene E1A-13S interacts with a specific isoform of the tumor suppressor PML to enhance viral transcription." Journal of Virology **87**(2): 965-977.

Betts, M. J. and R. B. Russell (2003). Amino Acid Properties and Consequences of Substitutions. Bioinformatics for Geneticists, John Wiley & Sons, Ltd**:** 289-316.

Bonen, D. K., Y. Ogura, D. L. Nicolae, N. Inohara, L. Saab, T. Tanabe, F. F. Chen, S. J. Foster, R. H. Duerr, S. R. Brant, J. H. Cho and G. Nunez (2003). "Crohn's disease-associated NOD2 variants share a signaling defect in response to lipopolysaccharide and peptidoglycan." Gastroenterology **124**(1): 140-146.

Boon, A. C. M., J. deBeauchamp, A. Hollmann, J. Luke, M. Kotb, S. Rowe, D. Finkelstein, G. Neale, L. Lu, R. W. Williams and R. J. Webby (2009). "Host Genetic Variation Affects Resistance to Infection with a Highly Pathogenic H5N1 Influenza A Virus in Mice." Journal of Virology **83**(20): 10417-10426.

Borden, K. L. B., E. J. CampbellDwyer and M. S. Salvato (1997). "The promyelocytic leukemia protein PML has a pro-apoptotic activity mediated through its RING domain." Febs Letters **418**(1-2): 30-34.

Boudinot, P., L. M. van der Aa, L. Jouneau, L. Du Pasquier, P. Pontarotti, V. Briolat, A. Benmansour and J. P. Levraud (2011). "Origin and Evolution of TRIM Proteins: New Insights from the Complete TRIM Repertoire of Zebrafish and Pufferfish." PLoS One **6**(7).

Burge, C. B. and S. Karlin (1998). "Finding the genes in genomic DNA." Current Opinion in Structural Biology **8**(3): 346-354.

Cai, X., S. Srivastava, Y. Sun, Z. Li, H. Wu, L. Zuvela-Jelaska, J. Li, R. S. Salamon, J. M. Backer and E. Y. Skolnik (2011). "Tripartite motif containing protein 27 negatively regulates CD4 T cells by ubiquitinating and inhibiting the class II PI3K-C2 beta." Proceedings of the National Academy of Sciences of the United States of America **108**(50): 20072-20077.

Cao, T. Y., K. L. B. Borden, P. S. Freemont and L. D. Etkin (1997). "Involvement of the rfp tripartite motif in protein-protein interactions and subcellular distribution." Journal of Cell Science **110**: 1563-1571.

Cao, T. Y., E. Duprez, K. L. B. Borden, P. S. Freemont and L. D. Etkin (1998). "Ret finger protein is a normal component of PML nuclear bodies and interacts directly with PML." Journal of Cell Science **111**: 1319-1329.

Carty, M. and A. G. Bowie (2010). "Recent insights into the role of Toll-like receptors in viral infection." Clinical and Experimental Immunology **161**(3): 397-406.

Chaix, R., C. Cao and P. Donnelly (2008). "Is Mate Choice in Humans MHC-Dependent?" PLoS Genet **4**(9): e1000184.

Chaves, L. D., S. B. Krueth and K. M. Reed (2009). "Defining the Turkey MHC: Sequence and Genes of the B Locus." Journal of Immunology **183**(10): 6530-6537.

Chelbi-Alix, M. K., F. Quignon, L. Pelicano, M. H. M. Koken and H. De The (1998). "Resistance to virus infection conferred by the interferon-induced promyelocytic leukemia protein." Journal of Virology **72**(2): 1043-1051.

Cheng, X. and H. Y. Kao (2012). "Microarray analysis revealing common and distinct functions of promyelocytic leukemia protein (PML) and tumor necrosis factor alpha (TNFalpha) signaling in endothelial cells." BMC Genomics **13**: 453.

Chu, Y. and X. Yang (2011). "SUMO E3 ligase activity of TRIM proteins." Oncogene **30**(9): 1108-1116.

Clark, K., M. Peggie, L. Plater, R. J. Sorcek, E. R. Young, J. B. Madwed, J. Hough, E. G. McIver and P. Cohen (2011). "Novel cross-talk within the IKK family controls innate immunity." Biochem J **434**(1): 93-104.

Cormican, P., A. T. Lloyd, T. Downing, S. J. Connell, D. Bradley and C. O'Farrelly (2009). "The avian Toll-Like receptor pathway-Subtle differences amidst general conformity." Developmental & Comparative Immunology **33**(9): 967-973.

Corpet, F. (1988). "Multiple sequence alignment with hierarchical clustering." Nucleic Acids Research **16**(22): 10881-10890.

D'Cruz, A. A., J. J. Babon, R. S. Norton, N. A. Nicola and S. E. Nicholson (2013). "Structure and function of the SPRY/B30.2 domain proteins involved in innate immunity." Protein Science **22**(1): 1-10.

De Thé, H., C. Chomienne, M. Lanotte, L. Degos and A. Dejean (1990). "The T(15-17) translocation of acte promyelocytic leukemia fuses the retinoic acid receptor-α gene to a novel transcribed locus." Nature **347**(6293): 558-561.

Deshaies, R. J. and C. A. P. Joazeiro (2009). "RING Domain E3 Ubiquitin Ligases." Annual Review of Biochemistry **78**: 399-434.

Dho, S. H. and K.-S. Kwon (2003). "The Ret finger protein induces apoptosis via its RING finger-B box-coiled-coil motif." Journal of Biological Chemistry **278**(34): 31902-31908.

Doyle, J. M., J. Gao, J. Wang, M. Yang and P. R. Potts (2010). "MAGE-RING Protein Complexes Comprise a Family of E3 Ubiquitin Ligases." Molecular Cell **39**(6): 963-974.

Dyck, J. A., G. G. Maul, W. H. Miller, J. D. Chen, A. Kakizuka and R. M. Evans (1994). "A novel macromolecular structure is a target of the promyelocyte-retinoic acid receptor oncoprotein." Cell **76**(2): 333-343.

Gack, M. U., R. A. Albrecht, T. Urano, K.-S. Inn, I. C. Huang, E. Carnero, M. Farzan, S. Inoue, J. U. Jung and A. Garcia-Sastre (2009). "Influenza A Virus NS1 Targets the Ubiquitin Ligase TRIM25 to Evade Recognition by the Host Viral RNA Sensor RIG-I." Cell Host & Microbe **5**(5): 439-449.

Gack, M. U., Y. C. Shin, C. H. Joo, T. Urano, C. Liang, L. J. Sun, O. Takeuchi, S. Akira, Z. J. Chen, S. S. Inoue and J. U. Jung (2007). "TRIM25 RING-finger E3 ubiquitin ligase is essential for RIG-I-mediated antiviral activity." Nature **446**(7138): 916-U912.

Ganser-Pornillos, B. K., V. Chandrasekaran, O. Pornillos, J. G. Sodroski, W. I. Sundquist and M. Yeager (2011). "Hexagonal assembly of a restricting TRIM5 alpha protein." Proceedings of the National Academy of Sciences of the United States of America **108**(2): 534-539.

Glusman, G., A. Bahar, D. Sharon, Y. Pilpel, J. White and D. Lancet (2000). "The olfactory receptor gene superfamily: data mining, classification, and nomenclature." Mamm Genome **11**(11): 1016-1023.

Gruen, J. R. and S. M. Weissman (1997). "Evolving views of the major histocompatibility complex." Blood **90**(11): 4252-4265.

Grutter, C., C. Briand, G. Capitani, P. R. E. Mittl, S. Papin, E. Tschopp and M. G. Grutter (2006). "Structure of the PRYSPRY-domain: Implications for autoinflammatory diseases." Febs Letters **580**(1): 99-106.

Hao, Y. H., J. M. Doyle, S. Ramanathan, T. S. Gomez, D. Jia, M. Xu, Z. J. J. Chen, D. D. Billadeau, M. K. Rosen and P. R. Potts (2013). "Regulation of WASH-Dependent Actin Polymerization and Protein Trafficking by Ubiquitination." Cell **152**(5): 1051-1064.

Harbers, M., T. Nomura, S. Ohno and S. Ishii (2001). "Intracellular localization of the Ret finger protein depends on a functional nuclear export signal and protein kinase C activation." Journal of Biological Chemistry **276**(51): 48596-48607.

Hemmi, H., O. Takeuchi, T. Kawai, T. Kaisho, S. Sato, H. Sanjo, M. Matsumoto, K. Hoshino, H. Wagner, K. Takeda and S. Akira (2001). "A Toll-like receptor recognizes bacterial DNA (vol 408, pg 740, 2000)." Nature **409**(6820): 646-U622.

Horby, P., N. Y. Nguyen, S. J. Dunstan and J. K. Baillie (2012). "The Role of Host Genetics in Susceptibility to Influenza: A Systematic Review." PLoS One **7**(3): e33180.

Horio, M., T. Kato, S. Mii, A. Enomoto, M. Asai, N. Asai, Y. Murakumo, K. Shibata, F. Kikkawa and M. Takahashi (2012). "Expression of RET finger protein predicts chemoresistance in epithelial ovarian cancer." Cancer medicine **1**(2): 218-229.

Hornung, V., J. Ellegast, S. Kim, K. Brzozka, A. Jung, H. Kato, H. Poeck, S. Akira, K.-K. Conzelmann, M. Schlee, S. Endres and G. Hartmann (2006). "5 '-triphosphate RNA is the ligand for RIG-I." Science **314**(5801): 994-997.

Horton, R., L. Wilming, V. Rand, R. C. Lovering, E. A. Bruford, V. K. Khodiyar, M. J. Lush, S. Povey, C. C. Talbot, M. W. WrighO, H. M. Wain, J. Trowsdale, A. Ziegler and S. Beck (2004). "Gene map of the extended human MHC." Nature Reviews Genetics **5**(12): 889-899.

Huang, B., Z. T. Qi, Z. Xu and P. Nie (2010). "Global characterization of interferon regulatory factor (IRF) genes in vertebrates: Glimpse of the diversification in evolution." BMC Immunology **11**: 22.

Huang, Y., Y. Li, D. W. Burt, H. Chen, Y. Zhang, W. Qian, H. Kim, S. Gan, Y. Zhao, J. Li, K. Yi, H. Feng, P. Zhu, B. Li, Q. Liu, S. Fairley, K. E. Magor, Z. Du, X. Hu, L. Goodman, H. Tafer, A. Vignal, T. Lee, K. W. Kim, Z. Sheng, Y. An, S. Searle, J. Herrero, M. A. M. Groenen, R. P. M. A. Crooijmans, T. Faraut, Q. Cai, R. G. Webster, J. R. Aldridge, W. C. Warren, S. Bartschat, S. Kehr, M. Marz, P. F. Stadler, J. Smith, R. H. S. Kraus, Y. Zhao, L. Ren, J. Fei, M. Morisson, P. Kaiser, D. K. Griffin, M. Rao, F. Pitel, J. Wang and N. Li (2013). "The duck genome and transcriptome provide insight into an avian influenza virus reservoir species." Nature Genetics **45**(7): 776-783.

Inoue, J.-i., T. Ishida, N. Tsukamoto, N. Kobayashi, A. Naito, S. Azuma and T. Yamamoto (2000). "Tumor necrosis factor receptor-associated factor (TRAF) family: Adapter proteins that mediate cytokine signaling." Experimental Cell Research **254**(1): 14-24.

James, L. C., D. L. Mallery, W. A. McEwan, S. R. Bidgood, G. J. Towers and C. M. Johnson (2010). "Antibodies mediate intracellular immunity through tripartite motif-containing 21 (TRIM21)." Proceedings of the National Academy of Sciences of the United States of America **107**(46): 19985-19990.

Jiang, X. M., L. N. Kinch, C. A. Brautigam, X. Chen, F. H. Du, N. V. Grishin and Z. J. J. Chen (2012). "Ubiquitin-Induced Oligomerization of the RNA Sensors RIG-I and MDA5 Activates Antiviral Innate Immune Response." Immunity **36**(6): 959-973.

Jourdain, E., G. Gunnarsson, J. Wahlgren, N. Latorre-Margalef, C. Bröjer, S. Sahlin, L. Svensson, J. Waldenström, Å. Lundkvist and B. Olsen (2010). "Influenza Virus in a Natural Host, the Mallard: Experimental Infection Data." PLoS One **5**(1): e8935.

Kamijo, R., T. Matsuyama, D. Shapiro, J. Le, T. Kimura, T. Taniguchi, T. W. Mak and J. Vilcek (1993). "Macrophages from mice lacking the IRF-1 gene fail to generate nitric oxide in response to IFN-gamma or IFN-alpha/beta." Lymphokine and Cytokine Research **12**(5): 348.

Kato, H., O. Takeuchi, S. Sato, M. Yoneyama, M. Yamamoto, K. Matsui, S. Uematsu, A. Jung, T. Kawai, K. J. Ishii, O. Yamaguchi, K. Otsu, T. Tsujimura, C. S. Koh, C. R. E. Sousa, Y. Matsuura, T. Fujita and S. Akira (2006). "Differential roles of MDA5 and RIG-I helicases in the recognition of RNA viruses." Nature **441**(7089): 101-105.

Kaufman, J., S. Milne, T. W. F. Gobel, B. A. Walker, J. P. Jacob, C. Auffray, R. Zoorob and S. Beck (1999). "The chicken B locus is a minimal essential major histocompatibility complex." Nature **401**(6756): 923-925.

Kawai, T. and S. Akira (2011). "Regulation of innate immune signalling pathways by the tripartite motif (TRIM) family proteins." EMBO Mol Med **3**(9): 513-527.

Kawai, T., K. Takahashi, S. Sato, C. Coban, H. Kumar, H. Kato, K. J. Ishii, O. Takeuchi and S. Akira (2005). "IPS-1, an adaptor triggering RIG-I- and Mda5-mediated type I interferon induction." Nat Immunol **6**(10): 981-988.

Kawakami, T., M. Matsumoto, M. Sato, H. Harada, T. Taniguchi and M. Kitagawa (1995). "Possible involvement of the transcription factor ISGF3-γ in virus-induced expression of the IFN-β gene." Febs Letters **358**(3): 225-229.

Keckesova, Z., L. M. J. Ylinen and G. J. Towers (2004). "The human and African green monkey TRIM5alpha genes encode Ref1 and Lv1 retroviral restriction factor activities." Proceedings of the National Academy of Sciences of the United States of America **101**(29): 10780-10785.

Kelley, J., L. Walter and J. Trowsdale (2005). "Comparative genomics of major histocompatibility complexes." Immunogenetics **56**(10): 683-695.

Kim, J. K., N. J. Negovetich, H. L. Forrest and R. G. Webster (2009). "Ducks: The "Trojan Horses" of H5N1 influenza." Influenza and Other Respiratory Viruses **3**(4): 121-128.

Kobasa, D., S. M. Jones, K. Shinya, J. C. Kash, J. Copps, H. Ebihara, Y. Hatta, J. H. Kim, P. Halfmann, M. Hatta, F. Feldmann, J. B. Alimonti, L. Fernando, Y. Li, M. G. Katze, H. Feldmann and Y. Kawaoka (2007). "Aberrant innate immune response in lethal infection of macaques with the 1918 influenza virus." Nature (London) **445**(7125): 319-323.

Krutzfeldt, M., M. Ellis, D. B. Weekes, J. J. Bull, M. Eilers, M. D. Vivanco, W. R. Sellers and S. Mittnacht (2005). "Selective ablation of retinoblastoma protein function by the RET finger protein." Mol Cell **18**(2): 213-224.

Kuchipudi, S. V., S. P. Dunham, R. Nelli, G. A. White, V. J. Coward, M. J. Slomka, I. H. Brown and K. C. Chang (2012). "Rapid death of duck cells infected with influenza: a potential mechanism for host resistance to H5N1." Immunology and cell biology **90**(1): 116-123.

Kumar, H., T. Kawai, H. Kato, S. Sato, K. Takahashi, C. Coban, M. Yamamoto, S. Uematsu, K. J. Ishii, O. Takeuchi and S. Akira (2006). "Essential role of IPS-1 in innate immune responses against RNA viruses." Journal of Experimental Medicine **203**(7): 1795-1803.

Lamothe, B., A. D. Campos, W. K. Webster, A. Gopinathan, L. Hur and B. G. Darnay (2008). "The RING Domain and First Zinc Finger of TRAF6 Coordinate Signaling by Interleukin-1, Lipopolysaccharide, and RANKL." Journal of Biological Chemistry **283**(36): 24871-24880.

Le, X. F., P. Yang and K. S. Chang (1996). "Analysis of the growth and transformation suppressor domains of promyelocytic leukemia gene, PML." Journal of Biological Chemistry **271**(1): 130-135.

Lee, J. T., J. Shan, J. Zhong, M. Li, B. Zhou, A. Zhou, R. Parsons and W. Gu (2013). "RFP-mediated ubiquitination of PTEN modulates its effect on AKT activation." Cell Research **23**(4): 552-564.

Li, X. and J. Sodroski (2008). "The TRIM5 alpha B-Box 2 Domain Promotes Cooperative Binding to the Retroviral Capsid by Mediating Higher-Order Self-Association." Journal of Virology **82**(23): 11495-11502.

Li, X., B. Song, S.-h. Xiang and J. Sodroski (2007). "Functional interplay between the B-box 2 and the B30.2(SPRY) domains of TRIM5 alpha." Virology **366**(2): 234-244.

Liang, Q., H. Deng, X. Li, X. Wu, Q. Tang, T. H. Chang, H. Peng, F. J. Rauscher, 3rd, K. Ozato and F. Zhu (2011). "Tripartite motif-containing protein 28 is a small ubiquitin-related modifier E3 ligase and negative regulator of IFN regulatory factor 7." Journal of Immunology **187**(9): 4754-4763.

Lienlaf, M., F. Hayashi, F. Di Nunzio, N. Tochio, T. Kigawa, S. Yokoyama and F. Diaz-Griffero (2011). "Contribution of E3-Ubiquitin Ligase Activity to HIV-1 Restriction by TRIM5 alpha(rh): Structure of the RING Domain of TRIM5 alpha." Journal of Virology **85**(17): 8725-8737.

Lund, J. M., L. Alexopoulou, A. Sato, M. Karow, N. C. Adams, N. W. Gale, A. Iwasaki and R. A. Flavell (2004). "Recognition of single-stranded RNA viruses by Toll-like receptor 7." Proceedings of the National Academy of Sciences of the United States of America **101**(15): 5598-5603.

MacDonald, M. R. W., J. Xia, A. L. Smith and K. E. Magor (2008). "The duck toll like receptor 7: Genomic organization, expression and function." Molecular Immunology **45**(7): 2055-2061.

Magor, K. E., D. Miranzo Navarro, M. R. Barber, K. Petkau, X. Fleming-Canepa, G. A. Blyth and A. H. Blaine (2013). "Defense genes missing from the flight division." Developmental and Comparative Immunology.

Mallery, D. L., W. A. McEwan, S. R. Bidgood, G. J. Towers, C. M. Johnson and L. C. James (2010). "Antibodies mediate intracellular immunity through tripartite motif-containing 21 (TRIM21)." Proceedings of the National Academy of Sciences of the United States of America **107**(46): 19985-19990.

Marin, I. (2012). "Origin and Diversification of TRIM Ubiquitin Ligases." PLoS One **7**(11).

Matsuura, T., Y. Shimono, K. Kawai, H. Murakami, T. Urano, Y. Niwa, H. Goto and M. Takahashi (2005). "PIAS proteins are involved in the SUMO-1 modification, intracellular translocation and transcriptional repressive activity of RET finger protein." Experimental Cell Research **308**(1): 65-77.

McNab, F. W., R. Rajsbaum, J. P. Stoye and A. O'Garra (2011). "Tripartite-motif proteins and innate immune regulation." Current Opinion in Immunology **23**(1): 46-56.

Meroni, G. and G. Diez-Roux (2005). "TRIM/RBCC, a novel class of 'single protein RING finger' E3 ubiquitin ligases." Bioessays **27**(11): 1147-1157.

Mesa, C. M., K. J. Thulien, D. A. Moon, S. M. Veniamin and K. E. Magor (2004). "The dominant MHC class I gene is adjacent to the polymorphic TAP2 gene in the duck, Anas platyrhynchos." Immunogenetics **56**(3): 192-203.

Metz, P., E. Dazert, A. Ruggieri, J. Mazur, L. Kaderali, A. Kaul, U. Zeuge, M. P. Windisch, M. Trippler, V. Lohmann, M. Binder, M. Frese and R. Bartenschlager (2012). "Identification of Type I and Type II Interferon-Induced Effectors Controlling Hepatitis C Virus Replication." Hepatology **56**(6): 2082-2093.

Meyer, M., S. Gaudieri, D. A. Rhodes and J. Trowsdale (2003). "Cluster of TRIM genes in the human MHC class I region sharing the B30.2 domain." Tissue Antigens **61**(1): 63-71.

Micheau, O. and J. Tschopp (2003). "Induction of TNF receptor I-mediated apoptosis via two sequential signaling complexes." Cell **114**(2): 181-190.

Milinski, M., S. Griffiths, K. M. Wegner, T. B. H. Reusch, A. Haas-Assenbaum and T. Boehm (2005). "Mate choice decisions of stickleback females predictably

modified by MHC peptide ligands." Proceedings of the National Academy of Sciences of the United States of America **102**(12): 4414-4418.

Moon, D. A., S. M. Veniamin, J. A. Parks-Dely and K. E. Magor (2005). "The MHC of the duck (Anas platyrhynchos) contains five differentially expressed class I genes." Journal of Immunology **175**(10): 6702-6712.

Morales, A. C., Jr., D. A. Hilt, S. M. Williams, M. J. Pantin-Jackwood, D. L. Suarez, E. Spackman, D. E. Stallknecht and M. W. Jackwood (2009). "Biologic Characterization of H4, H6, and H9 Type Low Pathogenicity Avian Influenza Viruses from Wild Birds in Chickens and Turkeys." Avian Diseases **53**(4): 552-562.

Morris-Desbois, C., V. Bochard, C. Reynaud and P. Jalinot (1999). "Interaction between the Ret finger protein and the int-6 gene product and colocalisation into nuclear bodies." Journal of Cell Science **112**(19): 3331-3342.

Mundt, E., L. Gay, L. Jones, G. Saavedra, S. M. Tompkins and R. A. Tripp (2009). "Replication and pathogenesis associated with H5N1, H5N2, and H5N3 low-pathogenic avian influenza virus infection in chickens and ducks." Archives of Virology **154**(8): 1241-1248.

Napolitano, L. M., E. G. Jaffray, R. T. Hay and G. Meroni (2011). "Functional interactions between ubiquitin E2 enzymes and TRIM proteins." Biochemical Journal **434**(Part 2): 309-319.

Niimura, Y. and M. Nei (2007). "Extensive Gains and Losses of Olfactory Receptor Genes in Mammalian Evolution." PLoS One **2**(8): e708.

Nisole, S., J. P. Stoye and A. Saib (2005). "TRIM family proteins: Retroviral restriction and antiviral defence." Nature Reviews Microbiology **3**(10): 799-808.

Ohgiya, D., H. Matsushita, M. Onizuka, N. Nakamura, J. Amaki, Y. Aoyama, H. Kawai, Y. Ogawa, H. Kawada and K. Ando (2012). "Association of promyelocytic leukemia protein with expression of IL-6 and resistance to treatment in multiple myeloma." Acta Haematol **128**(4): 213-222.

Ohman, T., J. Rintahaka, N. Kalkkinen, S. Matikainen and T. A. Nyman (2009). "Actin and RIG-I/MAVS Signaling Components Translocate to Mitochondria upon Influenza A Virus Infection of Human Primary Macrophages." Journal of Immunology **182**(9): 5682-5692.

Oshiumi, H., M. Matsumoto, S. Hatakeyama and T. Seya (2009). "Riplet/RNF135, a RING Finger Protein, Ubiquitinates RIG-I to Promote Interferon-beta Induction during the Early Phase of Viral Infection." Journal of Biological Chemistry **284**(2): 807-817.

Oshiumi, H., M. Matsumoto and T. Seya (2012). "Role of ubiquitin ligase in innate immune response in mammal." Seikagaku. The Journal of Japanese Biochemical Society **84**(6): 455-462.

Oshiumi, H., M. Miyashita, N. Inoue, M. Okabe, M. Matsumoto and T. Seya (2010). "The Ubiquitin Ligase Riplet Is Essential for RIG-I-Dependent Innate Immune Responses to RNA Virus Infection." Cell Host & Microbe **8**(6): 496-509.

Ozato, K., D. M. Shin, T. H. Chang and H. C. Morse (2008). "TRIM family proteins and their emerging roles in innate immunity." Nature Reviews Immunology **8**(11): 849-860.

Ozato, K., Shin, D. M., Chang, T. H. and H. C. Morse (2008). "TRIM family proteins and their emerging roles in innate immunity." Nature Reviews Immunology **8**(11): 849-860.

Pan, C., H. Zhao, L. Shen and J. Sheng (2011). "Molecular Characterization and Expression Pattern of Tripartite Motif Protein 39 in Gallus gallus with a Complete PRY/SPRY Domain." Int J Mol Sci **12**(6): 3797-3809.

Pantin-Jackwood, M. J. and D. E. Swayne (2009). "Pathogenesis and pathobiology of avian influenza virus infection in birds." Revue Scientifique et Technique Office International des Epizooties **28**(1): 113-136.

Patel, C. A. and G. Ghiselli (2005). "The RET finger protein interacts with the hinge region of SMC3." Biochemical and Biophysical Research Communications **330**(1): 333-340.

Perfetto, L., P. F. Gherardini, N. E. Davey, F. Diella, M. Helmer-Citterich and G. Cesareni (2013). "Exploring the diversity of SPRY/B30.2-mediated interactions." Trends in Biochemical Sciences **38**(1): 38-46.

Ponting, C., J. Schultz and P. Bork (1997). "SPRY domains in ryanodine receptors (Ca-2+-release channels)." Trends in Biochemical Sciences **22**(6): 193-194.

Rajsbaum, R., R. A. Albrecht, M. K. Wang, N. P. Maharaj, G. A. Versteeg, E. Nistal-Villan, A. Garcia-Sastre and M. U. Gack (2012). "Species-Specific Inhibition of RIG-I Ubiquitination and IFN Induction by the Influenza A Virus NS1 Protein." PLoS Pathogens **8**(11): e1003059.

Randall, R. E. and S. Goodbourn (2008). "Interferons and viruses: an interplay between induction, signalling, antiviral responses and virus countermeasures." Journal of General Virology **89**: 1-47.

Reymond, A., G. Meroni, A. Fantozzi, G. Merla, S. Cairo, L. Luzi, D. Riganelli, E. Zanaria, S. Messali, S. Cainarca, A. Guffanti, S. Minucci, P. G. Pelicci and A. Ballabio (2001). "The tripartite motif family identifies cell compartments." EMBO (European Molecular Biology Organization) Journal **20**(9): 2140-2151.

Rhodes, D. A., B. de Bono and J. Trowsdale (2005). "Relationship between SPRY and B30.2 protein domains. Evolution of a component of immune defence?" Immunology **116**(4): 411-417.

Ruby, T., B. Bed'Hom, H. Wittzell, V. Morin, A. Oudin and R. Zoorob (2005). "Characterisation of a cluster of TRIM-B30.2 genes in the chicken MHC B locus." Immunogenetics **57**(1-2): 116-128.

Ryu, J. H., C. H. Kim and J. H. Yoon (2010). "Innate Immune Responses of the Airway Epithelium." Molecules and Cells **30**(3): 173-183.

Salomon, R., P. Staeheli, G. Kochs, H.-L. Yen, J. Franks, J. E. Rehg, R. G. Webster and E. Hoffmann (2007). "Mx1 gene protects mice against the highly lethal human H5N1 influenza virus." Cell Cycle **6**(19): 2417-2421.

Sardiello, M., S. Cairo, B. Fontanella, A. Ballabio and G. Meroni (2008). "Genomic analysis of the TRIM family reveals two groups of genes with distinct evolutionary properties." BMC Evolutionary Biology **8**: 225.

Sato, M., N. Hata, M. Asagiri, T. Nakaya, T. Taniguchi and N. Tanaka (1998). "Positive feedback regulation of type I IFN genes by the IFN-inducible transcription factor IRF-7." Febs Letters **441**(1): 106-110.

Sato, M., H. Suemori, N. Hata, M. Asagiri, K. Ogasawara, K. Nakao, T. Nakaya, M. Katsuki, S. Noguchi, N. Tanaka and T. Taniguchi (2000). "Distinct and essential roles of transcription factors IRF-3 and IRF-7 in response to viruses for IFN-alpha/beta gene induction." Immunity **13**(4): 539-548.

Sato, M., N. Tanaka, N. Hata, E. Oda and T. Taniguchi (1998). "Involvement of the IRF family transcription factor IRF-3 in virus-induced activation of the IFN-beta gene." Febs Letters **425**(1): 112-116.

Sawyer, S. L., M. Emerman and H. S. Malik (2007). "Discordant evolution of the adjacent antiretroviral genes TRIM22 and TRIM5 in mammals." PLoS Pathogens **3**(12): 1918-1929.

Sawyer, S. L., Wu, L., Emerman, M. and H. S. Malik (2005). "Positive selection of primate TRIM5alpha identifies a critical species-specific retroviral restriction domain." Proceedings of the National Academy of Sciences of the United States of America **102**(8): 2832-2837.

Seth, R. B., L. J. Sun, C. K. Ea and Z. J. J. Chen (2005). "Identification and characterization of MAVS, a mitochondrial antiviral signaling protein that activates NF-kappa B and IRF3." Cell **122**(5): 669-682.

Shiina, T., Briles, W. E., Goto, R. M., Hosomichi, K., Yanagiya, K., Shimizu, S., Inoko, H., and M. M. Miller (2007). "Extended gene map reveals tripartite motif, C-type lectin, and Ig superfamily type genes within a subregion of the chicken MHC-B affecting infectious disease." Journal of Immunology **178**(11): 7162-7172.

Shimono, Y., H. Murakami, Y. Hasegawa and M. Takahashi (2000). "RET finger protein is a transcriptional repressor and interacts with enhancer of polycomb that has dual transcriptional functions." Journal of Biological Chemistry **275**(50): 39411-39419.

Shimono, Y., H. Murakami, K. Kawai, P. A. Wade, K. Shimokata and M. Takahashi (2003). "Mi-2 beta associates with BRG1 and RET finger protein at the distinct regions with transcriptional activating and repressing abilities." Journal of Biological Chemistry **278**(51): 51638-51645.

Sick, C., U. Schultz, U. Muenster, J. Meier, B. Kaspers and P. Staeheli (1998). "Promoter structures and differential responses to viral and nonviral inducers of chicken type I interferon genes." Journal of Biological Chemistry **273**(16): 9749-9754.

Sjöstrand, M., S. Brauner, M. Kvarnström, M. Wahren-Herlenius and A. Espinosa (2012). "TRIM genes are part of the interferon signature observed in patients with primary Sjögren's syndrome." Annals of the Rheumatic Diseases **71**(Suppl 1): A81.

Song, H. Y. and D. B. Donner (1995). "Association of a RING finger protein with cytoplasmic domain of the human type-2 tumour necrosis factor receptor." Biochemical Journal **309**(3): 825-829.

Srivastava, S., X. J. Cai, Z. Li, Y. Sun and E. Y. Skolnik (2012). "Phosphatidylinositol-3-Kinase C2 beta and TRIM27 Function To Positively and Negatively Regulate IgE Receptor Activation of Mast Cells." Molecular and Cellular Biology **32**(15): 3132-3139.

Stremlau, M., C. M. Owens, M. J. Perron, M. Kiessling, P. Autissier and J. Sodroski (2004). "The cytoplasmic body component TRIM5alpha restricts HIV-1 infection in Old World monkeys." Nature (London) **427**(6977): 848-853.

Stremlau, M., M. Perron, M. Lee, Y. Li, B. Song, H. Javanbakht, F. Diaz-Griffero, D. J. Anderson, W. I. Sundquist and J. Sodroski (2006). "Specific recognition and accelerated uncoating of retroviral capsids by the TRIM5alpha restriction factor." Proc Natl Acad Sci U S A **103**(14): 5514-5519.

Stremlau, M., Perron, M., Welikala, S., and J. Sodroski (2005). "Species-specific variation in the B30.2(SPRY) domain of TRIM5 alpha determines the potency of human immunodeficiency virus restriction." Journal of Virology **79**(5): 3139-3145.

Takahashi, M., Y. Inaguma, H. Hiai and F. Hirose (1988). "Developmentally regulated expression of a human finger-containing gene encoded by the 5'half of the Ret transforming gene." Molecular and Cellular Biology **8**(4): 1853-1856.

Tareen, S. U., S. L. Sawyer, H. S. Malik and M. Emerman (2009). "An expanded clade of rodent Trim5 genes." Virology **385**(2): 473-483.

Taylor, R. T., K. J. Lubick, S. J. Robertson, J. P. Broughton, M. E. Bloom, W. A. Bresnahan and S. M. Best (2011). "TRIM79 alpha, an Interferon-Stimulated Gene Product, Restricts Tick-Borne Encephalitis Virus Replication by Degrading the Viral RNA Polymerase." Cell Host & Microbe **10**(3): 185-196.

Tezel, G., T. Nagasaka, N. Iwahashi, N. Asai, T. Iwashita, K. Sakata and M. Takahashi (1999). "Different nuclear/cytoplasmic distributions of RET finger protein in different cell types." Pathology International **49**(10): 881-886.

Tezel, G. G., A. Uner, I. Yildiz, G. Guler and M. Takahashi (2009). "RET finger protein expression in invasive breast carcinoma: Relationship between RFP and ErbB2 expression." Pathology Research and Practice **205**(6): 403-408.

Trowsdale, J. and P. Parham (2004). "Mini-review: defense strategies and immunity-related genes." European Journal of Immunology **34**(1): 7-17.

Uchil, P. D., A. Hinz, S. Siegel, A. Coenen-Stass, T. Pertel, J. Luban and W. Mothes (2013). "TRIM Protein-Mediated Regulation of Inflammatory and Innate Immune Signaling and Its Association with Antiretroviral Activity." Journal of Virology **87**(1): 257-272.

Uchil, P. D., B. D. Quinlan, W.-T. Chan, J. M. Luna and W. Mothes (2008). "TRIM E3 ligases interfere with early and late stages of the retroviral life cycle." PLoS Pathogens **4**(2): e16.

van der Aa, L. M., J.-P. Levraud, M. Yahmi, E. Lauret, V. Briolat, P. Herbomel, A. Benmansour and P. Boudinot (2009). "A large new subset of TRIM genes highly diversified by duplication and positive selection in teleost fish." BMC Biology **7**: 7.

Vanderven, H. A., K. Petkau, K. E. E. Ryan-Jean, J. R. Aldridge, Jr., R. G. Webster and K. E. Magor (2012). "Avian influenza rapidly induces antiviral genes in duck lung and intestine." Molecular Immunology **51**(3-4): 316-324.

Versteeg, G. A., R. Rajsbaum, M. T. Sanchez-Aparicio, A. M. Maestre, J. Valdiviezo, M. Shi, K.-S. Inn, A. Fernandez-Sesma, J. Jung and A. Garcia-Sastre (2013). "The E3-ligase TRIM family of proteins regulates signaling pathways triggered by innate immune pattern-recognition receptors." Immunity **38**(2): 384-398.

Vieira, A. R., T. G. McHenry, S. Daack-Hirsch, J. C. Murray and M. L. Marazita (2008). "Candidate gene/loci studies in cleft lip/palate and dental anomalies finds novel susceptibility genes for clefts." Genet Med **10**(9): 668-674.

Wang, Z. G., D. Ruggero, S. Ronchetti, S. Zhong, M. Gaboli, R. Rivi and P. P. Pandolfi (1998). "Pml is essential for multiple apoptotic pathways." Nature Genetics **20**(3): 266-272.

Ware, C. F. (2011). "The TNF receptor super family in immune regulation." Immunological Reviews **244**(Sp. Iss. SI): 5-8.

Webster, R. G., W. J. Bean, O. T. Gorman, T. M. Chambers and Y. Kawaoka (1992). "Evolution and ecology of influenza A viruses." Microbiological Reviews **56**(1): 152-179.

Weinert, C., C. Gruetter, H. Roschitzki-Voser, P. R. E. Mittl and M. G. Gruetter (2009). "The Crystal Structure of Human Pyrin B30.2 Domain: Implications for Mutations Associated with Familial Mediterranean Fever." Journal of Molecular Biology **394**(2): 226-236.

Woo, J.-S., J.-H. Imm, C.-K. Min, K.-J. Kim, S.-S. Cha and B.-H. Oh (2006). "Structural and functional insights into the B30.2/SPRY domain." EMBO (European Molecular Biology Organization) Journal **25**(6): 1353-1363.

Wu, W.-S., Xu, Z.-X., Hittelman, W. N., Salomoni, P., Pandolfi, P. P. and K.-S. Chang (2003). "Promyelocytic leukemia protein sensitizes tumor necrosis factor alpha-induced apoptosis by inhibiting the NF-kappaB survival pathway." Journal of Biological Chemistry **278**(14): 12294-12304.

Yan, N. and Z. J. J. Chen (2012). "Intrinsic antiviral immunity." Nature Immunology **13**(3): 214-222.

Yap, M. W., Nisole, S., and J. P. Stoye (2005). "A single amino acid change in the SPRY domain of human Trim5 alpha leads to HIV-1 restriction." Current Biology **15**(1): 73-78.

Yoneyama, M., M. Kikuchi, T. Natsukawa, N. Shinobu, T. Imaizumi, M. Miyagishi, K. Taira, S. Akira and T. Fujita (2004). "The RNA helicase RIG-I has an essential function in double-stranded RNA-induced innate antiviral responses." Nature Immunology **5**(7): 730-737.

Zha, J., K.-J. Han, L.-G. Xu, W. He, Q. Zhou, D. Chen, Z. Zhai and H.-B. Shu (2006). "The Ret finger protein inhibits signaling mediated by the noncanonical and canonical IkappaB kinase family members." Journal of immunology (Baltimore, Md. : 1950) **176**(2): 1072-1080.

Zhang, L., J. M. Katz, M. Gwinn, N. F. Dowling and M. J. Khoury (2009). "Systems-based candidate genes for human response to influenza infection." Infection Genetics and Evolution **9**(6, Sp. Iss. SI): 1148-1157.

Zoumpoulidou, G., C. Broceno, H. Li, D. Bird, G. Thomas and S. Mittnacht (2012). "Role of the Tripartite Motif Protein 27 in Cancer Development." Journal of the National Cancer Institute (Cary) **104**(12): 941-952.

Appendix A.

Table A-1. Coding sequence predictions derived from the draft duck genome.
Accession numbers and number of independent read hits from the differential map to gene analysis of the scaffold618 gene predictions. Duck 408 lung samples are highly pathogenic IAV infected (VN1203) samples and duck 70 lung samples are low pathogenic IAV infected (BC500) samples (Duck genome consortium, results unpublished). Higher numbers of independent reads in duck 408 roughly indicates an upregulation of that gene in highly pathogenic AIV infected lung. By differential map to gene analysis of 408 to 70, all reads for genes within scaffold618 not significantly upregulated during highly pathogenic IAV infection ($p > 0.05$).

Internal Reference #	Scaffold #	NCBI Protein ID	NCBI Gene ID	Duck 408 Lung	Duck 70 Lung	Gene Annotation
Apl_13514	618	EOB02156.1	483514568	2	0	ZNF692; zinc finger protein 692
Apl_13515	618	EOB02161.1	483514573	0	0	TRIM7.2; Tripartite motif protein 7
Apl_13516	618	EOB02157.1	483514569	0	0	hypothetical LOC468804 ; K09228 KRAB domain-containing zinc finger protein
Apl_13517	618	EOB02158.1	483514570	0	0	LAO; L-amino-acid oxidase precursor ; K03334 L-amino-acid oxidase
Apl_13518	618	EOB02162.1	483514574	0	1	TRIM7; tripartite motif-containing 7 ; K12000 tripartite motif-containing protein 7
Apl_13519	618	EOB02159.1	483514571	1	0	TRIM27.2; hypothetical LOC430359
Apl_13520	618	EOB02163.1	483514575	1	0	TRIM27; tripartite motif-containing 27
Apl_13521	618	EOB02164.1	483514576	5	1	TRIM27; tripartite motif-containing 27
Apl_13522	618	EOB02160.1	483514572	0	0	TRIM41; tripartite motif-containing 41
Apl_13523	618	EOB02165.1	483514577	55	58	guanine nucleotide binding protein (G protein), beta polypeptide 2-like 1
Apl_13524	618	EOB02166.1	483514578	1	0	TRIM27; tripartite motif-containing 27
Apl_10900	878	EOB00009.1	483510966	0	0	PML; promyelocytic leukemia ; K10054 probable transcription factor PML
Apl_10902	878	EOB00003.1	483510960	0	0	PML; promyelocytic leukemia ; K10054 probable transcription factor PML
Apl_10903	878	EOB00004.1	483510961	0	0	PML; promyelocytic leukemia ; K10054 probable transcription factor PML
Apl_15985	1806	EOA95592.1	483502466	13*	0	TRIM14; tripartite motif-containing 14

* indicates a statistically significant expression level change between duck 408 and duck 70 ($p < 0.01$)

Table A-2. tRNAs predicted in scaffold618 genomic sequence.
We predicted the tRNAs in scaffold618 using the online web server ARAGORN, but the tRNAs of scaffold618 as since been annotated on NCBI. A total of 20 tRNA sequences were predicted in scaffold618

tRNA Amino acid	Anticodon	Start positon	End position	Orientation
Asn	GTT	43246	43319	antisense
Glu	CTC	67366	67437	antisense
Glu	CTC	72351	724022	antisense
Glu	TTC	69791	69862	antisense
Glu	TTC	70427	70498	sense
Leu	AAG	45087	45168	sense
Lys	CTT	64915	64989	antisense
Lys	CTT	66976	67048	antisense
Lys	CTT	71176	71249	sense
Lys	CTT	111054	111127	antisense
Lys	CTT	111984	112058	antisense
Thr	AGT	44383	44457	antisense
Thr	TGT	47268	47341	antisense
Val	AAC	45547	46521	antisense
Val	AAC	68785	68857	antisense
Val	AAC	69367	69439	antisense
Val	CAC	68318	68391	antisense
Val	CAC	69076	69148	antisense
Val	CAC	70722	70795	antisense
Val	CAC	111401	111474	antisense

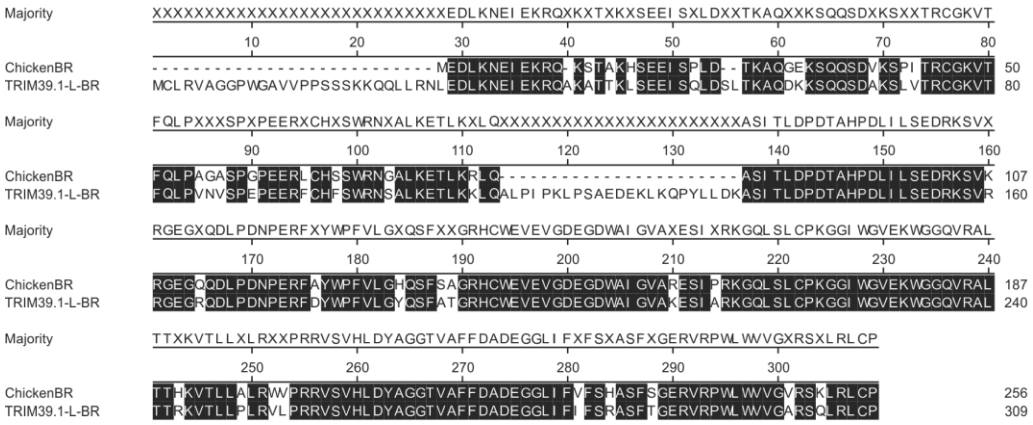

Figure A-1. Alignment of the chicken BR and TRIM39.1-L/BR amino acid sequence. This sequence was predicted in the intragenic region between *TRIM27.2* and *TRIM27.1a* in duck scaffold618.

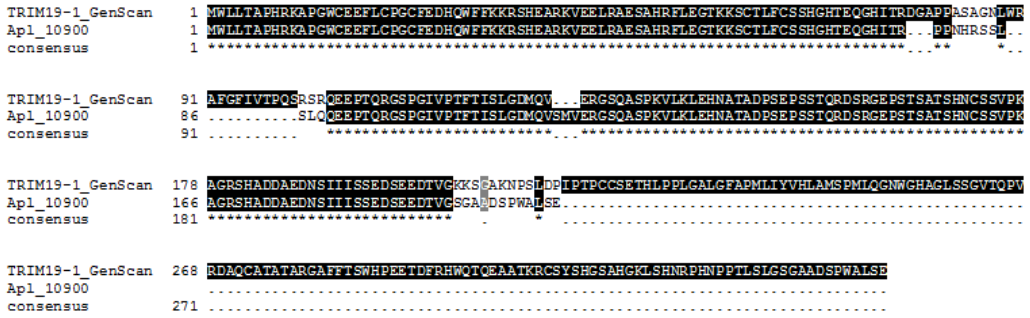

Figure A-2. Alignment of the PML-1 (TRIM19-1) predicted amino acid sequence and Apl_10900.

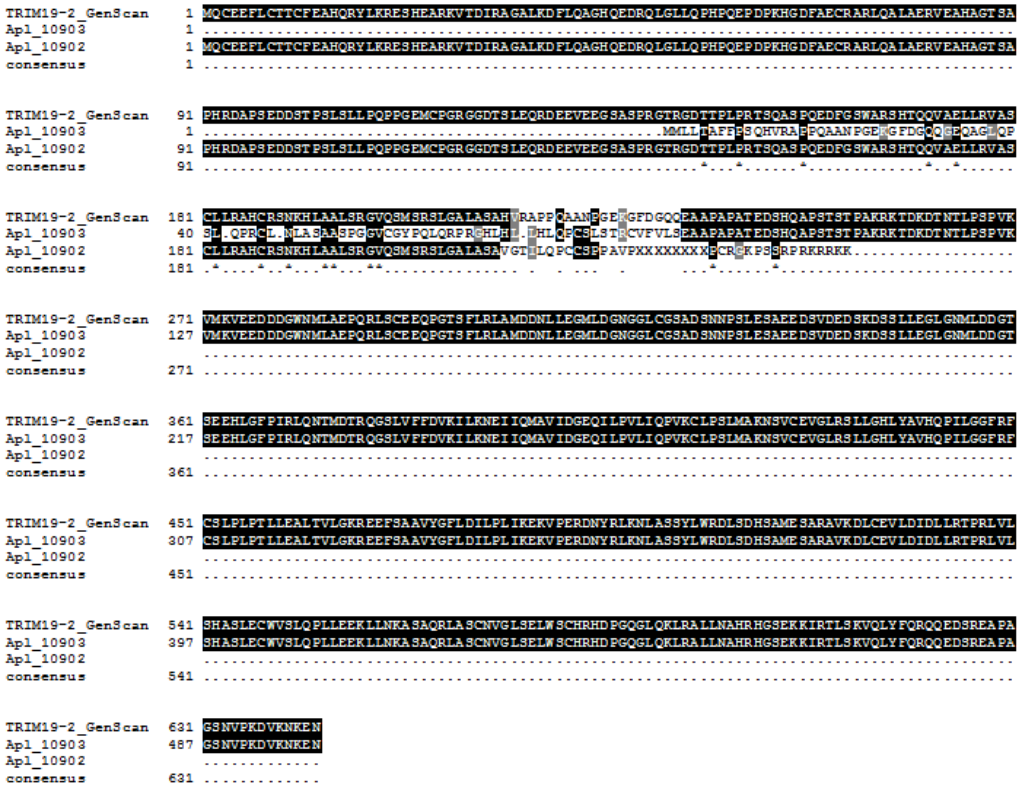

Figure A-3. Alignment of the TRIM19-2 predicted amino acid sequence and PML-L2 (Apl_10902) and PML-L3 (Apl_109003).

Table A-3. Clone numbers for each TRIM27.1a clones sequenced fully.

Duck Number	Allele	Clone Number
310	A	1-8
		1-18
	B	2-1
		1-4
312	A	9
		7
		4
		2
	B	10
		8
		6-1
401	A	2-15
		20
		19
		2
		6

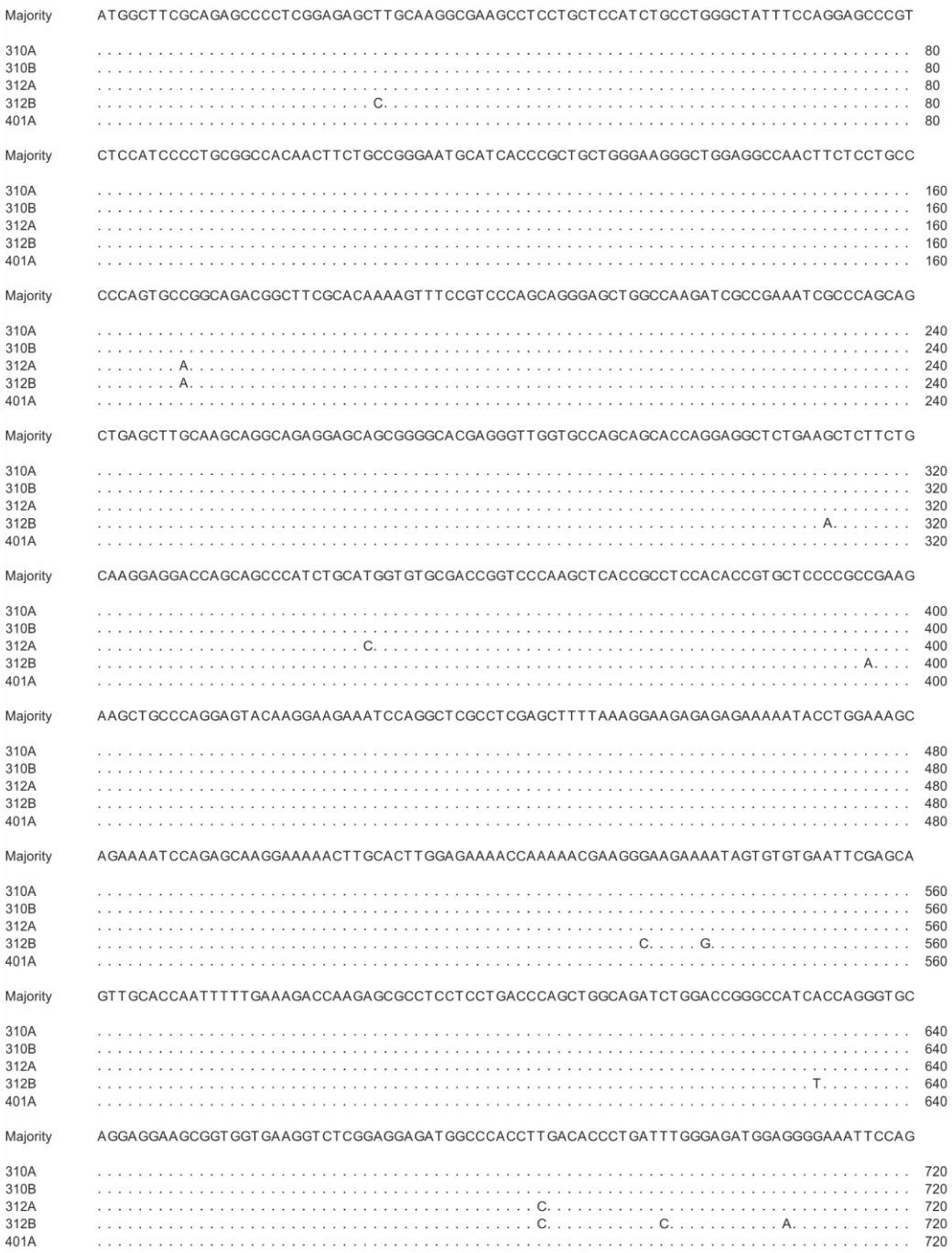

Figure A-4. Allele alignment of *TRIM27.1a* clones. Continues.

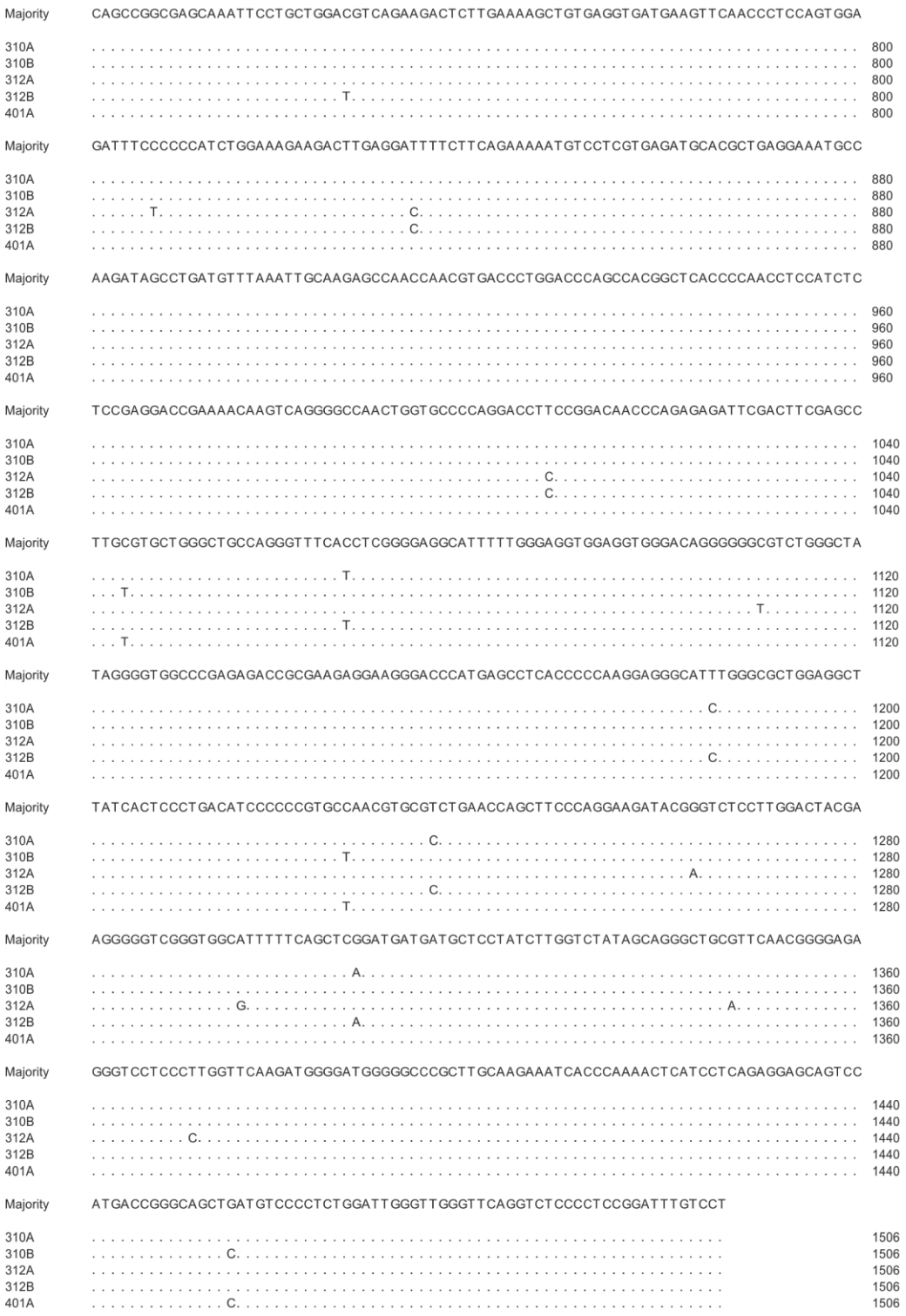

Figure A-4. Continued. Allele alignment of *TRIM27.1a* clones.

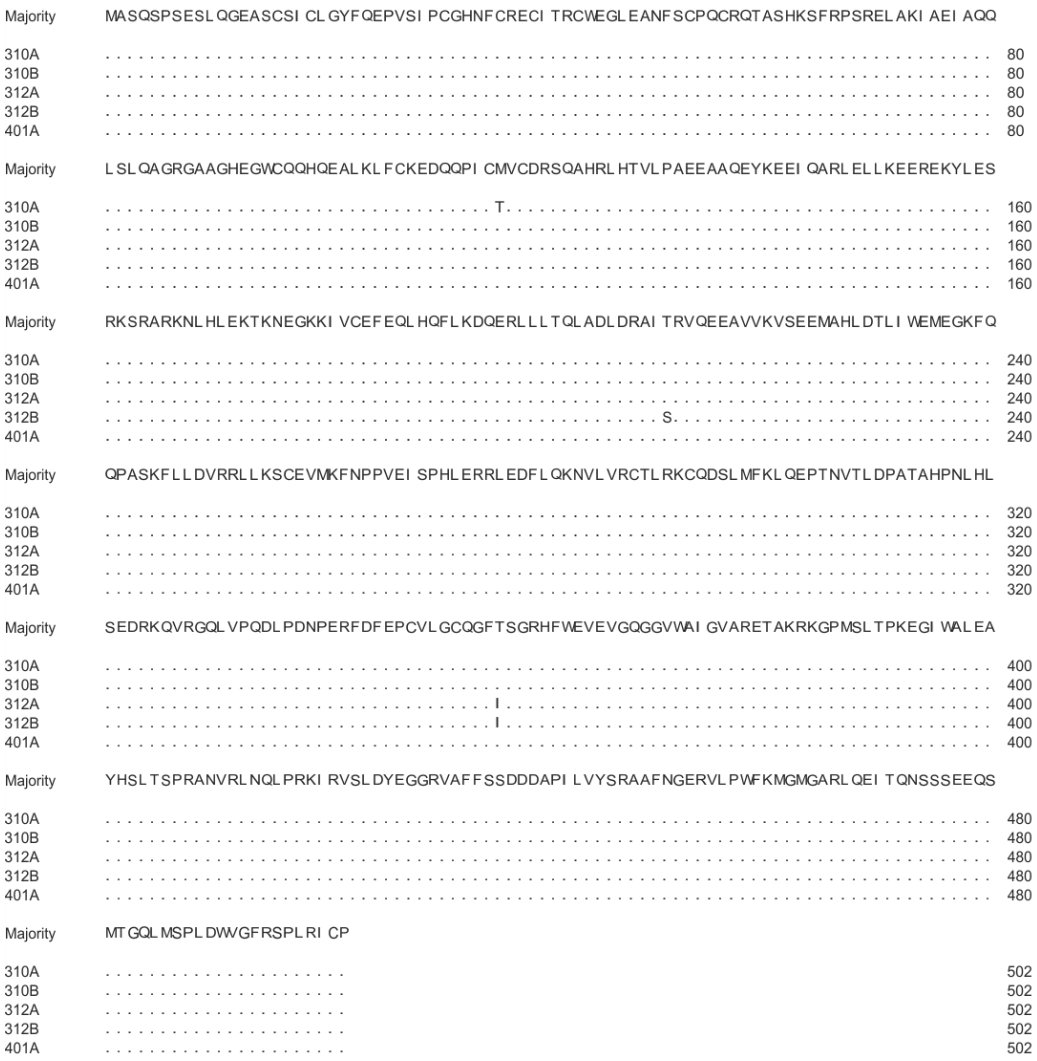

Figure A-5. Allele alignment of TRIM27.1a translations.

Table A-4. Clone numbers for allele screening of *TRIM27.1b* clones sequenced fully.

Duck Number	Allele	Clone Number
310	A	5-1
		5-2
		5-3
		5-6
	B	4-4
312	A	3
		7
		6
		9
	B	2
		4
		10
		5
401	A	3
		5
		8
		4
	B	2
		1

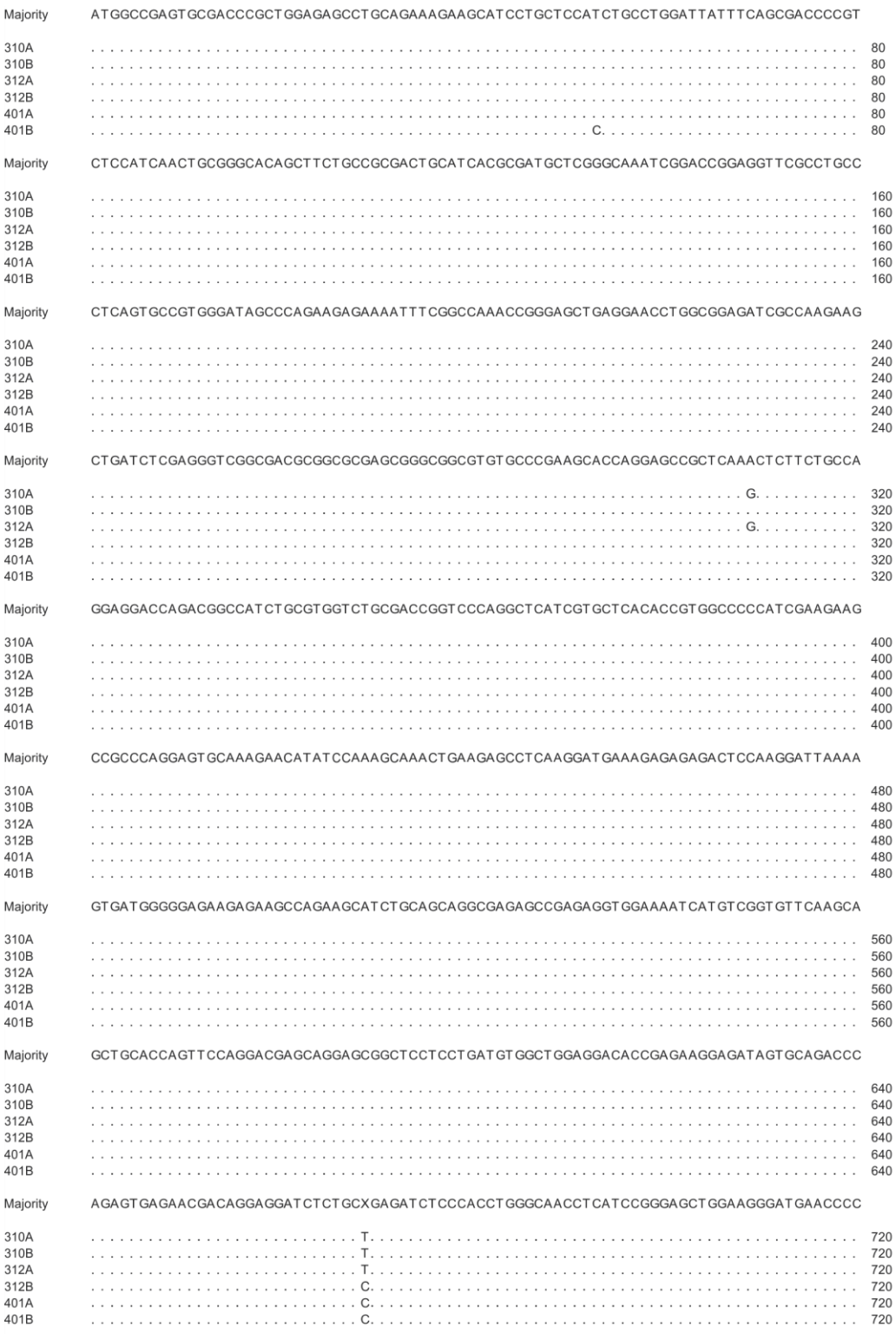

Figure A-6. Allele alignment of TRIM27.1b clones. Continues.

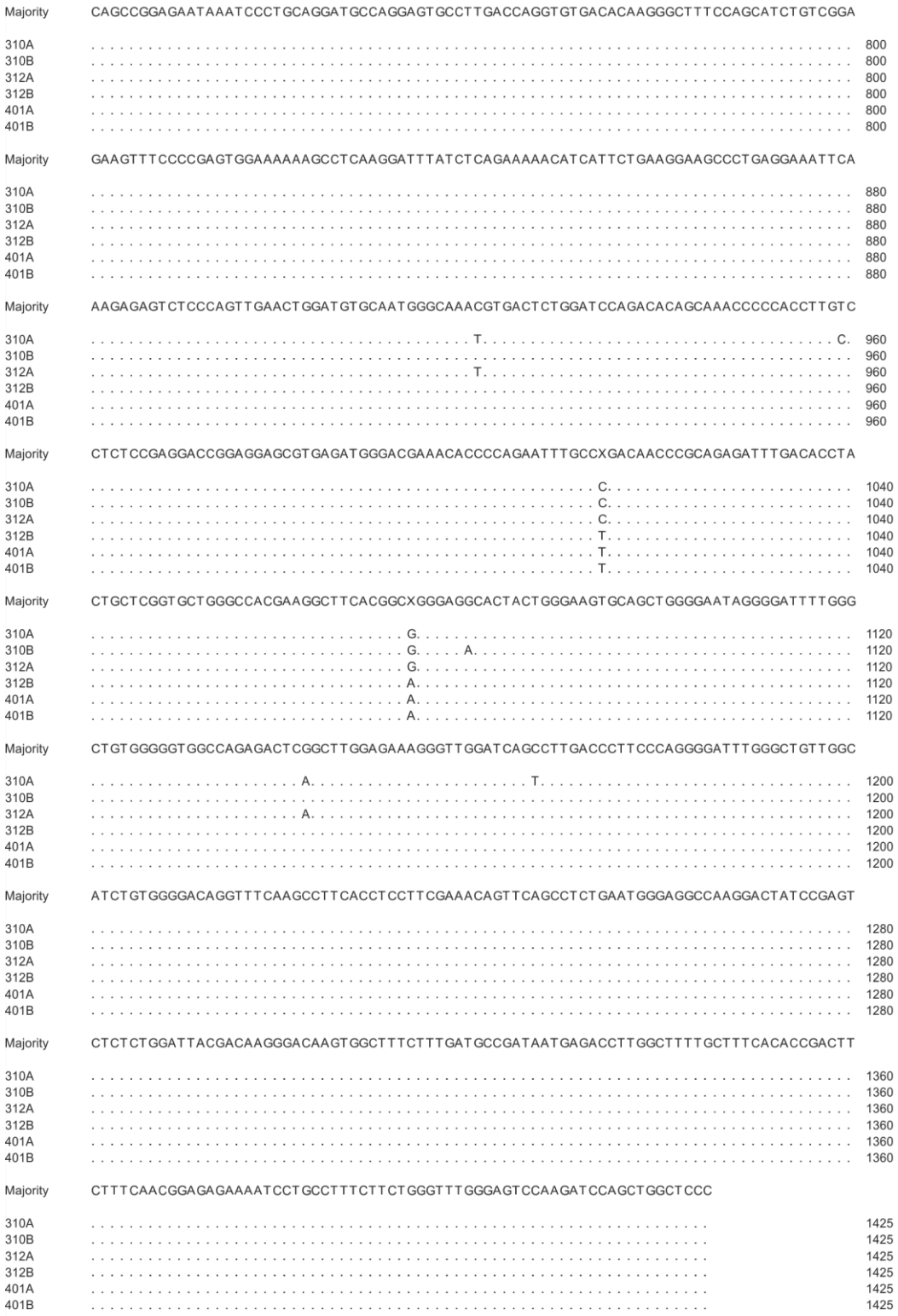

Figure A-6. Allele alignment of *TRIM27.1b* clones continued.

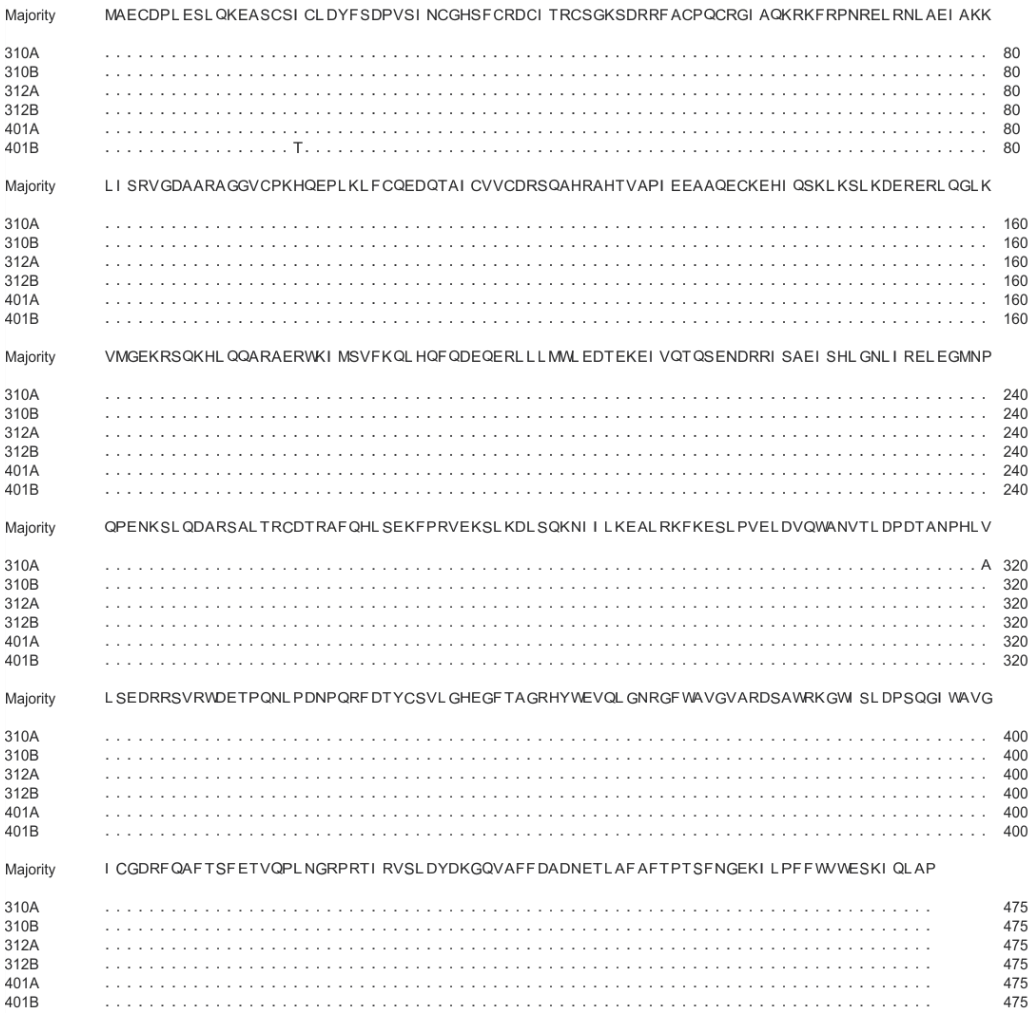

Figure A-7. Allele alignment of TRIM27.1b translations.

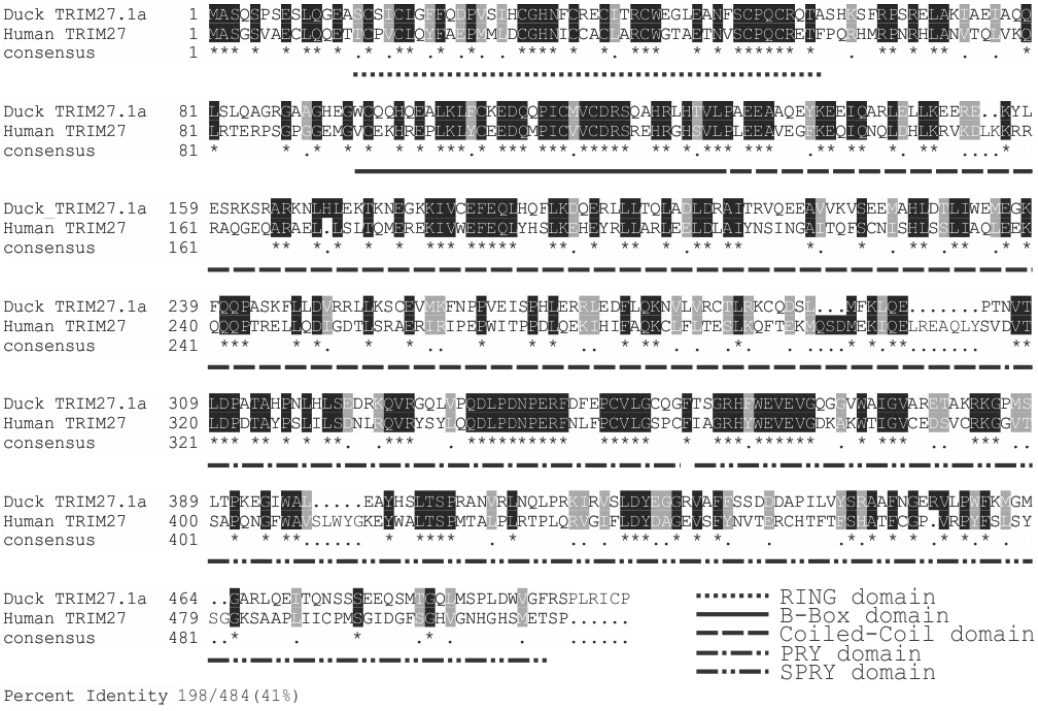

Figure A-8. Alignment of duck TRIM27.1a and human TRIM27.

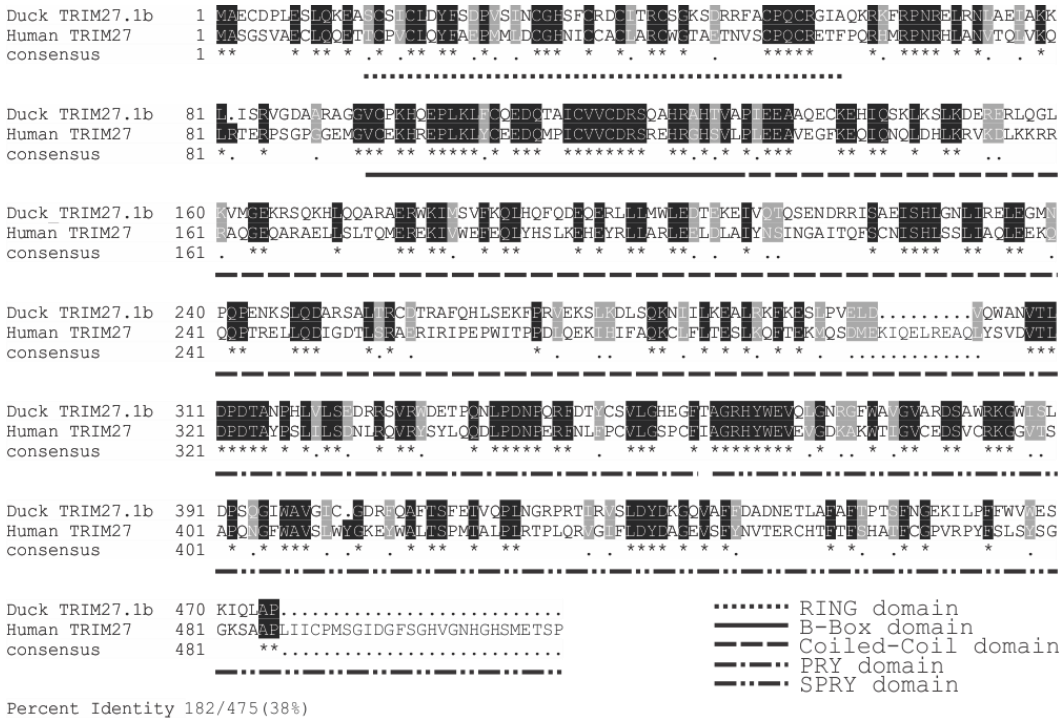

Figure A-9. Alignment of duck TRIM27.1b and human TRIM27.

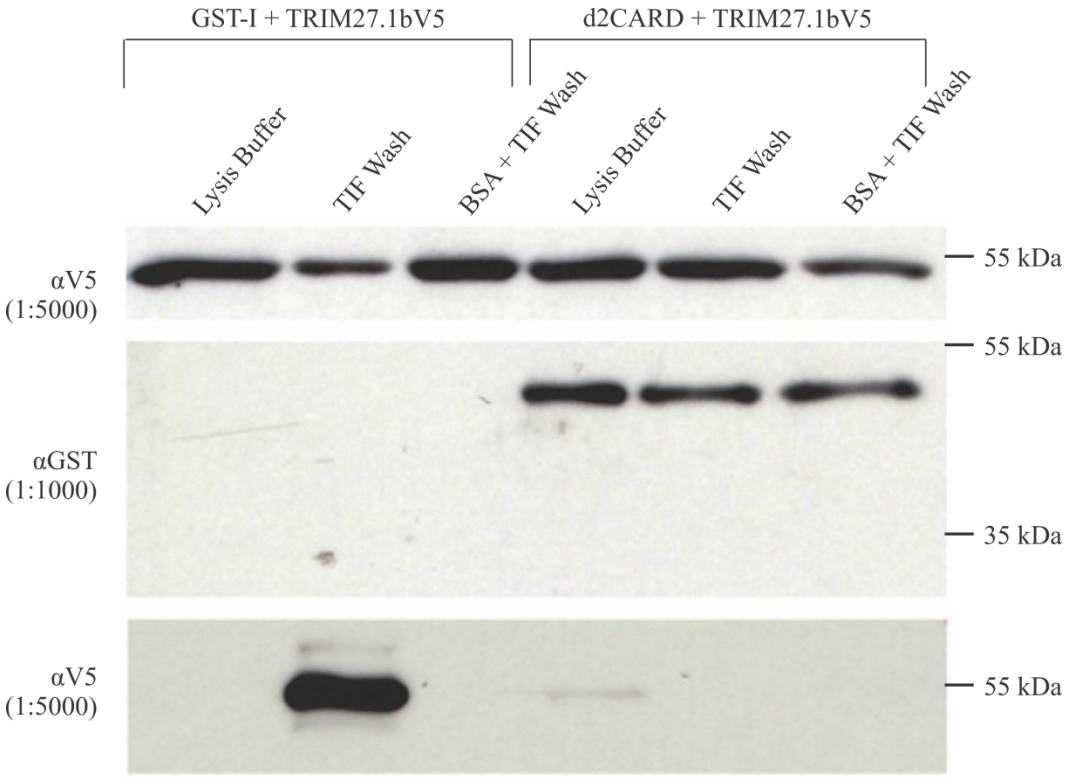

Figure A-10. TRIM27.1bV5 does not interact directly with GST-d2CARD fusion protein.
Using glutathione coated beads to pull-down the GST-d2CARD fusion protein and any interacting proteins, I were able to show that under stringent washing and pre-blocking conditions, TRIM27.1bV5 is not pulled down with GST-d2CARD indicating that TRIM27.1bV5 does not interact directly with the d2CARD to enhance transcriptional activation. A combination of TIF washing and 5% (w/v) BSA blocking of GST resin overnight provided a clean run with the GST-I+27.1b co transfection and the d2CARD+27.1b co-transfection experiments. This optimization experiment implies, although not well controlled, that TRIM27.1b does not seem to interact directly with duck RIG-I CARD domains.

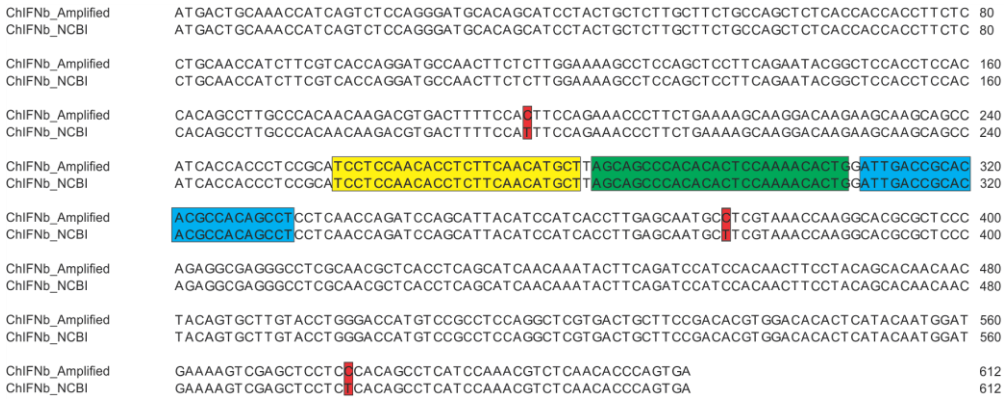

Figure A-11. Chicken *IFN-β* sequence from clones with probe binding regions. The amplified product of chicken *IFN-β* from DF1 cells aligned to the chicken *IFN-β* sequence from NCBI (NM_001024836.1) using ClustalW (MegAlign, DNAstar). There are 3 mismatches (indicated in red) in the sequence, but the qPCR primer (forward indicated in yellow, reverse in blue) and probe (indicated in green) binding sites are 100% homologous.

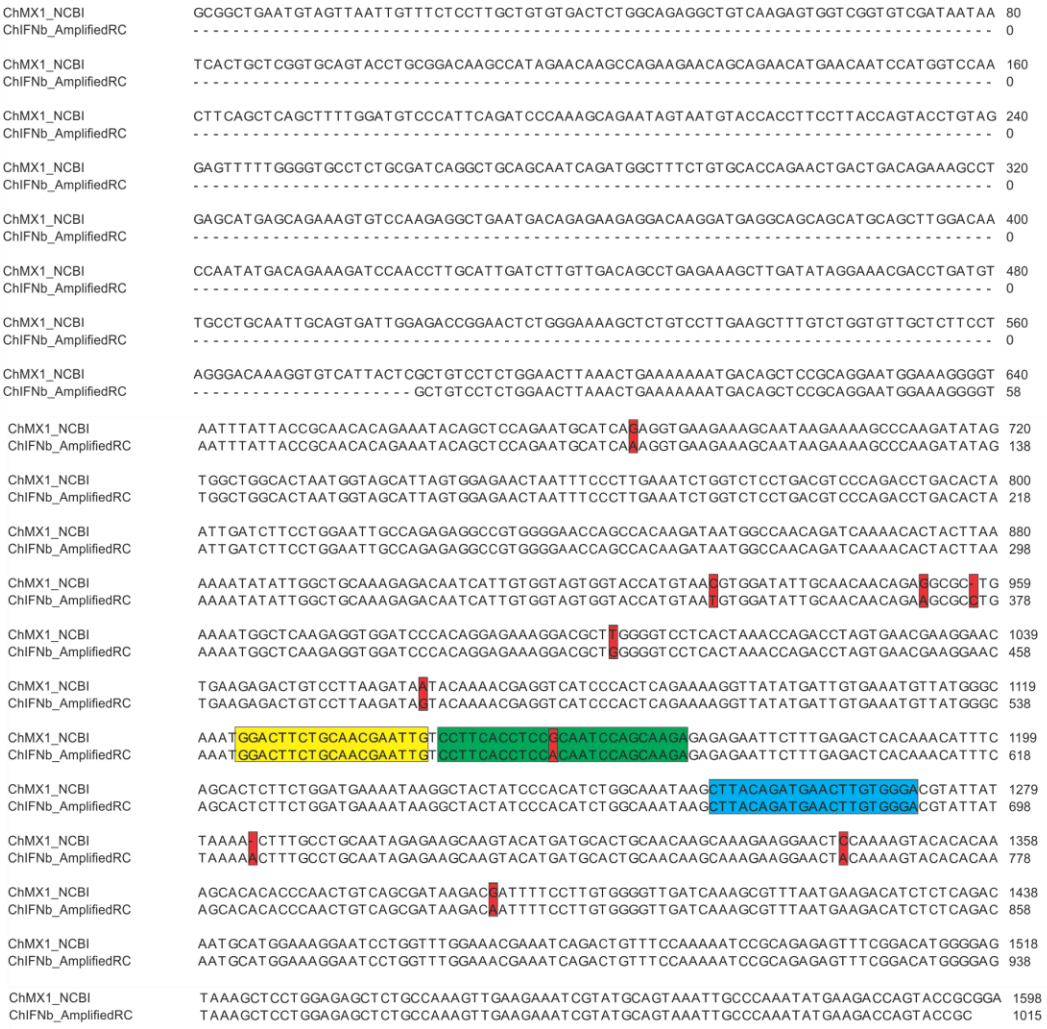

Figure A-12. Chicken *MX1fragment* sequence from clones with probe binding regions. Continues.

Chicken *MX1fragment* sequence used for abqPCR is aligned here with the predicted chicken *MX1* sequence amplified by ChickenMX1-F1 and ChickenMX1-R1 primers. The amplified product of chicken *MX1fragment* from DF1 cells aligned to the chicken *MX1* sequence from NCBI (NM_204609.1) using ClustalW (MegAlign, DNAstar). There are 10 mismatches (indicated in red) in the sequence. One mismatch in qPCR probe binding site. Of the 6 clones isolated with high fidelity enzyme all contained this A to G substitution. The primers (forward indicated in yellow, reverse in blue) and probe (indicated in green) binding sites are indicated.

Figure A-11. Continued. Chicken *MX1fragment* sequence from clones with probe binding regions.